ETH
Eidgenössische Technische Hochschule Zürich
Swiss Federal Institute of Technology Zurich

Computation of Measure Valued Solutions of the Incompressible Euler Equations

Master Thesis

S. Lanthaler

Advisor: Prof. Dr. S. Mishra

Department of Mathematics, ETH Zürich

Contents

Chapter 1

Introduction

The incompressible Euler equations (1.1) model the motion of an ideal inviscid fluid

$$\begin{cases} \partial_t v + \operatorname{div}(v \otimes v) + \nabla p = 0, \\ \operatorname{div}(v) = 0. \end{cases} \tag{1.1}$$

The vector field v is the flow vector field, the scalar function p represents the pressure. The solution of these equations requires the specification of the initial data $v|_{t=0} = v_0$ and, in addition, the specification of boundary conditions. We will consider periodic boundary conditions throughout this work. A derivation of the equations based on physical principles will be given below in section 1.1.

From a mathematical point of view, the Euler equations have proven to be difficult to study and many questions concerning the system (1.1) remain open. While there are by now well-known short-time existence and uniqueness theorems for smooth initial data [37], many problems persist, especially in the physical case of three spatial dimensions.

For two spatial dimensions, the theory is more complete. It has been understood that the vorticity, which is closely related to turbulence, is conserved along the flow and therefore the behaviour of solutions to (1.1) can be controlled to a certain extent. Indeed, existence and uniqueness results for smooth initial data were obtained not only for short times, but in the large [37]. The vorticity formulation will be discussed in section 1.4.

While these results answer the most pressing questions from a PDE perspective in the two dimensional case, they leave open the corresponding question for flows that lack smoothness. Among the most basic flows lacking smoothness are vortexsheets. A vortexsheet is a flow that is piecewise smooth, except for a smooth one-dimensional interface, across which the velocity field may have a discontinuity. For such flows, system (1.1) is to be solved in the

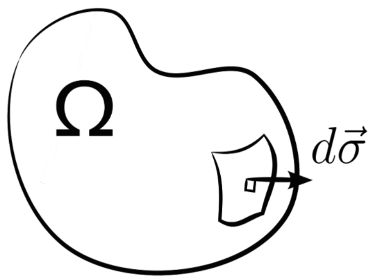

Figure 1.1: Domain Ω and surface element $d\vec{\sigma}$.

sense of distributions. An existence result for the case of vortexsheets was first obtained by Delort [17]. Delort proved that for vortexsheet initial data with vorticity a non-negative bounded measure in H^{-1}, there also exists a weak solution with vorticity a non-negative bounded measure in H^{-1}. The question of uniqueness was left open, however. More recently, Szekelyhidi obtained a non-uniqueness result for weak solutions to such initial conditions in a larger class of functions [49]. The counterexamples constructed in [49] are weak solutions belonging to L^2 for which the vorticity possibly is not a bounded measure. Thus, the question of uniqueness inside the class of flows considered by Delort remains open. We will come back to vortexsheet initial data in chapter 4, when we discuss the results of numerical experiments carried out to compute a measure-valued solution for such flows.

1.1 The incompressible Euler equations

We wish to provide a derivation of the Euler equations in this section. To this end, we fix a region $\Omega \subset \mathbb{R}^n$ in space. We assume that the fluid has a mass density distribution described by a positive function $\rho(x,t)$ and that the instantaneous velocity at point x and time t is given by the vector field $v(x,t)$.

1.1.1 Mass conservation

We make the physical assumption that mass can neither be created nor destroyed. The total mass contained in the region Ω at time t is given by $\int_\Omega \rho(x,t)\,dx$. Conservation of mass implies that any change of the mass contained inside Ω can only come from the influx or outflux of mass through the boundary $\partial\Omega$.

Mass is transported by the flow of $v(x,t)$. The flux through the boundary at time t is thus given by $-\int_{\partial\Omega} \rho(x,t)\,v(x,t)\cdot d\vec{\sigma}$. The negative sign stems from the fact that a flux in the direction of the outward normal $d\vec{\sigma}$ leads to a decrease of the mass inside Ω. Using the divergence theorem, we thus conclude that conservation of mass is expressed by

$$\frac{d}{dt}\int_{\Omega}\rho(x,t)\,dx = -\int_{\Omega}\operatorname{div}(\rho(x,t)v(x,t))\,dx.$$

This is true for an arbitrary region Ω. We can thus rewrite this integral equation in differential form and obtain

$$\partial_t\rho + \operatorname{div}(\rho\,v) = 0. \tag{1.2}$$

1.1.2 Momentum conservation

The second physical assumption that we will make concerns the conservation of momentum in an ideal fluid. The momentum density in the fluid is expressed by the vector field $M(x,t) = \rho(x,t)v(x,t)$. The total (vectorial) momentum in Ω at time t is thus given by $\int_{\Omega} M(x,t)\,dx$. By the same reasoning as above, this total momentum will change due to the flux of momentum through the boundary, $-\int_{\partial\Omega} M(x,t)\otimes v(x,t)\cdot d\vec{\sigma}$. However, in the present case there is a second way in which the momentum in Ω may change. By Newton's second law, a total force F_{Ω} acting on Ω, will induce a change of this momentum P_{Ω} by an amount given by $\frac{dP_{\Omega}}{dt} = F_{\Omega}$. Taking both of these two effects into account, we arrive at the general equation

$$\frac{d}{dt}\int_{\Omega} M(x,t)\,dx + \int_{\partial\Omega} M(x,t)\otimes v(x,t)\cdot d\vec{\sigma} = F_{\Omega}.$$

The question now is: What is the total force F_{Ω} acting on Ω at time t? In the modelling of an ideal fluid, we assume that this force is only due to the (as of yet unknown) pressure $p(x,t)$ of the fluid. Under this assumption, the force on Ω that is caused by the fluid element outside of Ω is obtained by integrating the pressure field over the boundary, i.e.

$$F_{\Omega} = -\int_{\partial\Omega} p\,d\vec{\sigma}.$$

Using the divergence-theorem once more, we conclude that the conservation of momentum in an ideal fluid can be written as

$$\frac{d}{dt}\int_{\Omega} M(x,t)\,dx + \int_{\Omega}\operatorname{div}(M(x,t)\otimes v(x,t))\,dx = -\int_{\Omega}\nabla p\,dx,$$

for any domain Ω. Since Ω is arbitrary, this integral equation can again be recast as a differential equation. Remembering also that $M = \rho v$, we conclude that

$$\partial_t(\rho v) + \operatorname{div}(\rho v\otimes v) + \nabla p = 0. \tag{1.3}$$

1.1.3 The incompressibility constraint

We want to model the motion of an *incompressible* fluid. A fluid is called incompressible, if the flow is volume-preserving, i.e. if the fluid does neither expand nor contract its volume locally. As is well-known, the flow associated to a vector field v is volume-preserving if and only if (see [37])

$$\operatorname{div}(v) = 0. \tag{1.4}$$

This is the incompressibility constraint that we have to impose in addition to conservation of mass and momentum. The incompressibility constraint allows us to rewrite $\operatorname{div}(\rho v) = v \cdot \nabla\rho + \rho \operatorname{div}(v) = v \cdot \nabla\rho$. The conservation of mass equation (1.2) can thus be formally rewritten in the form

$$\partial_t \rho + v \cdot \nabla\rho = 0. \tag{1.5}$$

This equation expresses the fact that the density ρ must be constant along the flow curves of v.

In many situations (e.g. if the fluid is liquid water), it is natural to make one additional assumption on the fluid being modelled. Namely, we assume that the fluid is homogeneous in the sense that the density ρ of the fluid has a constant value at the initial time, $\rho(x,0) = \rho_0 > 0$. By (1.5), this implies that $\rho(x,t) = \rho_0$ at all later times t. Plugging this into the momentum equation (1.3), we obtain

$$\partial_t v + \operatorname{div}(v \otimes v) + \frac{1}{\rho_0}\nabla p = 0.$$

We may now either redefine the function $p \to \frac{1}{\rho_0} p$ or set $\rho_0 = 1$, to arrive at the incompressible Euler equations:

$$\begin{cases} \partial_t v + \operatorname{div}(v \otimes v) + \nabla p = 0, \\ \operatorname{div}(v) = 0. \end{cases} \tag{1.6}$$

Remark 1.1 *If the fluid to be modelled is not ideal, then the friction forces between fluid elements have to be taken into account. This leads to the introduction of an additional force term in the momentum balance in the form of a stress tensor σ_{ij}. We will not give a detailed derivation of this case here, but instead only indicate the main points.*

The internal friction occurs when different fluid elements move at different velocities, so that there is a relative motion between them. Thus, σ_{ij} must depend on the space derivatives of the velocity. If the velocity gradients are small, we may assume that the viscous momentum transfer depends only on the first derivatives of v, and in the linear approximation that σ_{ij} is actually a linear function of ∇v. The trace of σ_{ij} leads to an isotropic force and can be incorporated in the pressure term, so that *we may assume σ_{ij} to be trace-free. Taking into account also the symmetries of the equations, it turns out that the only reasonable form of σ_{ij} under these assumptions is given by*

$$\sigma_{ij} = \nu \left(\nabla v + (\nabla v)^T - \frac{2}{3}\mathrm{div}(v) I \right),$$

where $\nu > 0$ is a constant. We then arrive at the incompressible Navier-Stokes equations

$$\begin{cases} \partial_t v + \mathrm{div}(v \otimes v) + \nabla p = \nu \Delta v, \\ \qquad\qquad\qquad\qquad \mathrm{div}(v) = 0. \end{cases} \tag{1.7}$$

The parameter ν is referred to as the kinematic viscosity. For a more detailed discussion we refer to [31, Chapter 2].

1.1.4 The role of the pressure

From our derivation of the incompressible Euler equations above, it might seem as if the pressure p had remained entirely undefined. Fortunately, this turns out not to be the case at closer inspection. To see why, we take the divergence of the evolution equation. Clearly, the liner term in v drops out due to the incompressibility constraint and we obtain the equation

$$-\Delta p = \mathrm{div}\,\mathrm{div}(v \otimes v),$$

for p. From standard elliptic theory we know that this equation possesses a unique solution given suitable conditions on v and given a further constraint such as $\int_{\mathbb{T}^n} p \, dx = 0$. We conclude that p is implicitly defined by the non-linear term. It's job is to keep v divergence-free at all times. Or said differently, p acts as a Lagrange multiplier to enforce the incompressibility constraint.

Remark 1.2 *This pressure term is responsible for much of the complexity of the incompressible Euler equations. Indeed, it is not only non-linear in v, but in addition it is also* non-local.

1.2 Classical Solutions

Before discussing more refined concepts of solutions and going into more details concerning the numerical approximation of the incompressible Euler equations, we make some fundamental observations about classical solutions.

The most fundamental result for the ensuing discussion concerns the physical principle of conservation of energy, which we now show to be satisfied by any classical solution of the Euler equations. We recall that the kinetic energy of a fluid with velocity field v is given by the expression

$$\int_{\mathbb{T}^n} \frac{1}{2}|v|^2\,dx.$$

To prove conservation of energy, we (formally) differentiate the expression above with respect to time and use the fact that v solves the Navier-Stokes equation, (1.7), with $\nu = 0$. This yields

$$\frac{d}{dt}\int_{\mathbb{T}^n} \frac{1}{2}|v|^2\,dx = \int_{\mathbb{T}^n} v\cdot\partial_t v = \int_{\mathbb{T}^n} v\cdot[-\mathrm{div}(v\otimes v) - \nabla p + \nu\Delta v]\,dx.$$

By the incompressibility constraint $\mathrm{div}(v) = 0$, and the fact that we are assuming periodic boundary conditions, we have $\int_{\mathbb{T}^n} v\cdot\nabla p\,dx = -\int_{\mathbb{T}^n}\mathrm{div}(v)\,p\,dx = 0$ after an integration by parts. Similarly, we obtain that

$$\begin{aligned}
\int_{\mathbb{T}^n} v\cdot\mathrm{div}(v\otimes v)\,dx &= \int_{\mathbb{T}^n}\sum_{i,j} v^i\partial_j(v^iv^j)\,dx\\
&= \int_{\mathbb{T}^n}\sum_{i,j}\partial_j\left(\frac{1}{2}(v^i)^2v^j\right)\,dx\\
&= \int_{\mathbb{T}^n}\mathrm{div}\left(\frac{1}{2}|v|^2v\right)\,dx\\
&= 0,
\end{aligned}$$

and

$$\int_{\mathbb{T}^n} v\cdot\nu\Delta v\,dx = -\nu\int_{\mathbb{T}^n}|\nabla v|^2\,dx.$$

Thus,

$$\frac{d}{dt}\int_{\mathbb{T}^n}\frac{1}{2}|v|^2\,dx = -\int_{\mathbb{T}^n} v\cdot[\mathrm{div}(v\otimes v) + \nabla p - \nu\Delta v]\,dx = -\nu\int_{\mathbb{T}^n}|\nabla v|^2\,dx.$$

Integration in time from 0 to t yields

$$\int_{\mathbb{T}^n}\frac{1}{2}|v|^2\,dx + \nu\int_0^t\int_{\mathbb{T}^n}|\nabla v|^2\,dx\,dt = \int_{\mathbb{T}^n}\frac{1}{2}|v_0|^2\,dx. \tag{1.8}$$

The term $\nu\int_0^t\int_{\mathbb{T}^n}|\nabla v|^2\,dx\,dt$ accounts for the energy dissipated due to friction. For classical solutions of (1.1), we can set $\nu = 0$. This proves the conservation of energy for classical solutions of (1.1).

The total momentum of the fluid is given by $\int_{\mathbb{T}^n} v\,dx$. Again, differentiation with respect to time yields

$$\frac{d}{dt}\int_{\mathbb{T}^n} v\,dx = -\int_{\mathbb{T}^n}[\mathrm{div}(v\otimes v) + \nabla p - \nu\Delta v]\,dx = 0, \tag{1.9}$$

for any classical solution v of (1.7). In particular, solutions of the Euler equations formally satisfy the principle of conservation of momentum.

1.3 Elements of the Mathematical Theory

1.3.1 Weak solutions

The question whether solution of the incompressible Euler equations which are smooth at an initial time will remain so for all later times, is still an outstanding problem. It has proven useful in the study of partial differential equations, to relax the solution concept and look for weak solutions which need not satisfy the equations in a pointwise sense. This can allow one to establish existence results first, and recover uniqueness and smoothness properties later on. Let us define what we mean by a weak solution in the context of the Euler equations.

Definition 1.3 *A vector field $v \in L^2(\mathbb{T}^n \times [0, +\infty); \mathbb{R}^n)$ is a weak solution of the incompressible Euler equations if*

$$\int_{\mathbb{T}^n} v \cdot \partial_t \varphi + (v \otimes v) : \nabla \varphi \, dx = 0,$$

for all $\varphi \in C_c^\infty(\mathbb{T}^n \times (0, +\infty); \mathbb{R}^n)$ with $\operatorname{div}(\varphi) = 0$, and

$$\int_{\mathbb{T}^n} v \cdot \nabla \psi \, dx = 0,$$

for all $\psi \in C^\infty(\mathbb{T}^n)$ and all times t.

A vector field $v \in L^2(\mathbb{T}^n \times [0, +\infty); \mathbb{R}^n)$ is a weak solution of the incompressible Euler equations with initial data v_0, if it is a weak solution and satisfies

$$\int_{\mathbb{T}^n} v \cdot \partial_t \varphi + (v \otimes v) : \nabla \varphi \, dx = -\int_{\mathbb{T}^n} v_0 \cdot \varphi(\,\cdot\,, 0) \, dx,$$

for all $\varphi \in C_c^\infty(\mathbb{T}^n \times [0, +\infty); \mathbb{R}^n)$ with $\operatorname{div}(\varphi) = 0$.

1.3.2 Existence and uniqueness

The mathematical theory underlying the incompressible Euler equations in the physical case, i.e. in three spatial dimensions, is still very incomplete. In particular, the study of the long time behaviour of solutions is beyond current understanding. More can be said for short time intervals. For sufficiently smooth initial conditions, we have the following well-posedness result at least for small times.

Theorem 1.4 (Existence and uniqueness) *[37, Corollary 3.2] Given a divergence-free initial data $v_0 \in H^m(\mathbb{T}^n; \mathbb{R}^n)$, $m \geq \left[\frac{n}{2}\right] + 2$, there exists a time T depending on the H^m-norm of v_0, such that there exists a unique solution*

$$v \in C([0, T); H^m(\mathbb{T}^n; \mathbb{R}^n)) \cap C^1([0, T); H^{m-2}(\mathbb{T}^n; \mathbb{R}^n)).$$

1.3.3 Vorticity

As has already been mentioned above, the vorticity is a quantity of central importance in the study of turbulent flows. The vorticity, which will be denoted by η, is simply defined as the curl of the velocity field $\eta = \operatorname{curl} v$.

To obtain the corresponding evolution equation for η, we will make use of the following elementary identities from vector calculus, valid for any smooth vector fields A, B and any smooth function f.

$$
\begin{aligned}
\operatorname{div}(A \otimes A) &= A \cdot \nabla A + \operatorname{div}(A) A, && (1.10)\\
A \cdot \nabla A &= \frac{1}{2}\nabla |A|^2 - A \times \operatorname{curl} A, && (1.11)\\
\operatorname{curl} \nabla f &= 0, && (1.12)\\
\operatorname{div}(\operatorname{curl} A) &= 0, && (1.13)\\
\operatorname{curl}(A \times B) &= \operatorname{div}(B) A - \operatorname{div}(A) B + B \cdot \nabla A - A \cdot \nabla B. && (1.14)
\end{aligned}
$$

We take the curl of $\partial_t v + \operatorname{div}(v \otimes v) + \nabla p = 0$. We use the vector calculus identity (1.11)

$$v \cdot \nabla v = \frac{1}{2}\nabla |v|^2 - v \times \eta,$$

and the fact that by (1.10)

$$\operatorname{div}(v \otimes v) = v \cdot \nabla v,$$

provided that $\operatorname{div}(v) = 0$. By (1.12), we have $\operatorname{curl} \nabla p = 0$ for any p.

Taking the curl of $\partial_t v = -(\operatorname{div}(v \otimes v) + \nabla p)$, we formally arrive at

$$
\begin{aligned}
\partial_t \eta &= -\operatorname{curl}(\operatorname{div}(v \otimes v) + \nabla p)\\
&= -\operatorname{curl}\left(\nabla \left(\frac{1}{2}|v|^2 + p\right) - v \times \eta\right).
\end{aligned}
$$

The term involving the gradient vanishes again by (1.12). Finally, by (1.14), we have

$$\operatorname{curl}(v \times \eta) = \operatorname{div}(\eta) v - \operatorname{div}(v) \eta + \eta \cdot \nabla v - v \cdot \nabla \eta \quad = \eta \cdot \nabla v - v \cdot \nabla \eta,$$

using also the fact that by (1.13), $\operatorname{div} \operatorname{curl} = 0$ and once more that $\operatorname{div}(v) = 0$. Thus, we arrive at the evolution equation for the vorticity η:

$$
\begin{cases}
\partial_t \eta + v \cdot \nabla \eta = \eta \cdot \nabla v,\\
\operatorname{curl} v = \eta, \operatorname{div} v = 0.
\end{cases}
\tag{1.15}
$$

The term $\eta \cdot \nabla v$ is called the vortex stretching term. It acts as a source term in the advection equation for η and can have the effect of, well, stretching η. Since v depends on η, the vortex stretching term could potentially lead to a fatal feed-back and cause η to blow up after a finite time, even when starting from smooth initial data.

The vorticity equation is especially convenient to work with in the two-dimensional case. In this case, η is a (pseudo-)scalar and the vortex stretching term vanishes. The evolution equation for η thus is simply a transport equation. I.e. η is a solution of

$$\partial_t \eta + v \cdot \nabla \eta = 0. \tag{1.16}$$

The vorticity can also be used to reconstruct the velocity field. Let $\nabla^\perp$ denote the gradient operator, rotated by 90 degrees,

$$\nabla^\perp = (-\partial_{x_2}, \partial_{x_1})^t,$$

Then v can be (formally) obtained from η as follows. Because of $\operatorname{div}(v) = 0$, we have $v = \nabla^\perp \psi$ for some function ψ. This ψ then solves

$$\eta = \operatorname{curl} v = \operatorname{curl}(\nabla^\perp \psi) = \Delta \psi. \tag{1.17}$$

On the other hand, if ψ solves (1.17), then $v := \nabla^\perp \psi$ is automatically divergence-free and solves $\operatorname{curl} v = \eta$. The evolution equation for η is thus formally equivalent to the incompressible Euler equations.

The fact that there is no vortex stretching term in two dimensions simplifies the analysis of the Euler equation considerably. In fact, *global* existence for smooth solutions has been proven in the two dimensional case.

Theorem 1.5 ([Corollary 3.3) *, [37]] Given a 2D initial velocity field $v_0 \in C^\infty(\mathbb{T}^2; \mathbb{R}^2)$, there exists a for all time a unique smooth solution $v \in C^\infty([0, +\infty) \times \mathbb{T}^2; \mathbb{R}^2)$ of the Euler equations.*

We will encounter equation (1.16) again, when we discuss spectral schemes in two spatial dimensions.

Chapter 2

Measure valued solutions

2.1 Introduction

In this section, we recapitulate the notion of measure-valued solutions for the Euler equations. Measure-valued solutions were introduced to study the behaviour of weakly convergent sequences of solutions, or approximate solutions, to the Euler equations by DiPerna and Majda [19].

They address the following problem. Strong solutions of the Euler equations conserve energy $\|v(t)\|_{L^2} = \|v_0\|_{L^2}$. Given a sequence v_n of solutions to the Euler equations with uniformly bounded L^2-norm, we can extract a weakly convergent subsequence $v_n \rightharpoonup v$ in $L^2([0,+\infty) \times \mathbb{T}^n; \mathbb{R}^n)$. If each v_n is a solution of the Euler equations, then for any test function $\varphi \in C_c^\infty((0,+\infty) \times \mathbb{T}^n; \mathbb{R}^n)$, with $\operatorname{div}\varphi = 0$, we have

$$\int_0^\infty \int_{\mathbb{T}^n} v_n \partial_t \varphi + (v_n \otimes v_n) : \nabla\varphi \, dx\, dt = 0.$$

We would like to pass to the limit in this equation to show that the limiting flow vector field v is again a weak solution of the Euler equations. However, as the v_n are only known converge weakly in L^2, we cannot deduce that the non-linear term converges, i.e. we may have $v_n \otimes v_n \not\rightharpoonup v \otimes v$ in general. This possible lack of convergence is due to the effects of sustained oscillations and concentrations. We illustrate the point with the following example due to DiPerna and Majda [19].

Example 2.1 *We present an example of a sequence of solutions to the incompressible Euler equations which exhibit persistent oscillations. We begin with the following remark. If $v(x_1, x_2, t) = (v_1(x_1, x_2, t), v_2(x_1, x_2, t))$ is a divergence free field, then $(v_1(x_1, x_2, t), v_2(x_1, x_2, t), v_3(x_1, x_2, t))$ will be a solution to the incompressible Euler equations provided that v_3 solves the transport equation*

$$\partial_t v_3 + v_1 \partial_{x_1} v_3 + v_2 \partial_{x_2} v_3 = 0.$$

Let $u(x_1, x_2)$ be given, such that $\xi \mapsto u(\xi, x_2)$ is 1-periodic and has mean zero, i.e. such that $\int_0^1 u(\xi, x_2)\, d\xi = 0$ for all x_2. We consider the initial data given by

$$v_\varepsilon\big|_{t=0} = \left(u\left(\frac{x_2}{\varepsilon}, x_2\right), 0, w(x_1, x_2)\right).$$

for $\varepsilon > 0$. Clearly, $v_\varepsilon|_{t=0}$ defined in this way is divergence-free. The corresponding solution of the incompressible Euler equations can be written down explicitly. It is given by

$$v_\varepsilon(x, t) = \left(u\left(\frac{x_2}{\varepsilon}, x_2\right), 0, w\left(x_1 - t\, u\left(\frac{x_2}{\varepsilon}, x_2\right), x_2\right)\right).$$

We thus have obtained a one-parameter family of solutions of the Euler equations. Evidently, v_ε will be uniformly bounded in L^∞, hence in L^2_{loc}. We want to consider the limiting behaviour as $\varepsilon \to 0$.

By the Riemann-Lebesgue lemma, it is known that for any function $f(x_1, x_2)$ which is 1-periodic in the first variable, we have

$$f\left(\frac{x_2}{\varepsilon}, x_2\right) \rightharpoonup \int_0^1 f(\xi, x_2)\, d\xi, \quad \text{as } \varepsilon \to 0, \quad \text{weakly in } L^2. \tag{2.1}$$

In particular, this implies that

$$v_\varepsilon \rightharpoonup \overline{v} = \left(0, 0, \int_0^1 w\left(x_1 - t\, u\left(\xi, x_2\right), x_2\right)\, d\xi\right) \quad \text{as } \varepsilon \to 0.$$

The vector field $\overline{v}$ will be a solution of the incompressible Euler equations if and only if $\partial_t \overline{v_3} = 0$, i.e. if and only if

$$\int_0^1 w\left(x_1 - t\, u\left(\xi, x_2\right), x_2\right)\, d\xi$$

is independent of t. It is clear that this will not be the case for general u, w (except if w is independent of the first variable). So $\overline{v}$ is not a solution of the incompressible Euler equations in general.

We summarize the conclusions to be drawn from example 2.1:

There exist solutions v_ε to the Euler equations, such that v_ε converges weakly to a limit $\overline{v}$ as $\varepsilon \to 0$, but such that this limit $\overline{v}$ is not a solution of the Euler equations. In particular, this shows that we cannot use simple compactness arguments based on estimates on the kinetic energy $\frac{1}{2}\|v_\varepsilon\|^2_{L^2}$, in order to prove the existence of weak solutions of the Euler equations.

The limiting behaviour of solution sequences of the Euler equations may be too complex to be captured properly by a single-valued function. In order to make sense of such limits, we must extend our notions and consider measure-valued functions, or Young measures, instead.

2.2 (Generalized) Young measures

The general limiting behaviour of a weakly convergent sequence including oscillation and concentration effects can in very general terms be captured by the notion of a generalised Young measure [1], [14], [18], [19]. Let $v_n \in L^\infty((0,T); L^2(\mathbb{T}^n;\mathbb{R}^n))$ be a sequence of vector fields with uniformly bounded norm $\sup_t \|v_n\|_{L^2} \leq C$. According to the theory of Young measures, there exists a triple $(\nu, \lambda, \nu^\infty)$ such that (after extraction of a subsequence)

$$f(v_n)\,dx\,dt \overset{*}{\rightharpoonup} \left(\int_{\mathbb{R}^n} f\,d\nu_{x,t}\right)dx\,dt + \left(\int_{\mathbb{S}^{n-1}} f^\infty\,d\nu^\infty_{x,t}\right)\lambda(\,dx\,dt) \tag{2.2}$$

for every continuous function $f \in C(\mathbb{R}^n)$ for which $f^\infty(\theta) = \lim_{s\to\infty} s^{-2} f(s\theta)$ exists. A generalised Young measure $(\nu, \lambda, \nu^\infty)$ thus consists of

- the oscillation measure ν, which is a probability measure on phase space $\mathbb{R}^n$ accounting for the persistence of oscillations in the sequence v_n,
- the concentration measure $\lambda = \lambda_t \otimes dt$, where λ_t is a measure in physical space $\mathbb{T}^n$ that is singular with respect to Lebesgue measure,
- the concentration-angle measure ν^∞, a probability measure on $\mathbb{S}^{n-1}$.

We will call $(\nu, \lambda, \nu^\infty)$ an associated Young measure to the sequence v_n, if we can extract a subsequence for which (2.2) holds. In particular, this allows us to obtain a limiting object for the limiting behaviour of sequences of the Euler equations in the nonlinear term $f(v) = v \otimes v$. We will frequently use the notation $\langle \nu_{x,t}, f\rangle := \int_{\mathbb{R}^n} f\,d\nu_{x,t}$ in the following.

Definition 2.2 *We denote by $\mathcal{F}$ the space of test functions g that are of the form $g(\xi) = \tilde{g}(\xi)(1+|\xi|^2)$, where $\tilde{g}$ is a continuous and bounded function on $\mathbb{R}^n$, and for which the recession function $\tilde{g}^\infty(\xi) = \lim_{s\to\infty} \tilde{g}(s\xi)$ exists and is a continuous function on $\mathbb{S}^{n-1}$.*

We have the following theorem about the limiting behaviour of uniformly bounded sequences of L^2-functions.

Theorem 2.3 *([19], [1]) Let (v_k) be a bounded sequence in $L^\infty((0,T); L^2(\mathbb{T}^n;\mathbb{R}^n))$. There exists a subsequence (not reindexed), a nonnegative Radon measure λ and parametrized families of probability measures $\nu \in L^\infty_{w^*}(\mathbb{T}^n \times (0,T); \mathcal{P}(\mathbb{R}^n))$, $\nu^\infty \in L^\infty_{w^*}(\mathbb{T}^n \times (0,T); \mathcal{P}(\lambda; \mathbb{S}^{n-1}))$ such that:*

$$g(v_k) \overset{*}{\rightharpoonup} \langle \nu, g\rangle + \langle \nu^\infty, g^\infty\rangle\lambda$$

in the sense of measures, for every $g \in \mathcal{F}$. The concentration measure λ is singular with respect to Lebesgue measure $dx\,dt$.

In addition, the concentration measure λ can be disintegrated in the form $\lambda(dx, dt) = \lambda_t(dx) \otimes dt$, where λ_t is a non-negative measure on $\mathbb{T}^n$, parametrized by time t.

Having introduced the concept of Young measures, we return to example 2.1.

Example 2.4 *We wish to compute the limiting Young measure corresponding to the sequence v_ε of example 2.1, where*

$$v_\varepsilon(x,t) = \left(u\left(\frac{x_2}{\varepsilon}, x_2\right), 0, w\left(x_1 - t\, u\left(\frac{x_2}{\varepsilon}, x_2\right), x_2\right)\right).$$

Let $g \in \mathcal{F}$. By the homogenization equation (2.1)*, we have that*

$$g(v_\varepsilon(x,t)) \rightharpoonup \int_0^1 g\left(u\left(\xi, x_2\right), 0, w\left(x_1 - t\, u\left(\xi, x_2\right), x_2\right)\right)\, d\xi.$$

This expression does not depend on the recession function g^∞ of g. We thus observe that there is no concentration effect in this example, and the lack of convergence in the strong L^2 sense arises from the persistence of oscillations in the limit. In particular, we have $\lambda = 0$ in this case.

The oscillation measure $\nu_{x,t}$ on the other hand satisfies

$$\begin{aligned}\int_{\mathbb{R}^n} g(\xi)\, d\nu_{x,t}(\xi) &= \int_0^1 g\left(u\left(\rho, x_2\right), 0, w\left(x_1 - t\, u\left(\rho, x_2\right), x_2\right)\right)\, d\rho \\ &= \int_0^1 g \circ \Phi_{x,t}(\rho)\, d\rho,\end{aligned}$$

where $\Phi_{x,t}(\rho) = \left(u\left(\rho, x_2\right), 0, w\left(x_1 - t\, u\left(\rho, x_2\right), x_2\right)\right)$. It follows that $\nu_{x,t} = (\Phi_{x,t})_* d\rho$ is given by the push forward of the line element $d\rho$ under the map $\rho \mapsto \Phi_{x,t}(\rho)$.

Note that (as was to be expected from example 2.1) the limiting Young measure $(\nu_{x,t}, \lambda_t, \nu^\infty_{x,t})$ is non-atomic*!*

2.3 A Generalized Solution Concept

Measure-valued solutions (MVS) are a generalisation of the usual weak solution concept based on generalized Young measures introduced by DiPerna-Majda [19]. We give the slightly more general definition found in [22].

Definition 2.5 *A Young measure $v = (\nu, \lambda, \nu^\infty)$ is a measure-valued solution of the incompressible Euler equations* (1.1) *with initial data σ, if it satisfies*

$$\begin{aligned}&\int_0^\infty \int_{\mathbb{T}^n} \langle \nu_{x,t}, \xi \rangle \partial_t \varphi + \langle \nu_{x,t}, \xi \otimes \xi \rangle : \nabla \varphi \; dx\, dt \\ &\quad + \int_0^\infty \int_{\mathbb{S}^{n-1}} \langle \nu^\infty_{x,t}, \theta \otimes \theta \rangle : \nabla \varphi \; \lambda(\, dx\, dt) + \int_{\mathbb{T}^n} \langle \sigma_x, \xi \rangle \varphi(x,0)\; dx = 0\end{aligned} \tag{2.3}$$

for all $\varphi \in C_c^\infty([0,+\infty) \times \mathbb{T}^n; \mathbb{R}^n)$ *with* $\operatorname{div}\varphi = 0$*, and*

$$\int_0^\infty \int_{\mathbb{T}^n} \langle \nu_{x,t}, \xi \rangle \cdot \nabla \psi = 0 \tag{2.4}$$

for $\psi \in C_c^\infty([0,+\infty) \times \mathbb{T}^n)$.

One of the main motivations for introducing MVS in [19] was the observation that the limiting behaviour of solutions to the Navier-Stokes equations (1.7) in the zero-viscosity limit can naturally be captured by MVS. This is relevant because a general existence theorem for the Navier-Stokes equations is already known, and real physical flows will exhibit some viscous behaviour.

In 1934, Jean Leray [34] gave a proof of the existence of weak solutions v_ν to the Navier-Stokes equations with kinematic viscosity ν and for given initial data v^0. His solutions satisfy the natural energy estimate expected from the formal identity (1.8):

$$\frac{1}{2}\|v_\nu(t)\|^2_{L^2(\mathbb{T}^3)} + \nu \int_0^t \|\nabla v_\nu(s)\|^2_{L^2(\mathbb{T}^3)}\, ds \leq \frac{1}{2}\|v^0\|^2_{L^2(\mathbb{T}^3)}, \tag{2.5}$$

for all $t \in [0,+\infty)$.

The Euler equations now have a natural interpretation as the zero viscosity limit of the Naviar-Stokes equations. One would therefore like to study the limiting behaviour of the familiy $\{v_\nu\}_{\nu>0}$ as $\nu \to 0$.

The main problem in taking this limit is that the a priori estimate for ∇v_ν obtained from (2.5) blows up as $\nu \to 0$. The only uniform estimate we can obtain from (2.5) apparently is the L^2 estimate

$$\|v_\nu(t)\|^2_{L^2(\mathbb{T}^3)} \leq \|v^0\|^2_{L^2(\mathbb{T}^3)}.$$

However, without any a priori control on ∇v_ν, we cannot use compactness arguments to show that there exists a limit $v_\nu \to v$ as $\nu \to 0$ in any strong (point-wise) sense. What can be said about the limiting behaviour is a consequence of the following proposition due to DiPerna-Majda [19].

Proposition 2.6 *Assume* v_ε *is a sequence of functions satisfying* $\operatorname{div}(v_\varepsilon) = 0$.

(a) Weak Stability: *There exists a constant* $C > 0$ *such that*

$$\int_{\mathbb{T}^n} |v_\varepsilon|^2\, dx \leq C, \tag{2.6}$$

(b) Weak Consistency: *For all divergence-free test functions* $\varphi \in C^\infty(\mathbb{T}^n \times (0,T); \mathbb{R}^n)$,

$$\lim_{\varepsilon \to 0} \int_{\mathbb{T}^n \times (0,T)} \varphi_t \cdot v_\varepsilon + \nabla\varphi : v_\varepsilon \otimes v_\varepsilon\, dx\, dt = 0. \tag{2.7}$$

If $v = (\nu, \lambda, \nu^\infty)$ is the associated generalized Young measure from Theorem 2.3, then v is a measure-valued solution of the Euler equations on $\mathbb{T}^n \times (0,T)$.

Proof Let v_ε be a sequence satisfying the assumptions of proposition 2.6. By theorem 2.3 and the weak stability assumption (a), there exists a Young measure $v = (\nu, \lambda, \nu^\infty)$ and a subsequence v_ε (not reindexed) converging to it, i.e. such that for any test function $\varphi \in C_c^\infty([0,+\infty) \times \mathbb{T}^n)$ and for $g \in \mathcal{F}$:

$$\int_{\mathbb{T}^n \times (0,T)} g(v_\varepsilon)\varphi \, dx \, dt \to \int \langle \nu, g \rangle \, \varphi \, dx \, dt + \int_{\mathbb{T}^n \times (0,T)} \langle \nu^\infty, g^\infty \rangle \varphi \, d\lambda_t^\infty \, dt.$$

We apply this component-wise to $g(v) = v$ (so $g^\infty(\theta) = 0$) and with test function $\partial_t \varphi$, to obtain

$$\int_{\mathbb{T}^n \times (0,T)} v_\varepsilon \partial_t \varphi \, dx \, dt \to \int_{\mathbb{T}^n \times (0,T)} \langle \nu, \xi \rangle \, \partial_t \varphi \, dx \, dt. \tag{2.8}$$

On the other hand, for the vector test function $\nabla \psi$, where $\psi \in C_c^\infty(\mathbb{T}^n \times (0,T))$, we corrispondingly have

$$\int_{\mathbb{T}^n \times (0,T)} v_\varepsilon \cdot \nabla \psi \, dx \, dt \to \int_{\mathbb{T}^n \times (0,T)} \langle \nu, \xi \rangle \cdot \nabla \psi \, dx \, dt. \tag{2.9}$$

Further, for $g(v) = v \otimes v$ (so $g^\infty(\theta) = \theta \otimes \theta$) and with test function $\nabla \varphi$, we obtain

$$\int_{\mathbb{T}^n \times (0,T)} v_\varepsilon \otimes v_\varepsilon : \nabla \varphi \, dx \, dt \to \int_{\mathbb{T}^n \times (0,T)} \langle \nu, \xi \otimes \xi \rangle : \nabla \varphi \, dx \, dt. \tag{2.10}$$

Since $\operatorname{div}(v_\varepsilon) = 0$, all the terms on the left hand side in (2.9) are $= 0$. Hence, we also have

$$\int_{\mathbb{T}^n \times (0,T)} \langle \nu, \xi \rangle \cdot \nabla \psi \, dx \, dt = 0.$$

We see that the limiting Young measure satisfies the incompressiblity constraint (2.4). On the other hand, summing (2.8) and (2.10) and using the weak consistency assumption (b), we find that

$$\begin{aligned} &\int_0^\infty \int_{\mathbb{T}^n} \langle \nu_{x,t}, \xi \rangle \partial_t \varphi + \langle \nu_{x,t}, \xi \otimes \xi \rangle : \nabla \varphi \; dx \, dt \\ &\quad + \int_0^\infty \int_{\mathbb{S}^{n-1}} \langle \nu_{x,t}^\infty, \theta \otimes \theta \rangle : \nabla \varphi \; \lambda(\, dx \, dt) + \int_{\mathbb{T}^n} \langle \sigma_x, \xi \rangle \varphi(x,0) \; dx \end{aligned}$$

is the limit of $\int_{\mathbb{T}^n \times (0,T)} v_\varepsilon \partial_t \varphi \, dx \, dt + \int_{\mathbb{T}^n \times (0,T)} v_\varepsilon \otimes v_\varepsilon : \nabla \varphi \, dx \, dt$. But, by (b)

$$\int_{\mathbb{T}^n \times (0,T)} v_\varepsilon \partial_t \varphi \, dx \, dt + \int_{\mathbb{T}^n \times (0,T)} v_\varepsilon \otimes v_\varepsilon : \nabla \varphi \, dx \, dt \to 0.$$

Thus, we conclude that

$$\int_0^\infty \int_{\mathbb{T}^n} \langle \nu_{x,t}, \xi \rangle \partial_t \varphi + \langle \nu_{x,t}, \xi \otimes \xi \rangle : \nabla \varphi \, dx \, dt$$
$$+ \int_0^\infty \int_{\mathbb{T}^n} \langle \nu_{x,t}^\infty, \theta \otimes \theta \rangle : \nabla \varphi \, \lambda(\, dx \, dt) + \int_{\mathbb{T}^n} \langle \sigma_x, \xi \rangle \varphi(x, 0) \, dx = 0,$$

and the limiting Young measure v is a also solution of (2.3). This shows that v is a MVS of the incompressible Euler equations. □

It is now easy to prove the following theorem.

Theorem 2.7 ([19]) *Let v^0 be given initial data for the Euler equations. For $\varepsilon > 0$, let v_ε be a Leray solution of the incompressible Navier-Stokes equations with viscosity ε and initial data v^0. Then, up to extraction of a subsequence, $v_\varepsilon \xrightarrow{*} \nu$ converges to a MVS of the incompressible Euler equations with initial data v^0 in the sense of Young measures.*

Proof It suffices to show that v_ε satisfies the assumptions of proposition 2.6. By assumption, we have $\operatorname{div}(v_\varepsilon) = 0$ for all ε. Weak stability follows from the estimate (2.5).

The weak consistency follows from the following estimate: For any $\varphi \in C^\infty(\mathbb{T}^n \times (0, T); \mathbb{R}^n)$, we have

$$\int_{\mathbb{T}^n \times (0,+\infty)} \varphi_t \cdot v_\varepsilon + \nabla \varphi : v_\varepsilon \otimes v_\varepsilon \, dx \, dt = \varepsilon \int_{\mathbb{T}^n \times (0,+\infty)} v_\varepsilon \cdot \Delta \varphi \, dx \, dt.$$

Thus, by Cauchy-Schwarz,

$$\begin{aligned} \left| \int_{\mathbb{T}^n \times (0,+\infty)} \varphi_t \cdot v_\varepsilon + \nabla \varphi : v_\varepsilon \otimes v_\varepsilon \, dx \, dt \right| &\le \varepsilon \|v_\varepsilon\|_{L^2} \|\Delta \varphi\|_{L^2} \\ &\le C(v^0, \varphi) \varepsilon, \end{aligned}$$

where $C(v^0, \varphi)$ is a constant depending on v^0 and φ, but independent of ε. This implies that

$$\lim_{\varepsilon \to 0} \int_{\mathbb{T}^n \times (0,+\infty)} \varphi_t \cdot v_\varepsilon + \nabla \varphi : v_\varepsilon \otimes v_\varepsilon \, dx \, dt = 0.$$

We conclude that v_ε satisfies weak consistency. Now we apply proposition 2.6 to conclude. □

In particular, this proves global existence of solutions to the Euler equations *in the measure-valued sense*, using the corresponding result for weak Leray solutions. However, even assuming that Leray solutions to the Navier-Stokes equations are unique – based on the a priori estimate (2.5), there is no reason to assume that the zero-viscosity limit will necessarily be an atomic

MVS. It is also unknown, whether there is a *unique* MVS obtained in the zero-viscosity limit, or whether different subsequences might converge to different MVS.

In general, measure-valued solutions have a large scope for non-uniqueness. One reason for this is the moment closure problem: Equation (2.3) is an evolution equation for the first moment of ν, only. Nothing is prescribed for the evolution of higher order moments. The lack of uniqueness becomes very clear upon rewriting (2.3) in terms of the mean $\overline{v}(x,t) = \langle \nu_{x,t}, \xi \rangle$ and the covariance matrix $\langle \nu_{x,t}, (\xi - \overline{v}) \otimes (\xi - \overline{v}) \rangle$. Namely, ν is a MVS to (1.1), provided that

$$\partial_t \overline{v} + \overline{v} \cdot \nabla \overline{v} + \nabla p = -\mathrm{div}(\langle \nu_{x,t}, (\xi - \overline{v}) \otimes (\xi - \overline{v}) \rangle), \quad \mathrm{div}(\overline{v}) = 0.$$

Since $\langle \nu_{x,t}, (\xi - \overline{v}) \otimes (\xi - \overline{v}) \rangle$ is independent of $\overline{v}$, we see that the notion of MVS can encompass not only the classical Euler equations, corresponding to a complete lack of variance

$$\langle \nu_{x,t}, (\xi - \overline{v}) \otimes (\xi - \overline{v}) \rangle = 0,$$

but also the Navier-Stokes equations, in which the fluctuations are modelled by

$$\langle \nu_{x,t}, (\xi - \overline{v}) \otimes (\xi - \overline{v}) \rangle \approx -\frac{1}{2\,\mathrm{Re}} \left(\nabla \overline{v} + \nabla \overline{v}^T - \frac{2}{3} \mathrm{div}(\overline{v}) \ \mathrm{id} \right).$$

In view of this, additional criteria are required to filter out the physically correct solution.

What these additional criteria should be, remains an open problem that we cannot answer at the present time. Energy admissibility is an obvious physical constraint. Other constraints might for example be motivated by the study of the hydrodynamic limit of more fundamental physical theories, notably the Boltzmann equation. It has also been suggested that a unique weak solution might be obtained by a principle of maximal energy dissipation. For arguments in support of this idea, we refer to [11]. In the context of scalar conservation laws, such a minimizer is unique and known to coincide with the usual Kruskov entropy solution.

2.4 Admissibility Criteria

2.4.1 Energy admissibility

To remedy this lack of uniqueness for MVS, one can try to impose additional constraints on physically relevant solutions. This procedure for filtering out unphysical weak solutions to recover uniqueness is well-known in the theory of scalar conservation laws. There, one imposes so-called entropy constraints on solutions, which reflect the fact that physical conservation laws describe the zero-viscosity limit of slightly diffusive processes. In the context of the incompressible Euler equations, one such physical constraint should clearly come from the principle of conservation of energy. In the weak formulation, we might need to relax the equality $\|v(t)\|_{L^2} = \|v_0\|_{L^2}$, valid for classical solutions to an inequality.

In accordance with [16], we give the following definition.

Definition 2.8 *A MVS $v = (\nu, \lambda, \nu^\infty)$ with initial data σ, is called* admissible, *if*

$$\int_{\mathbb{T}^n} \langle \nu_{x,t}, |\xi|^2 \rangle \, dx + \lambda_t(\mathbb{T}^n) \leq \int_{\mathbb{T}^n} \langle \sigma_x, |\xi|^2 \rangle \, dx$$

for almost all $t \in [0, +\infty)$.

2.4.2 Weak-strong uniqueness

Although it is known that admissibility by itself does not recover uniqueness of MVS [16], [14], we nevertheless have the following weak-strong uniqueness result which implies in particular that *if* a classical solution exists, this classical solution is the only admissible MVS [5].

Theorem 2.9 *Let $v \in C([0, T]; L^2(\mathbb{T}^n; \mathbb{R}^n))$ be a weak solution of* (1.1) *with*

$$\int_0^T \|\nabla v + \nabla v^T\|_{L^\infty} \, dt < \infty$$

and let $(\nu, \lambda, \nu^\infty)$ be an admissible measure-valued solution with atomic initial data $\sigma = \delta_{v(x,0)}$. Then $\nu_{x,t} = \delta_{v(x,t)}$ and $\lambda = 0$, i.e. v is the unique admissible MVS in this situation.

Proof To illustrate the basic idea, we will give a proof of the theorem under an additional smoothness assumption on ν and leave the less illuminating proof of the general case for the appendix.

Let us assume that the measure-valued solution ν is smooth both in space and time, in the sense that $(x, t) \mapsto \langle \nu_{x,t}, g \rangle$ is smooth for every $g \in C^\infty(\mathbb{R}^n)$, $|g(\xi)| \leq C(1 + |\xi|^2)$. Assume also that $\lambda = 0$.

If this is the case, then the equation $\partial_t \overline{\nu}_{x,t} + \operatorname{div}\langle \nu_{x,t}, \xi \otimes \xi \rangle = 0$ holds in the strong sense and, making use of the admissibility condition, we obtain

$$\begin{aligned}
\frac{d}{dt}\int \langle \nu_{x,t}, \frac{1}{2}|\xi - v|^2\rangle \, dx &= \frac{d}{dt}\int \langle \nu_{x,t}, \frac{1}{2}|\xi|^2\rangle \, dx + \frac{d}{dt}\int \frac{1}{2}|v|^2 \, dx \\
&\quad - \int \partial_t \left(\overline{v} \cdot v\right) \, dx \\
&\leq - \int \partial_t \left(\overline{v} \cdot v\right) \, dx \\
&= - \int \left(\partial_t \overline{v}\right) \cdot v + \overline{v} \cdot \left(\partial_t v\right) \, dx \\
&= \int \operatorname{div}\left(\langle \nu_{x,t}, \xi \otimes \xi\rangle\right) \cdot v \, dx + \int \overline{v} \cdot \left(v \cdot \nabla v\right) \, dx \\
&= - \int \langle \nu_{x,t}, \xi \otimes \xi\rangle : \nabla v \, dx + \int v \cdot \nabla v \cdot \overline{v} \, dx.
\end{aligned}$$

Due to the incompressibility constraint on both $\overline{v}$ and v, we have $\int \overline{v} \cdot \nabla v \cdot v \, dx = 0$ and $-\int v \cdot \nabla v \cdot v \, dx = 0$. Adding these two terms yields the estimate

$$\begin{aligned}
\frac{d}{dt}\int \langle \nu_{x,t}, \frac{1}{2}|\xi - v|^2\rangle \, dx &\leq - \int \Big[\langle \nu_{x,t}, \xi \otimes \xi\rangle : \nabla v - \left(v \otimes \overline{v}\right) : \nabla v \\
&\qquad - \left(\overline{v} \otimes v\right) : \nabla v + \left(v \otimes v\right) : \nabla v\Big] \, dx \\
&= - \int \langle \nu_{x,t}, (\xi - v) \otimes (\xi - v)\rangle : \nabla v \, dx \\
&= - \int \langle \nu_{x,t}, \frac{1}{2}(\xi - v) \otimes (\xi - v)\rangle : \left(\nabla v + \nabla v^T\right) \, dx \\
&\leq \|\nabla v + \nabla v^T\|_{L^\infty} \int \langle \nu_{x,t}, \frac{1}{2}|\xi - v|^2\rangle \, dx
\end{aligned}$$

By Gronwall's inequality, this implies that

$$\int \langle \nu_{x,t}, \frac{1}{2}|\xi - v|^2\rangle \, dx \leq e^{\int_0^T \|\nabla v + \nabla v^T\|_{L^\infty} \, dt} \int \langle \sigma_x, \frac{1}{2}|\xi - v_0|^2\rangle \, dx.$$

Since $\sigma_x = \delta_{v_0(x)}$, the right hand side vanishes and we must have $\nu_{x,t} = \delta_{v(x,t)}$ and the claim follows for this special case. □

Owing to the local existence and smoothness theorem 1.4 for solutions of (1.1), Theorem 2.9 guarantees in particular the existence and uniqueness of admissible MVS with smooth initial conditions at least on a finite time interval.

2.5 Non-uniqueness, non-well-posedness

The first results on measure-valued solutions, due to DiPerna and Majda, have been known since the 80's. More recent results due to DeLellis, Szekelyhidi and co-workers have shed a new light on this solution concept. A

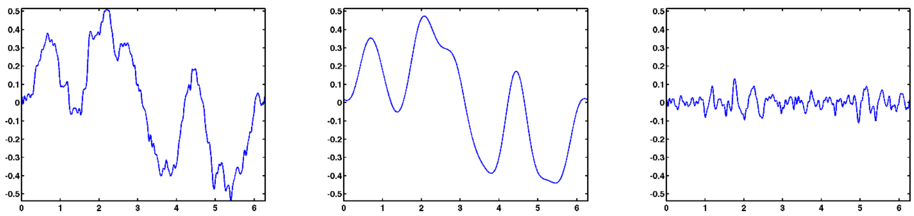

(a) Complete flow v. (b) Coarse-grained flow $\overline{v}$. (c) Fine-str. flow v'.

Figure 2.1: Illustration of the splitting of $v = \overline{v} + v'$ into a coarse-grained part $\overline{v}$ and a fine-structure part v'. The illustrated splitting is based on splitting by high/low Fourier modes.

detailed discussion of their results is definitely beyond the scope of this Master's thesis. We will contend ourselves with the (rough) underlying idea and the statements of two of their main results.

The starting point is the following observation concerning the coarse-grained portion of the flow. We split the velocity field v into two parts $v = \overline{v} + v'$, as illustrated by figure 2.1c

The component $\overline{v}$ represents the coarse-grained flow and is obtained by some averaging procedure. The averaging map $v \mapsto \overline{v}$ is hereby supposed to be linear and satisfy $\overline{\overline{v}} = \overline{v}$ (i.e. it is a projection). We obtain the evolution equation satisfied by $\overline{v}$ by averaging the evolution equation for v:

$$\partial_t \overline{v} + \operatorname{div}(\overline{v} \otimes \overline{v}) + \nabla \overline{p} = -\operatorname{div}(\overline{(v-\overline{v}) \otimes (v-\overline{v})}), \quad \operatorname{div}(\overline{v}) = 0.$$

The tensor

$$R = \overline{(v-\overline{v}) \otimes (v-\overline{v})} = \overline{v \otimes v} - \overline{v} \otimes \overline{v} = \overline{v' \otimes v'}$$

is commonly called the Reynolds stress tensor. It expresses the effect of the local fluctuations v' on the coarse-grained flow $\overline{v}$.

Remark 2.10 *This Reynolds averaging is very relevant in the engineering context. In many situations, one is not interested in the smallest scale features of the flow, but rather in the average values, so that e.g. the pressure of the fluid on a built structure can be estimated. In such situations, it might be advisable to consider the Reynolds averaged version of the Euler equations instead of the full system* (1.1)*. One can then try to find a model for the Reynolds tensor as a function of $\overline{v}$, in order to close the evolution equation. In this way, the coarse-grained flow $\overline{v}$ can be approximately computed, without having to resolve all the small-scale features. This is called large-eddy simulation (LES). For a detailed discussion of LES, see [44].*

From the perspective of MVS, we observe that every MVS corresponds to a Reynolds averaged solution, where

$$\overline{v}(x,t) = \langle \nu_{x,t}, \xi \rangle, \quad R(x,t) = \langle \nu_{x,t}, (\xi - \overline{v}(x,t)) \otimes (\xi - \overline{v}(x,t)) \rangle .$$

The idea of Szekelyhidi and DeLellis is now to start from a Reynolds averaged version of the Euler equations with a Reynolds stress R, and then to reintroduce local fluctuations step by step. Thus, given $\overline{v}$ satisfying an equation

$$\partial_t \overline{v} + \mathrm{div}(\overline{v} \otimes \overline{v}) + \nabla \overline{p} = -\mathrm{div}(\overline{R}), \quad \mathrm{div}(\overline{v}) = 0.$$

with suitable $\overline{R}$, they show how to construct v' via the introduction of local fluctuations. These fluctuations are constructed so that the resulting $v = \overline{v} + v'$ is closer to being a solution of the original Euler equations in the sense that v solves

$$\partial_t v + \mathrm{div}(v \otimes v) + \nabla p = -\mathrm{div}(R), \quad \mathrm{div}(v) = 0.$$

with $R < \overline{R}$. After an infinite number of such perturbation steps, it is shown that $R \to 0$ and that the limit (obtained by adding up all perturbations) is a weak solution of the incompressible Euler equations. Their construction involves infinitely many arbitrary choices, which ultimately lead to the non-uniqueness of the limit.

We cite two theorems. The first shows that non-uniqueness is generic in L^2.

Theorem 2.11 ([14]) *Let $n \geq 2$. There exist initial data $v_0 \in L^\infty \cap L^2$ for which there are infinitely many bounded solution of* (1.1) *which are strongly L^2-continuous and satisfy the admissibility constraint. Furthermore, the set of such wild initial data is dense in the space of L^2 solenoidal vector fields.*

The second theorem shows that weak solutions and measure-valued solutions satisfying the admissibility constraint are, in a very precise sense, equally badly behaved.

Theorem 2.12 ([48]) *Let $(\nu, \lambda, \nu^\infty)$ be a measure-valued solution of the incompressible Euler equations. There exists a sequence of weak solutions v_k with bounded energy converging to $(\nu, \lambda, \nu^\infty)$ in the sense of Young measures.*

In particular, we can interpret this result as saying that a solution concept based on Young measures is just as good or bad as the more commonly accepted weak solution concept, at least from a mathematical point of view.

2.6 Discussion

In this chapter, we have reviewed the concept of measure-valued solutions for the incompressible Euler equations which was introduced by DiPerna-Majda [19]. We have given a proof, which first appeared in [19], that Leray solutions to the incompressible Navier-Stokes equations converge to measure-valued solutions of the Euler equations in the zero viscosity limit. In particular, this provides a global existence result for the incompressible Euler equations in the measure-valued sense. We have also discussed, how the known a priori estimates for the Navier-Stokes equations could indicate that measure-valued solutions are a natural concept in the context of turbulence. Uniqueness questions for measure-valued solutions have also been considered. In particular, we provided a proof that energy admissibility implies weak-strong uniqueness. This result is due to Brenier-Szekelyhidi-DeLellis [5].

We finished this chapter with a very brief discussion of recent non-uniqueness results due to Szekelyhidi, De Lellis and coworkers, as well as their connection to measure-valued solutions.

Chapter 3

Spectral Method

3.1 A Numerical Scheme

In this section, we are going to describe a semi-discrete spatial discretisation scheme based on spectral methods and we prove convergence to an energy admissible measure-valued solution of the incompressible Euler equations. We will restrict our attention to flows with periodic boundary conditions throughout.

3.1.1 The Euler equations in Fourier space

Let (v, p) be a solution of the Euler equations (where we formally write $\operatorname{div}(v \otimes v) = v \cdot \nabla v$, since $\operatorname{div}(v) = 0$):

$$\begin{cases} \partial_t v + v \cdot \nabla v + \nabla p = 0, \\ \operatorname{div}(v) = 0. \end{cases} \tag{3.1}$$

defined on $\mathbb{T}^n \times [0, +\infty)$ (i.e. n space dimensions, with periodic boundary conditions).

Consider the spatial Fourier expansion $v(x,t) = \sum_k \widehat{v}_k(t) e^{ikx}$ of v, with coefficients given by

$$\widehat{v}_k(t) = \frac{1}{(2\pi)^n} \int_{\mathbb{T}^n} v(x,t)\, e^{-ikx}\, dx.$$

If v is a solution of (3.1), then the above expression yields

$$\begin{aligned}
\frac{d}{dt}\widehat{v}_k &= \frac{1}{(2\pi)^n}\int_{\mathbb{T}^n} \partial_t v\, e^{-ikx}\,dx \\
&= -\frac{1}{(2\pi)^n}\int_{\mathbb{T}^n} (v\cdot\nabla v + \nabla p)\, e^{-ikx}\,dx \\
&= -\frac{1}{(2\pi)^n}\int_{\mathbb{T}^n} \sum_{\ell,m}(\widehat{v}_\ell \cdot im)\widehat{v}_m e^{i(\ell+m-k)x} \\
&\quad -\frac{1}{(2\pi)^n}\int_{\mathbb{T}^n} \sum_{\ell} \widehat{p}_\ell i\ell e^{i(\ell-k)x}\,dx \\
&= (-i)\sum_{\substack{\ell,m\\ \ell+m-k=0}} (\widehat{v}_\ell\cdot m)\widehat{v}_m - i\widehat{p}_k k.
\end{aligned}$$

We note that $\operatorname{div}(v) = i\sum_k(\widehat{v}_k\cdot k)e^{ikx} = 0$ is equivalent to $\widehat{v}_k \perp k$ for all k. Using $m = k-\ell$ and $\widehat{v}_\ell \perp \ell$ for all terms in the summation, we can rewrite the last equation in the form

$$\frac{d}{dt}\widehat{v}_k = (-i)\sum_{\substack{\ell,m\\ \ell+m-k=0}} (\widehat{v}_\ell\cdot k)\widehat{v}_m - i\widehat{p}_k k. \tag{3.2}$$

This is the Fourier space version of the Euler equations (1.1). It becomes evident that the pressure term $-i\widehat{p}_k k$, which is collinear to k, serves as the orthogonal L^2 projection of the non-linear term

$$(-i)\sum_{\substack{\ell,m\\ \ell+m-k=0}} (\widehat{v}_\ell\cdot k)\widehat{v}_m$$

to the orthogonal complement of k, thus keeping v divergence-free.

For the coefficient $\widehat{v}_k$ with $k=0$, equation (3.2) yields $\frac{d}{dt}\widehat{v}_0 = 0$. This corresponds to *conservation of momentum*. Using Galilean invariance for the incompressible Euler equations, we can without loss of generality assume that $\widehat{v}_0 = \frac{1}{(2\pi)^n}\int_{\mathbb{T}^n} v\,dx = 0$, in the following.

3.1.2 Semi-discretization in Space

To obtain a discretized approximation to system (3.2), we restrict our attention to only the Fourier modes below some threshold N. We thus consider divergence-free fields of the form $v(x,t) = \sum_{|k|\le N}\widehat{v}_k(t)\,e^{ikx}$, and we have to project the non-linear term to this space. We denote the corresponding projection operator by $\mathbf{P}_N$. The projection operator is a combination of both Fourier truncation and projection to the space of divergence-free fields. More explicitely, $\mathbf{P}_N$ is given by

$$\mathbf{P}_N \left(\sum_{k \in \mathbb{Z}^2} \widehat{w}_k e^{ikx} \right) = \sum_{|k| \leq N} \left(\widehat{w}_k - \frac{\widehat{w}_k \cdot k}{|k|^2} k \right) e^{ikx},$$

yielding a divergence-free vector field with Fourier modes $|k| \leq N$. We also add a small amount of numerical viscosity to ensure the stability of the resulting scheme.

This idea results in the following scheme: For given initial data $v_0(x)$, we obtain an approximate solution $v_N(x,t) \approx v(x,t)$ by solving the finite-dimensional problem

$$\begin{cases} \partial_t v_N + \mathbf{P}_N \left(v_N \cdot \nabla v_N \right) = \nu \Delta v_N, \\ \quad v_N(x,0) = \mathbf{P}_N v_0(x). \end{cases} \tag{3.3}$$

In this scheme, the small number $\nu > 0$ is an artificial numerical viscosity that depends on N and $\nu \to 0$ as $N \to \infty$.

A refined version of this basic scheme was introduced by Tadmor [50]. In that version, we choose a small number $\varepsilon > 0$ and an integer $m \leq N$. The integer m serves as a threshold between small and large Fourier modes. We apply a viscous regularization only to the large Fourier modes. With a judicious choice of $\varepsilon = \varepsilon(N)$, $m = m(N)$, the resulting method can be shown to be spectrally accurate [51], [2]. We obtain the corresponding approximate system

$$\begin{cases} \partial_t v_N + \mathbf{P}_N \left(v_N \cdot \nabla v_N \right) = \varepsilon \operatorname{div} \left(\mathbf{Q}_N \nabla v_N \right), \\ \quad v_N(x,0) = \mathbf{P}_N v_0(x), \end{cases} \tag{3.4}$$

where $\mathbf{Q}_N = \mathbf{I} - \mathbf{P}_m$, denotes the projection onto the higher modes. System (3.4) includes (3.16) for the special choice $m = 0$, $\varepsilon = \nu$.

3.2 Convergence to MVS

Multiplying equation (3.4) by v_N and integrating over space, we obtain after an integration by parts, and using also the fact that all boundary terms vanish due to the periodic boundary conditions,

$$
\begin{aligned}
\frac{d}{dt}\frac{1}{2}\int_{\mathbb{T}^2}|v_N|^2\,dx &= \int_{\mathbb{T}^2} -v_N\cdot\mathbf{P}_N\left(v_N\cdot\nabla v_N\right) + v_N\cdot\varepsilon\,\mathrm{div}\left((\mathbf{I}-\mathbf{P}_m)\nabla v_N\right)\,dx \\
&= \int_{\mathbb{T}^2} -\mathbf{P}_N v_N\cdot(v_N\cdot\nabla v_N) - \varepsilon\nabla v_N : (\mathbf{I}-\mathbf{P}_m)\nabla v_N\,dx \\
&= \int_{\mathbb{T}^2} -v_N\cdot(v_N\cdot\nabla v_N) - \varepsilon(\mathbf{I}-\mathbf{P}_m)\nabla v_N : (\mathbf{I}-\mathbf{P}_m)\nabla v_N\,dx \\
&= \int_{\mathbb{T}^2} -\mathrm{div}\left(\frac{1}{2}|v_N|^2 v_N\right) - \varepsilon|(\mathbf{I}-\mathbf{P}_m)\nabla v_N|^2\,dx \\
&= -\varepsilon\int_{\mathbb{T}^n}|(\mathbf{I}-\mathbf{P}_m)\nabla v_N|^2\,dx,
\end{aligned}
$$

i.e. we have

$$
\frac{d}{dt}\int_{\mathbb{T}^n}\frac{1}{2}|v_N|^2\,dx + \varepsilon\int_{\mathbb{T}^n}|(\mathbf{I}-\mathbf{P}_m)\nabla v_N|^2\,dx = 0. \tag{3.5}
$$

Integrating in time from 0 to t, we obtain

Lemma 3.1 *If v_N is the solution of the semi-discrete system* (3.4)*, then*

$$
\frac{1}{2}\|v_N\|_{L^2}^2 + \varepsilon\int_0^t \|(\mathbf{I}-\mathbf{P}_m)\nabla v_N\|_{L^2}^2\,dt = \frac{1}{2}\|\mathbf{P}_N v_0\|_{L^2}^2 \le \frac{1}{2}\|v_0\|_{L^2}^2. \tag{3.6}
$$

In particular, we have $\|v_N\|_{L^2} \le \|v_0\|_{L^2}$, independently of N, m, ε.

The simple estimate of Lemma 3.1 is already the main step towards proving convergence of our semi-discretized scheme to a MVS. To finish our proof, we use the result of Proposition 2.6 about convergence to MVS due to DiPerna, Majda [19, Proposition 5.1].

Let us check that the conditions of Theorem 2.3 are satisfied for the sequence generated by the spectral scheme. We have already seen in Lemma 3.1 that

$$
\int_0^T\int_{\mathbb{T}^n}|v_N(x,t)|^2\,dx\,dt \le T\|v_0\|_{L^2}^2.
$$

Thus, condition (A), equation (2.6), is satisfied for all N. It remains to show that (B), equation (2.7), is also satisfied. Rewriting (3.4) and using that $\mathrm{div}(v_N) = 0$, we have

$$
\partial_t v_N + \mathrm{div}\left(v_N\otimes v_N\right) + \nabla p_N = \mathrm{div}\left((\mathbf{I}-\mathbf{P}_N)(v_N\otimes v_N)\right) + \varepsilon\,\mathrm{div}\left((\mathbf{I}-\mathbf{P}_m)\nabla v_N\right).
$$

Hence, for any divergence-free test function $\varphi \in C_c^\infty(\mathbb{T}^n \times (0,T);\mathbb{R}^n)$ we obtain after an integration by parts

$$\begin{aligned}
\int_{\mathbb{T}^n\times(0,T)} \partial_t\varphi \cdot v_N + \nabla\varphi : v_N \otimes v_N \, dx\, dt &= -\int_{\mathbb{T}^n\times(0,T)} \varphi \cdot \left(\partial_t v_N + \operatorname{div}(v_N \otimes v_N)\right) \, dx\, dt \\
&= -\int_{\mathbb{T}^n\times(0,T)} \varphi \cdot \operatorname{div}\left((\mathbf{I}-\mathbf{P}_N)\,(v_N \otimes v_N)\right) \, dx\, dt \\
&\quad - \varepsilon \int_{\mathbb{T}^n\times(0,T)} \varphi \cdot \operatorname{div}\left((\mathbf{I}-\mathbf{P}_m)\nabla v_N\right) \, dx\, dt \\
&= (A) + (B).
\end{aligned}$$

Now

$$\begin{aligned}
(A) &= -\int_{\mathbb{T}^n\times(0,T)} \varphi \cdot \operatorname{div}\left((\mathbf{I}-\mathbf{P}_N)\,(v_N \otimes v_N)\right) \, dx\, dt \\
&= \int_{\mathbb{T}^n\times(0,T)} \nabla\varphi : \left((\mathbf{I}-\mathbf{P}_N)\,(v_N \otimes v_N)\right) \, dx\, dt \\
&= \int_{\mathbb{T}^n\times(0,T)} \nabla(\mathbf{I}-\mathbf{P}_N)\varphi : (v_N \otimes v_N) \, dx\, dt
\end{aligned}$$

We notice that for a constant C_n depending on the space dimension n only:

$$\begin{aligned}
|v_N|_{L^\infty} &\le \sum_{|k|\le N} |\widehat{(v_N)}_k| \le C_n N^{n/2}\Big(\sum_{|k|\le N} |\widehat{(v_N)}_k|^2\Big)^{1/2} \\
&= C_n N^{n/2}\|v_N\|_{L^2} \le C_n N^{n/2}\|v_0\|_{L^2}.
\end{aligned}$$

Thus we can continue to estimate the term (A) as

$$\begin{aligned}
|(A)| &\le \int_0^T \|v_N\|_{L_x^\infty}\|v_N\|_{L_x^2}\|\nabla(\mathbf{I}-\mathbf{P}_N)\varphi\|_{L_x^2}\, dt \\
&\le C_n N^{n/2}\|v_0\|_{L^2}^2 \int_0^T \|\nabla(\mathbf{I}-\mathbf{P}_N)\varphi\|_{L_x^2}\, dt \\
&\le C_n \|v_0\|_{L^2}^2 \int_0^T \|(\mathbf{I}-\mathbf{P}_N)\varphi\|_{H_x^{n/2+1}}\, dt
\end{aligned}$$

Since φ is smooth, it follows that $\int_0^T \|(\mathbf{I}-\mathbf{P}_N)\varphi\|_{H_x^{n/2+1}}\, dt \to 0$ as $N \to \infty$. Hence, we obtain that $(A) \to 0$.

The term (B) is handled similarly. We have

$$\begin{aligned}(B) &= -\varepsilon \int_{\mathbb{T}^n\times(0,T)} \varphi \cdot \operatorname{div}\left((\mathbf{I}-\mathbf{P}_m)\nabla \mathbf{v}_N\right)\,dx\,dt \\ &= \varepsilon \int_{\mathbb{T}^n\times(0,T)} \operatorname{div}\left((\mathbf{I}-\mathbf{P}_m)\nabla \varphi\right)\cdot \mathbf{v}_N\,dx\,dt \\ &= \varepsilon \int_{\mathbb{T}^n\times(0,T)} \left((\mathbf{I}-\mathbf{P}_m)\Delta \varphi\right)\cdot \mathbf{v}_N\,dx\,dt.\end{aligned}$$

This yields

$$|(B)| \le \varepsilon \int_0^T \|(\mathbf{I}-\mathbf{P}_m)\varphi\|_{H^2_x}\|v_N\|_{L^2}\,dt \le \varepsilon\|v_0\|_{L^2}\int_0^T \|(\mathbf{I}-\mathbf{P}_m)\varphi\|_{H^2_x}\,dt,$$

and again we see that the right hand side again converges to 0, if either $\varepsilon \to 0$ or $m \to \infty$.

We conclude that

Theorem 3.2 *Let $v_0 \in L^2(\mathbb{T}^n;\mathbb{R}^n)$ be a given divergence-free vector field. Let v_N, $N \in \mathbb{N}$, be obtained by solving* (3.4). *Let $\varepsilon = \varepsilon(N) \to 0$, $m = m(N) \to \infty$. Then, up to extraction of a subsequence, v_N converges in the sense of Young measures to an admissible measure-valued solution $v = (\mu, \nu, \nu^\infty)$ of the Euler equations with initial data v_0, in the sense of Definitions 2.5, 2.8.*

Proof By our discussion above, the assumptions of Theorem 2.3 are fulfilled. Furthermore, we observe that, by construction, $v_N(x,0) = \mathbf{P}_N v_0(x) \to v_0(x)$ in L^2. Admissibility follows from the fact that $\|v_N\|_{L^2} \le \|v_0\|_{L^2}$ for all N. The result follows. $\square$

Remark 3.3 *The arguments used in the derivation of the estimates for Theorem 3.2 also yield uniform Lipschitz continuity $v_N \in \mathrm{Lip}([0,T]; H^{-n/2-1}(\mathbb{T}^n;\mathbb{R}^n))$ for $n \ge 2$. Indeed, we have*

$$\partial_t v_N = -\mathbf{P}_N \operatorname{div}(v_N \otimes v_N) + \varepsilon \operatorname{div}((\mathbf{I}-\mathbf{P}_m)\nabla v_N). \tag{3.7}$$

The $H^{-n/2-1}$-bound for the first term is essentially obtained in the estimate for (A), while the estimate for (B) implies an upper bound on the H^{-2}-norm. From the inclusion $H^{-2} \subset H^{-n/2-1}$, we obtain an upper bound for the right hand side of (3.7)*, and upon integration in time, the claimed Lipschitz continuity of v_N in $H^{-n/2-1}$ with respect to time. This shows that the spectral scheme* (3.4) *produces an approximate-solution sequence in the sense of DiPerna, Majda [20].*

We should point out that there is some evidence to indicate that the measure-valued solution obtained from Theorem 3.2 could depend on the particular choice of $\varepsilon(N) \to 0, m(N) \to \infty$. Frisch et al. [30] have observed resonance phenomena in the solutions of the purely Fourier truncated Euler system (3.4) (corresponding to the choice $\varepsilon = 0$), which occur after some finite time. An analogous effect is also observed to occur when solving the purely Fourier truncated Burgers equation after shock formation. In the Burgers case, these spurious oscillations are due to the fact that the entropy solution exhibits anomalous energy dissipation in the shocks, which is not reflected in the energy-conservative truncated Fourier approximation. Thus, the purely Fourier truncated can not converge to the entropy solution in the limit. For an analytical discussion of the Burgers case and the importance of a sufficient amount of energy dissipation in the numerical approximation using the spectrally vanishing viscosity method, see also [2].

The fact that this same effect occurs for both systems is intriguing. In the Burgers case it is due to the formation of shocks, whereas in the case of the incompressible Euler equations it occurs because of the turbulent motion of the fluid and the corresponding formation of small scale features. Both effects are also associated with anomalous energy dissipation [42]. This might be seen as an indication that there should indeed a close analogy between the two phenomena of shock formation and the generation of small scale features in turbulence.

Using the weak-strong uniqueness result obtained in Theorem 2.9, we obtain the following convergence result for the spectral scheme.

Corollary 3.4 *Let v be a classical solution of the Euler equations on $[0, T] \times \mathbb{T}^n$ with initial data v_0, such that $\int_0^T \|\nabla v + \nabla v^T\|_{L^\infty}\, dt < \infty$. Then any approximating sequence v_N solving* (3.4)*, where $\varepsilon = \varepsilon(N) \to 0$, $m = m(N) \to \infty$, converges to v strongly in L^2.*

Proof By Theorem 3.2, for any subsequence of $\{v_N\}$ we can extract a further subsequence converging to an admissible MVS of (1.1). By the weak-strong uniqueness result of Theorem 2.9, the associated Young measure is atomic and concentrated on v. It follows that each subsequence contains a further subsequence converging strongly in L^2 to v. This implies that also $v_N \to v$ strongly in L^2. $\square$

Remark 3.5 *Combining Corollary 3.4 with classical existence, uniqueness and regularity results for the Euler equation in the two-dimensional case yields the convergence of the spectral scheme in L^2 for Lipschitz continuous initial data.*

We can also give a proof of global existence of MVS to the incompressible Euler equations that is independent of the proof that follows from combining the global existence result for Leray solutions of the Navier-Stokes equations and the convergence result for the zero-viscosity limit, theorem 2.7.

Corollary 3.6 *Let $v_0 \in L^2(\mathbb{T}^n; \mathbb{R}^n)$ be divergence-free initial data for the incompressible Euler equations. There exists a global measure-valued solution $(\nu, \lambda, \nu^\infty)$ with initial data given by $\delta_{v_0(x)}$.*

Proof For each $N \in \mathbb{N}$, let $v_N(x,t)$ be the approximate solution obtained from the spectral scheme (3.4). By theorem 3.2, the sequence v_N converges up to extraction of a subsequence to a MVS $(\nu, \lambda, \nu^\infty)$ with initial data given by v_0. In particular, a MVS $(\nu, \lambda, \nu^\infty)$ with initial data given by v_0 exists. $\square$

3.2.1 An ensemble based algorithm to compute admissible measure valued solutions

Next, we will combine the spectral (viscosity) method with the ensemble based algorithm of the paper [22] in order to compute admissible measure valued solutions of the incompressible Euler equations. First, we assume that the initial velocity field is an arbitrary Young measure i.e, $v(x,0) = \sigma_x$, which satisfies the divergence constraint in a weak sense. Then, an algorithm for computing measure valued solutions is specified with the following steps:

Algorithm 3.7

Step 1: *Let $v_0 : \Omega \mapsto L^2(\mathbb{T}^n; \mathbb{R}^n)$ be a random field on a probability space $(\Omega, \mathcal{F}, P)$ such that the initial Young measure σ is the law of the random field v_0. The existence of such a random field can be shown analogous to [22, proposition A.3].*

Step 2: *We evolve the initial random field v_0 by applying the spectral (viscosity) scheme* (3.4) *for every $\omega \in \Omega$ to obtain an approximation $v_N(\omega)$, to the solution random field $v(\omega)$, corresponding to the initial random field $v_0(\omega)$.*

Step 3: *Define the approximate measure-valued solution ν^N as the law of v_N.*

Then from proposition A. 3. 1 of the paper [22], ν^N is a Young measure. Next, we show that these approximate Young measures will converge in the appropriate sense to an admissible measure valued solution of the incompressible Euler equations (1.1).

Theorem 3.8 *Let the (kinetic) energy of the initial Young measure σ be finite i.e,*

$$\int_{\mathbb{T}^n} \langle \sigma_x, |\xi|^2 \rangle dx \leq C < \infty,$$

then the approximate Young measure $\nu^N_{x,t}$, generated by the algorithm 3.7 converges (upto a subsequence) to an (admissible) measure valued solution $(\nu, \lambda, \nu^\infty)$ of the incompressible Euler equations (1.1).

Proof Given the initial bound on the energy and the fact that the energy estimate (3.6) holds for every realization ω, it is straightforward to see that for all $T \in (0, +\infty)$, we obtain

$$\int_D |v_N(\omega)|^2 dxdt \leq C(D), \quad \forall \omega \in \Omega.$$

Here we have set $D = \mathbb{T}^n \times (0, T)$. Given the fact that ν^N is the law of the random field v_N, the above estimate translates to

$$\int_D \langle \nu^N_{x,t}, |\xi|^2 \rangle dxdt \leq C(D).$$

Therefore, by a straightforward modification of the Young measure theorem of [1] (see recent paper [23]), we obtain as $N \to \infty$, that (upto a subsequence), ν^N converges (narrowly) to a (generalized) Young measure $(\nu, \lambda, \nu^\infty)$, such that

$$\int_D \langle \nu^N, g \rangle \varphi \, dx \, dt \to \int_D \langle \nu_{x,t}, g \rangle \varphi \, dx \, dt + \int_D \langle \nu^\infty_{x,t}, g^\infty \rangle \varphi \, \lambda(\, dx \, dt),$$

for all $\varphi \in C_0^\infty(D)$.

In particular, we can apply this to the particular choice $g(\xi) = \xi$ with $g^\infty \equiv 0$ and test function $\partial_t \varphi$ (for each component) to obtain,

$$\int_D \partial_t \varphi \cdot \langle \nu^N_{x,t}, \xi \rangle \, dx \, dt \to \int_D \partial_t \varphi \cdot \langle \nu_{x,t}, \xi \rangle \, dx \, dt.$$

Similarly, with $g(\xi) = \xi \otimes \xi$, $g^\infty(\theta) = \theta \otimes \theta$ and test function $\nabla \varphi$, we obtain

$$\int_D \nabla \varphi : \langle \nu^N_{x,t}, \xi \otimes \xi \rangle \, dx \, dt \to \int_D \nabla \varphi : \langle \nu_{x,t}, \xi \otimes \xi \rangle \, dx \, dt + \int_D \nabla \varphi : \langle \nu^\infty_{x,t}, \theta \otimes \theta \rangle \, \lambda(\, dx \, dt).$$

Furthermore, the consistency property (2.7) also holds for every $\omega \in \Omega$, therefore,

$$\lim_{N \to \infty} \int_D \partial_t \varphi \cdot v_N(\omega) + \nabla \varphi : v_N(\omega) \otimes v_N(\omega) \, dx \, dt = 0, \quad \forall \omega \in \Omega. \tag{3.8}$$

In terms of the Young measure ν^N, the above consistency is expressed as,

$$\lim_{N \to \infty} \int_D \partial_t \varphi \cdot \langle \nu^N_{x,t}, \xi \rangle + \nabla \varphi : \langle \nu^N_{x,t}, \xi \otimes \xi \rangle \, dx \, dt = 0. \tag{3.9}$$

Thus, we obtain,

$$\begin{aligned} &\int_D \partial_t \varphi \cdot \langle \nu_{x,t}, g \rangle \, dx \, dt + \int_D \nabla \varphi : \langle \nu_{x,t}, \xi \otimes \xi \rangle \, dx \, dt + \int_D \nabla \varphi : \langle \nu^\infty_{x,t}, \theta \otimes \theta \rangle \, \lambda(\, dx \, dt) \\ &\quad = \lim_{N \to \infty} \int_D \partial_t \varphi \cdot \langle \nu^N_{x,t}, \xi \rangle + \nabla \varphi : \langle \nu^N_{x,t}, \xi \otimes \xi \rangle \, dx \, dt = 0. \end{aligned}$$

Similarly, we obtain for any $\psi \in C_0^\infty(D)$ that

$$\int_D \nabla \psi \cdot \langle \nu_{x,t}, \xi \rangle \, dx \, dt = \lim_{N \to \infty} \int_D \nabla \psi \cdot \langle \nu^N_{x,t}, \xi \rangle \, dx \, dt = 0,$$

since $\operatorname{div}(v_N(\omega)) = 0$, $\forall \omega \in \Omega$. Thus, we prove that ν^N is a measure valued solution of the incompressible Euler equations (1.1). Admissibility follows as a straightforward consequence of the energy estimate (3.6). $\square$

3.2.2 Approximate measure valued solutions for atomic initial data

The case of atomic initial data i.e $\sigma = \delta_{v_0}$ with a divergence free velocity field $v_0 \in L^2$ is particularly interesting for applications as it represents the zero uncertainty (in the initial conditions) limit. To compute the measure valued solutions associated with atomic initial data, we use the following algorithm,

Algorithm 3.9 *Let $(\Omega, \mathcal{F}, P)$ be a probability space and let $X : \Omega \to L^2(\mathbb{T}^n; \mathbb{R}^n)$ be a random field satisfying $\|X\|_{L^2(\mathbb{T}^n)} \leq 1$ P-almost surely.*

Step 1: *Fix a small number $\varepsilon > 0$. Perturb v_0 by defining $v_0^\varepsilon(\omega, x) := v_0(x) + \varepsilon X(\omega, x)$. Let σ^ε be the law of v_0^ε.*

Step 2: *For each $\omega \in \Omega$ and $\varepsilon > 0$, let $v_N^\varepsilon(\omega)$ be the solution computed by the spectral method* (3.4)*, corresponding to the initial data v_0^ε.*

Step 3: *Let $\nu^{N,\varepsilon}$ be the law of v_N^ε.*

Theorem 3.10 *Let $\{\nu^{N,\varepsilon}\}$ be the family of approximate measure valued solutions constructed by algorithm 3.9. Then there exists a subsequence $(N_n, \varepsilon_n) \to 0$ such that*

$$\nu^{N_n, \varepsilon_n} \to (\nu, \lambda, \nu^\infty),$$

with $(\nu, \lambda, \nu^\infty)$ being an admissible measure valued solution of the incompressible Euler equations (1.1) *with atomic initial data v_0.*

The proof of this theorem is a straightforward extension of the proof of theorem 3.2 and we omit it here.

Remark 3.11 *There is an analogy between the zero viscosity limit and the zero uncertainty limit considered above. It is commonly argued that in real-world systems, viscosity effects are unavoidable. In order to obtain the correct solution in e.g. the context of conservation laws, a small amount of viscosity should therefore be added to the equations. In situations where viscosity effects are assumed to play a secondary role, the zero viscosity viscosity limit must then be considered and will lead to the correct physical solution.*

Along the same lines it can be argued that in real-world systems, uncertainties in the initial data, arising e.g. from uncertainties in measurements, are unavoidable. To account for this fact a small amount of uncertainty should be introduced. If the uncertainties are assumed to be negligible, the correct solution should correspondingly be obtained in the zero uncertainty limit as described in algorithm 3.9 and theorem 3.10.

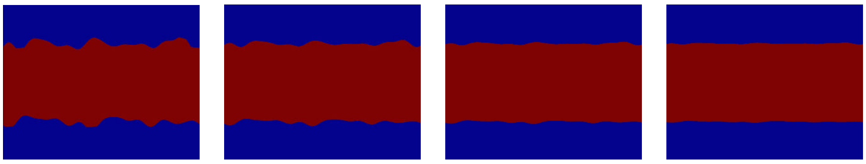

Figure 3.1: Illustration of the 'zero uncertainty limit' in the initial data.

3.2.3 Computation of space-time averages

The algorithms 3.7 and 3.9 compute space-time averages with respect to the measure ν^N,

$$\int_{\mathbb{T}^n}\int_{\mathbb{R}_+} \varphi(x,t)\langle \nu^N_{x,t}, g\rangle dxdt, \tag{3.10}$$

for smooth test functions φ and for admissible functions g, i.e. $g \in C^\infty(\mathbb{R}^n)$ for which $g^\infty(\theta) = \lim_{r\to\infty} g(r\theta)/r^2$ exists and $g^\infty \in C(\mathbb{S}^{n-1})$ is continuous.

Following [22], we will compute space-time averages (3.10) by using a Monte-Carlo sampling procedure To this end, we utilize the equivalent representation of the measure ν^N as the law of the *random field* v_N:

$$\langle \nu^N_{x,t}, g\rangle := \int\limits_{\mathbb{R}^n} g(\xi)\, d\nu^N_{(x,t)}(\xi) = \int_\Omega g(v_N(\omega; x,t))\, dP(\omega). \tag{3.11}$$

We will approximate this integral by a Monte Carlo sampling procedure:

Algorithm 3.12 *Let $N > 0$ and let M be a positive integer. Let σ be the initial Young measure and let v_0 be a (spatially divergence free) random field $v_0 : \Omega \times \mathbb{T}^n \to \mathbb{R}^n$ such that σ is the law of v_0.*

Step 1: *Draw M independent and identically distributed random fields v_0^k for $k = 1, \dots, M$.*

Step 2: *For each k and* for a fixed *$\omega \in \Omega$, use the spectral method* (3.4) *to numerically approximate the incompressible Euler equations with initial data $v_0^k(\omega)$. Denote $v_{N,k}(\omega)$ as the computed solution.*

Step 3: *Define the approximate measure-valued solution*

$$\nu^{N,M} := \frac{1}{M}\sum_{k=1}^{M} \delta_{v_{N,k}(\omega)}.$$

For every admissible test function g, the space-time average (3.10) is then approximated by

$$\int_{\mathbb{T}^n}\int_{\mathbb{R}_+} \varphi(x,t)\langle \nu^N_{x,t}, g\rangle dxdt \approx \frac{1}{M}\sum_{k=1}^{M}\int_{\mathbb{R}_+}\int_{\mathbb{T}^n} \varphi(x,t) g\big(v_{N,k}(\omega; x,t)\big)\, dxdt. \tag{3.12}$$

The convergence of the approximate Young measures $\nu^{N,M}$ to a measure valued solution of the incompressible Euler equations (1.1) as $N, M \to \infty$ follows as a consequence of the law of large numbers. The proof is very similar to that of theorem 4.9 of [22].

3.3 Simplifications in 2D

Let us now specialize our discussion to the case of fluid flow in two dimensions. We recall that the divergence-free condition $\operatorname{div}(v) = 0$ is equivalent to the requirement that $\widehat{v}_k \perp k$ for all Fourier coefficients $\widehat{v}_k$ of v. In two spatial dimensions, this implies that we can write $\widehat{v}_k = a_k \mathbf{J} k$ for scalar coefficients a_k and where $\mathbf{J}$ denotes the rotation matrix

$$\mathbf{J} = \begin{pmatrix} 0 & -1 \\ 1 & 0 \end{pmatrix}.$$

The corresponding evolution equations for the coefficients a_k are found by taking the inner product of $\frac{d}{dt}\widehat{v}(k)$ with $\mathbf{J}\,k/k^2$. This yields the following equivalent form of (3.2):

$$\frac{da_k}{dt} = \frac{(-i)}{k^2} \sum_{\substack{\ell,m \\ \ell+m-k=0}} (\mathbf{J}k \cdot \ell)(k \cdot m)\, a_\ell a_m. \tag{3.13}$$

It is now natural to define a (real-valued) function ψ by

$$\psi(x,t) = (-i) \sum_k a_k(t) e^{ikx}.$$

This function is usually referred to as the stream function.

If $\nabla^\top$ denotes the operator $(-\partial_{x_2}, \partial_{x_1})^T = \mathbf{J}\nabla$ acting on functions, then v is given by $v = \nabla^\top \psi$. Thus, ψ determines v uniquely. On the other hand, given v, we can recover ψ by solving $\Delta\psi = \operatorname{curl} v$. This equation has a unique solution for sufficiently smooth v if we require in addition that $\int \psi\, dx = 0$.

We can now rewrite the equations of fluid motion in terms of ψ. If v solves (1.1), then $\psi = \Delta^{-1} \operatorname{curl} v$ solves

$$\partial_t \psi + \Delta^{-1} \operatorname{curl}(v \cdot \nabla v) + \Delta^{-1} \operatorname{curl} \nabla p = 0.$$

Clearly, $\operatorname{curl} \nabla = 0$, and the pressure term drops out. Let us consider the nonlinear term in more detail. A short (formal) calculation reveals that

$$\operatorname{curl}(v \cdot \nabla v) = \nabla^\top \psi \cdot \nabla(\Delta\psi).$$

We thus obtain

$$\partial_t \psi + \Delta^{-1} \nabla^\top \psi \cdot \nabla(\Delta\psi) = 0.$$

or the equivalent formulation

$$\partial_t(\Delta\psi) + \nabla^\top\psi \cdot \nabla(\Delta\psi) = 0.$$

This last equation is actually an equation for the vorticity $\eta = \operatorname{curl} v = \Delta\psi$. According to these calculations, we once again arrive at the vorticity formulation of the Euler equations (1.16), which we reproduce here for convenience.

$$\begin{cases} \partial_t\eta + v \cdot \nabla\eta = 0, \\ \operatorname{curl} v = \eta, \operatorname{div} v = 0. \end{cases} \tag{3.14}$$

Corresponding to (3.4), we also obtain the semi-discretized version for to the vorticity formulation.

$$\begin{cases} \quad \partial_t\eta_N + \mathbf{P}_N\left(v_N \cdot \nabla\eta_N\right) = \varepsilon \operatorname{div}\left((\mathbf{I} - \mathbf{P}_m)\nabla\eta_N\right), \\ \eta_N(x,0) = \operatorname{curl} \mathbf{P}_N v_0(x). \end{cases} \tag{3.15}$$

The system of equations (3.14) is formally equivalent to (1.1).[1] The important observation for us is the following: Even though the two full systems of equations might not be strictly speaking equivalent, their Fourier truncated versions *are* equivalent.

Lemma 3.13 *The truncated systems with spectrally small vanishing viscosity* (3.4) *for v_N and* (3.15) *for η_N are equivalent.*

Proof Let v_N and η_N be solutions of (3.4) and (3.15), respectively. Since v_N is smooth and because the projection operators $\mathbf{P}_N$ commute with differentiation, we can take the curl of (3.4) to obtain

$$\begin{cases} \partial_t \operatorname{curl} v_N + \mathbf{P}_N\left(\operatorname{curl}(v_N \cdot \nabla v_N)\right) = \varepsilon \operatorname{div}\left((\mathbf{I} - \mathbf{P}_m)\nabla \operatorname{curl} v_N\right), \\ \qquad \operatorname{curl} v_N(x,0) = \operatorname{curl} \mathbf{P}_N v_0(x). \end{cases} \tag{3.16}$$

We note that $\operatorname{curl}(v_N \cdot \nabla v_N) = v_N \cdot \nabla \operatorname{curl} v_N$. Hence, both η_N and $\operatorname{curl} v_N$ satisfy system (3.15). By classical uniqueness results for ODEs, we must have $\eta_N = \operatorname{curl} v_N$ and the two systems are seen to be equivalent. □

In particular, by Lemma 3.13 we may use the apperently simpler system (3.15) for our numerical computations, rather than the larger system (3.4). This reduces the computational cost and was furthermore observed to lead to better stability properties of the resulting fully discretized numerical scheme. In particular, in the vorticity formulation there is no need to project to the space of divergence-free fields after each time step, which would involve the solution of a Poisson equation.

[1] The two equations are strictly equivalent *only if the flow is sufficiently smooth.*

We would like to point out one subtlety concerning the previous discussion. Numerically, we obtain the initial conditions $v_N(x,0)$ not by truncating the exact Fourier series of v_0 (which is usually not available), but rather by sampling v_0 on the numerical grid and finding the unique trigonometric polynomial which coincides with v_0 at these points. Let us denote the corresponding pseudo-spectral truncation-projection by $\widetilde{\mathbf{P}}_N$. Projection with $\widetilde{\mathbf{P}}_N$ introduces an aliasing error which is usually very small for *smooth* v_0, but may not necessarily be negligible otherwise. In particular, we *numerically* would not get the same initial conditions for the coefficients $\widehat{v}_k = a_k \mathbf{J}k$, $|k| \leq N$, if we simply took $\omega_N(x,0) = \widetilde{\mathbf{P}}_N \omega_0(x) = \widetilde{\mathbf{P}}_N \nabla^\perp \cdot v_0(x)$ as our initial value, because the resulting aliasing error $\|(\mathbf{P}_N - \widetilde{\mathbf{P}}_N)(\nabla^\perp \cdot v_0)\|_{L^2}$ might be very large.

This problem will not occur if we take $\omega_N(x,0) = \nabla^\perp \cdot \widetilde{\mathbf{P}}_N v_0(x)$, instead. In the latter case, the two discretizations are entirely equivalent.

3.4 Time stepping.

In the previous sections, we have discussed schemes for the spatial discretization of the incompressible Euler equations, and based on this, the computation of MVS. To obtain a fully discretized scheme, we also need a time-stepping procedure.

Our preferred time-stepping scheme is a strong stability preserving (SSP) Runge-Kutta scheme of order 3, a discussion of which can be found in [27]. It approximates $v(n\Delta t)$, $n = 0, 1, \dots$, of the ODE $v' = L(v)$, with initial data v_0, by $v^0 := v_0$ and

$$\begin{cases} \tilde{v}^n = v^n + \Delta t L(v^n), \\ \tilde{\tilde{v}}^n = \frac{3}{4} v^n + \frac{1}{4}\tilde{v}^n + \frac{1}{4}\Delta t L(\tilde{v}^n), \\ v^{n+1} = \frac{1}{3} v^n + \frac{2}{3}\tilde{\tilde{v}}^n + \frac{2}{3}\Delta t L(\tilde{\tilde{v}}^n). \end{cases} \tag{3.17}$$

This scheme can be shown to be formally of 3rd order.

Chapter 4

Numerical experiments

In this section, we will provide numerical experiments that demonstrate the theory developed in the previous section (particularly the convergence of algorithm 4.2).

4.1 Rotating vortex patch

The rotating vortex patch can be simulated by consider the two-dimensional Euler equations with initial data with piecewise constant vorticity

$$\eta_0(x) = \begin{cases} 1, & (x_1 - \pi)^2 + (x_2 - \pi)^2 \leq \pi/2, \\ 0, & \text{otherwise.} \end{cases}$$

Since our objective is to test the algorithm 4.2, we consider a perturbed version of the rotating vortex patch (see step 1 of algorithm 4.2). The perturbation is achieved as follows. In radial coordinates about the center $(x_1, x_2) = (\pi, \pi)$, we define a random perturbation

$$p_\delta(\theta) = 1 + \sum_{k=1}^{K} a_k \sin(b_k + (20 + k)\theta),$$

with $a_1, \ldots, a_K \in [0, 1]$, $b_1, \ldots, b_K \in [0, 2\pi]$ i.i.d. random variable chosen according to a uniform distribution with renormalization $\sum_{k=1}^{K} |a_k|^2 = \delta$. In our computations, we made the choice $K = 20$. The perturbed initial data depending on the perturbation parameter $\delta > 0$ are given by their vorticity $\eta_0^\delta(r, \theta) = \eta_0(r - p_\delta(\theta), \theta)$. The corresponding velocity field v_0^δ is obtained from the Biot-Savart law.

First, we fix a realization of the random field $v_0^\delta(\omega)$ by setting $\delta = 0.0128$. This initial data is evolved using the spectral (viscosity) method with $\varepsilon =$

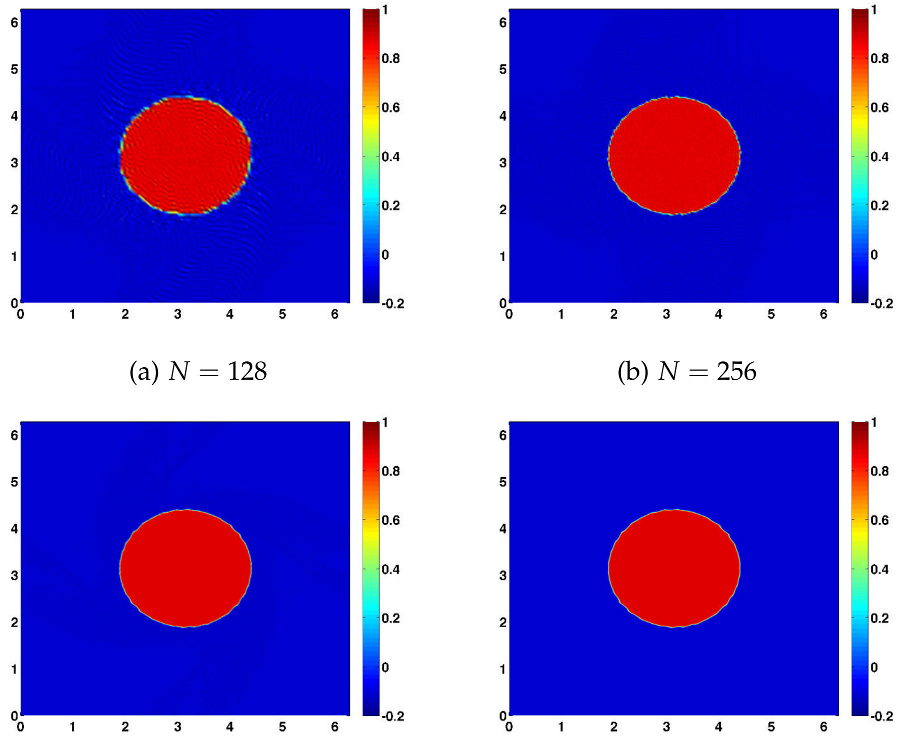

(a) $N = 128$ (b) $N = 256$

(c) $N = 512$ (d) $N = 1024$

Figure 4.1: Rotating vortex patch: Illustration of the sample convergence with respect to the number of Fourier modes N.

10^{-5}, $m = 0$. The resulting system of ODE's is approximately solved using the SSP Runge-Kutta scheme (3.17) with time step $\Delta t = 1/(2N)$.

The results are then presented in figures 4.1 and 4.2. In figure 4.1, we present the vorticity as the number of modes N is increased. We see that the vortex patch is well resolved with increasing resolution. Next, we compute the differences between successive resolutions,

$$\|v_N^{\delta}(t) - v_{N/2}^{\delta}(t)\|_{L^2}^2 \tag{4.1}$$

at different time levels. This difference, shown in figure 4.2 (left) clearly converges as $N \to \infty$. Consequently, the sequence of approximations (for a single realization) forms a Cauchy sequence and hence converges.

Since, the algorithm 4.2 is based on setting the perturbation amplitude $\delta \to 0$, we fix the number of approximating Fourier modes $N = 512$ and decrease δ. The corresponding difference between two successive values of δ is shown in figure 4.1 (right) and shows that the approximations clearly converge

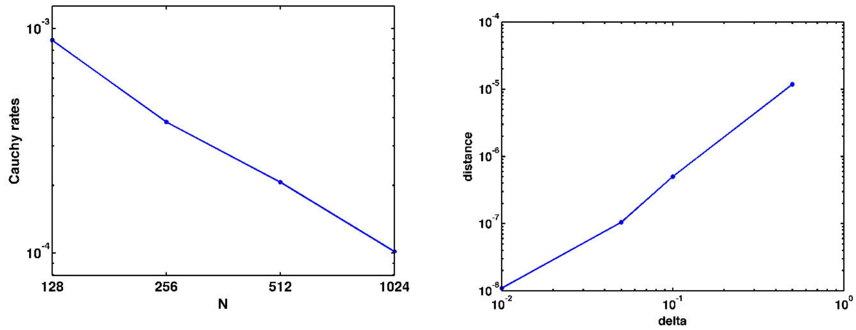

(a) Cauchy rates with respect to N at constant perturbation magnitude $\delta = 0.0128$.

(b) Cauchy rates with respect to δ at constant grid size $N = 512$.

Figure 4.2: Convergence behaviour of the rotating vortex patch for a single sample.

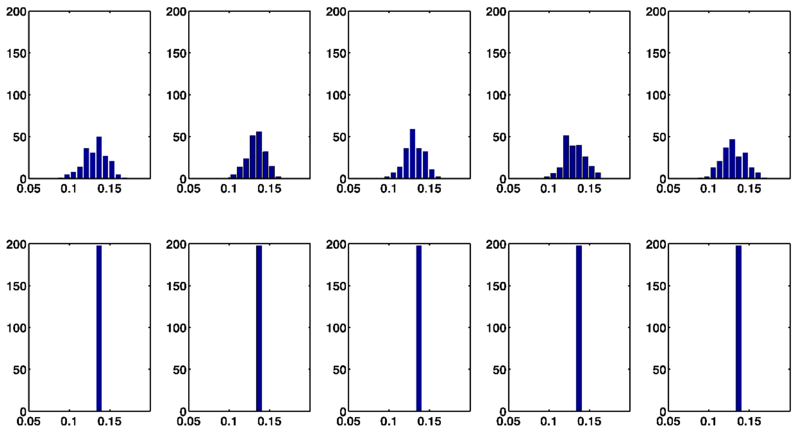

Figure 4.3: Rotating vortex patch: PDF with respect to time $t = 0, 0.5, 1, 2, 4$ at two different delta values $\delta = 0.512$ (top), $\delta = 0.0064$ (bottom) at $x = 2\pi \cdot (0.65, 0.55)$ illustrating atomicity

as the perturbation amplitude is reduced. Thus, for each fixed realization (sample), we already observe convergence of the spectral method as well as stability of the computed solutions with respect to perturbations in initial data. Although the initial data is not smooth (the vorticity is discontinuous), this convergence and stability are not surprising as the solution does not possess any fine scale features. Consequently, the computed measure valued solution ν is *atomic* as shown in figure 4.3.

4.2 Flat vortex sheet

Next, we consider a flat vortex sheet as a prototype for two-dimensional Euler flows with singular behavior. To this end, the underlying initial data is,

$$v^0(x) = \begin{cases} (-1,0), & \text{if } \pi/2 < x_2 \le 3\pi/2, \\ (1,0), & \text{if } x_2 \le \pi/2 \text{ or } 3\pi/2 < x_2, \end{cases} \tag{4.2}$$

on a periodic domain $[0,2\pi]^2$. The initial vorticity in this case is a bounded measure.

It is straightforward to check that the initial data for the flat vortex sheet (4.4) is a weak solution of the two-dimensional Euler equations. In fact, it is a steady state (stationary) solution. However, this datum also belongs to the class of *wild initial data* in the sense of Szekelyhidi [49]. Thus, infinitely many admissible weak solutions were constructed in [49], corresponding to this initial datum. See theorem 2.11.

Our objective is to compute the (admissible) measure valued solution, corresponding to this atomic initial data, by employing the algorithm 4.2. To this end, we mollify the initial data v^0 to obtain a smooth approximation $v^0_\rho = \left(\pi_1 v^0_\rho, \pi_2 v^0_\rho\right)$ of (4.4). Concretely, we used

$$\pi_1 v^0_\rho(x_1,x_2) = \left\{ \begin{array}{ll} \tanh\left(\dfrac{x_2 - \pi/2}{\rho}\right), & (x_2 \le \pi) \\ \tanh\left(\dfrac{3\pi/2 - x_2}{\rho}\right), & (x_2 > \pi) \end{array} \right\}, \quad \pi_2 v^0_\rho(x_1,x_2) = 0.$$

with a small parameter ρ. The parameter ρ controls the sharpness of the transition from -1 to $+1$ across the interfaces. A small value of ρ corresponds to a very sharp transition.

To obtain a random field (as required by Step 1 of algorithm 4.2, we further introduce perturbations of the two interfaces by making a *perturbation ansatz for each interface* of the form

$$p_\delta(x) = \sum_{k=1}^{K} \alpha_k \sin(kx_1 - \beta_k),$$

for randomly chosen numbers $\alpha_1,\dots,\alpha_K \in \mathbb{R}$, $\beta_1,\dots,\beta_K \in [0,2\pi)$ with $\sum_{k=1}^{K} |\alpha_k|^2 = \delta$. For our computations, we used a fixed value of $K = 10$ perturbation modes.

The result of this ansatz is a random field $v^0_\rho(x_1, x_2 - p_\delta(x_1))$ depending on two parameters ρ and δ. The parameter δ controls the magnitude of the permutation, while ρ determines the smoothness across the interfaces.

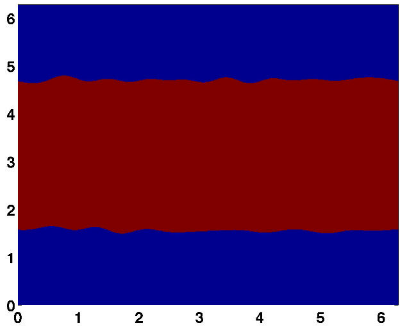

Figure 4.4: Perturbation with $\delta = 0.0512$.

Projecting this random field back to the space of divergence-free vector fields (using the Leray projection), we obtain our initial random perturbation $X^0_{\rho,\delta}$, as illustrated in Figure 4.4. For a fixed number of Fourier modes N, we aim to compute the corresponding approximate Young measure $\nu_N^{\rho,\delta}$ (Step 2 of algorithm). Then, the measured valued solution of (1.1) will be realized as a limit of $\nu_N^{\rho,\delta}$ as $N \to \infty, \rho, \delta \to 0$.

First, we fix a single realization of the random field $v_0(\omega)$. To visualize the resulting approximate solutions, we show a passive tracer (advected by the velocity field) in figure 4.5, at time $t = 2$ and with $(\delta, \rho) = (0.01, 0.001)$, at different Fourier modes N. We see from the figure that as the resolution is refined, finer and finer scale feature emerge, indicating that the tracer is getting mixed by the fluid at smaller and smaller scales. Furthermore, this indicates that the underlying velocity field may not emerge as the number of Fourier modes is increased. This is indeed verified in figure 4.6 (left), where we show the successive differences (4.1) of the approximate solution in L^2 (for a single sample). The differences do not seem to converge, indicating the approximate solutions may not form a Cauchy sequence. Hence and in contrast with the vortex patch example, the approximate solutions for a single realization (sample) do not converge.

Next, we consider the stability of the approximate solutions (for a single realization) with respect to the perturbation parameter δ. For a fixed $N = 512$ and time $t = 2$, we show a passively advected tracer, for different values of δ in figure 4.7. Again, the fine scale structure of the solutions is very different for each value of δ. As shown in figure 4.6 (right), the difference (in L^2) for successive values of δ does not decrease as δ decreases. This indicating that the perturbed solutions do not converge as the perturbation tends to zero, indicating instability of the flat vortex sheet (4.4) with respect to perturbations.

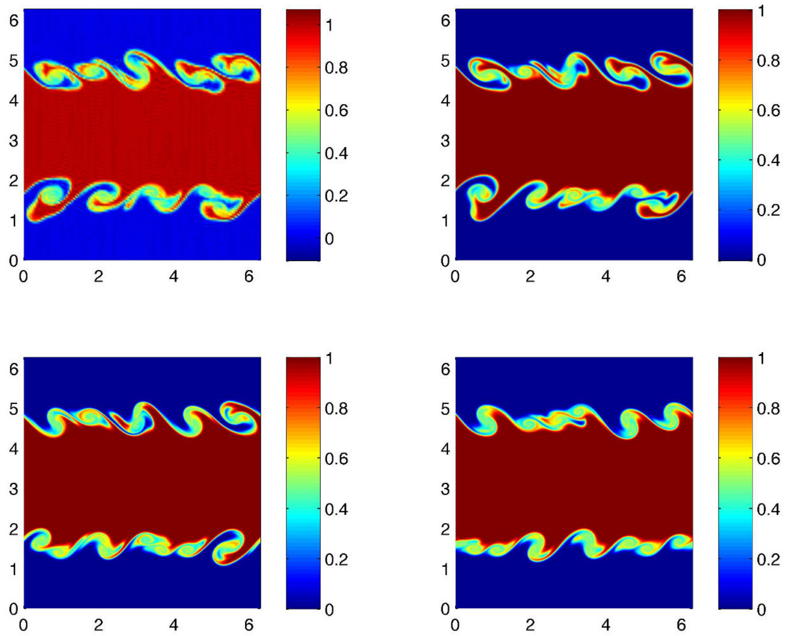

Figure 4.5: Flat vortex sheet (sample): Non-convergence with respect to N. A passive tracer (advected by the velocity field) is shown at time $t = 2$ for different Fourier modes. Top left $N = 128$, Top right $N = 256$, Bottom left $N = 512$, Bottom right $N = 1024$.

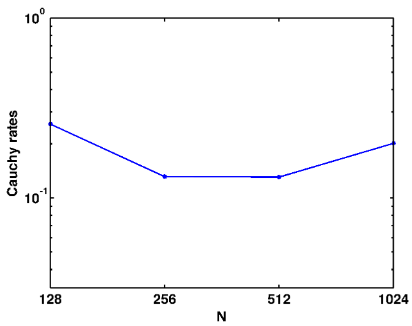

(a) Cauchy rates with respect to N.

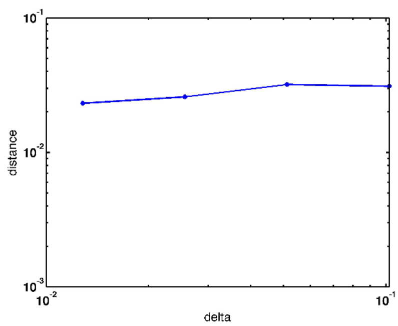

(b) Cauchy rates with respect to δ.

Figure 4.6: Flat vortex sheet (sample): (left) Cauchy rates with respect to N at fixed δ, (right) Cauchy rates with respect to δ at fixed N for a single sample. Convergence is not observed.

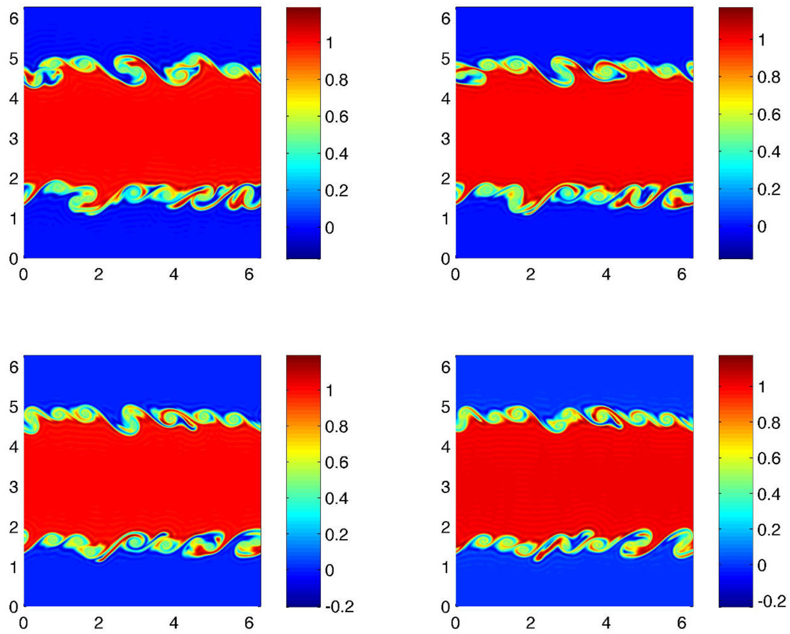

Figure 4.7: Passively advected tracer at $t = 2$ for $\delta = 0.0512$, 0.0256, 0.0128, 0.0064.

Having seen the lack of convergence (and stability) for single realizations of the perturbed vortex sheet, we apply the algorithm 4.2 to compute the approximate Young measure. To this end, we use the Monte Carlo algorithm 3.12 with $M = 400$ samples. We compute the mean of the approximate Young measure by setting $g(\xi) = \xi$ in (3.11). Similarly, the second moments are computed by setting $g(\xi) = \xi \otimes \xi$ in (3.11). The mean of the first component and variance of the second component at time $t = 2$, for different number of Fourier are shown in figures 4.8 and 4.9, respectively. In complete contrast to figure 4.5 (single sample) and as predicted by Theorem 3.10, both the mean as well as the variance seem to converge as the number of Fourier modes is increased. This convergence is further verified in figure 4.10, where successive L^2 differences of the mean velocity field and the second $\xi_2\xi_2$ moment are displayed. The convergence in the second moment is slower than than that of the mean. This is not unexpected as we use the same number of samples for the computation of both the mean and the second-moment. Furthermore, from figure **??**, we observe that small scale features are averaged out in the statistical quantities such as the mean of the passive tracer. In contrast, computations of single realizations (samples) revealed increasing fine small scale features as the number of Fourier modes was increased.

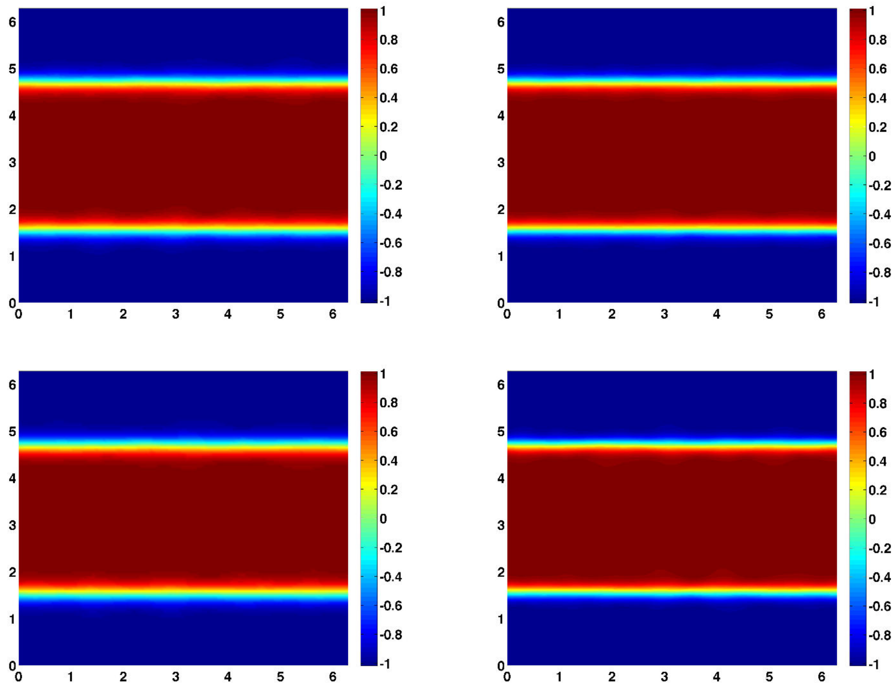

Figure 4.8: Flat vortex sheet: Convergence of mean of the first component of the velocity field at time $t = 2$ with respect to N (number of Fourier modes). Top left $N = 128$, Top right $N = 256$, Bottom left $N = 512$, Bottom right $N = 1024$.

As we are approximating atomic initial Young measure concentrated on the flat vortex sheet (4.4) by the perturbation based algorithm 4.2, we will let the perturbation parameter $\delta \to 0$. For this purpose, we fix $N = 512$ and consider approximate Young measures $\nu_N^{\rho,\delta}$ for successively smaller values of δ. The results for the mean of the first component of the velocity field and the variance of the second component of the velocity field are plotted in figures 4.8 and 4.9 and show that these statistical quantifies also converge with decreasing perturbation amplitude. This convergence is verified in figure 4.11, where successive differences of the mean and the second moment in L^2 are displayed.

The convergence results for statistical quantities such as the mean and the variance, with respect of the resolution as well as the perturbation parameter, are consistent with the prediction of narrow convergence in Theorem 3.10. Is the convergence even stronger than the predicted narrow convergence ? To test this assertion, we follow [22] and compute the Wasserstein distance for $\nu_{x,t}^{\delta,\rho}$ as probability measures in phase space. Again, we have computed the 1-Wasserstein distance between successive approximations δ vs. $\delta/2$, as

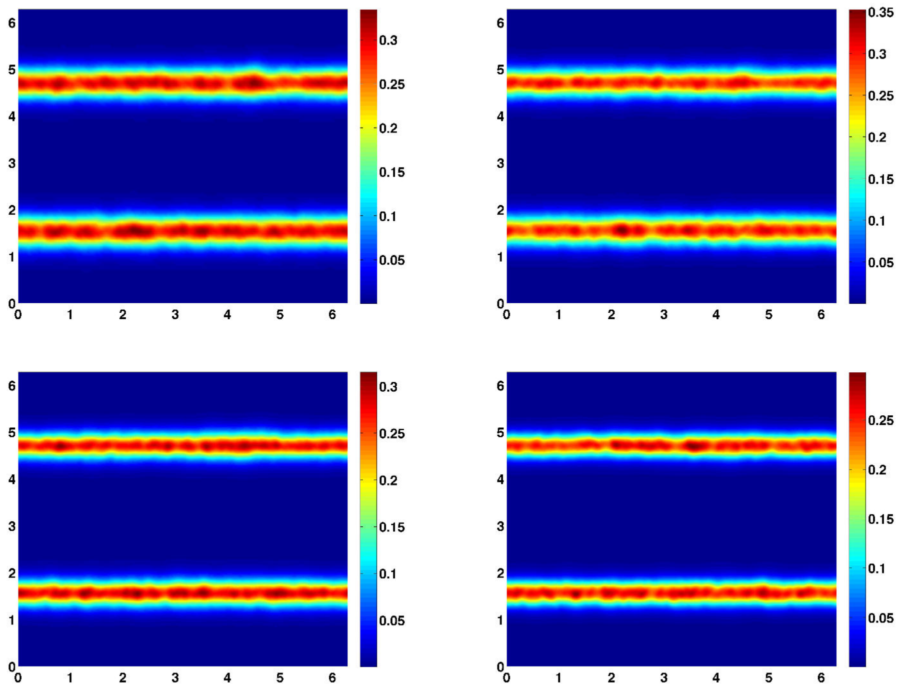

Figure 4.9: Flat vortex sheet: Convergence of second moment $\xi_2\xi_2$ of the velocity field at time t with respect to N (number of Fourier modes). Top left $N = 128$, Top right $N = 256$, Bottom left $N = 512$, Bottom right $N = 1024$.

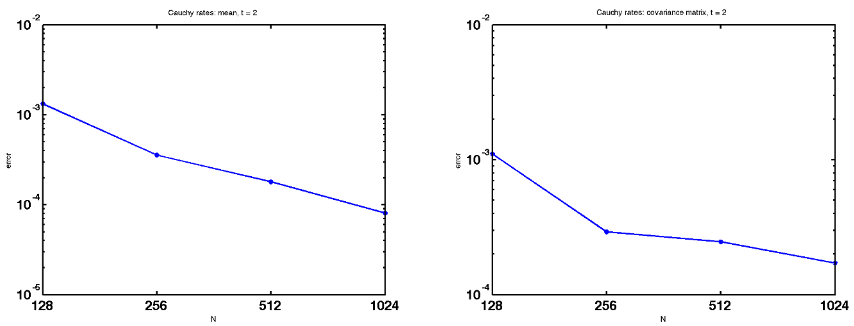

(a) Mean (b) Second moment

Figure 4.10: Flat vortex sheet: Cauchy rates with respect to N left (mean) right (second moment).

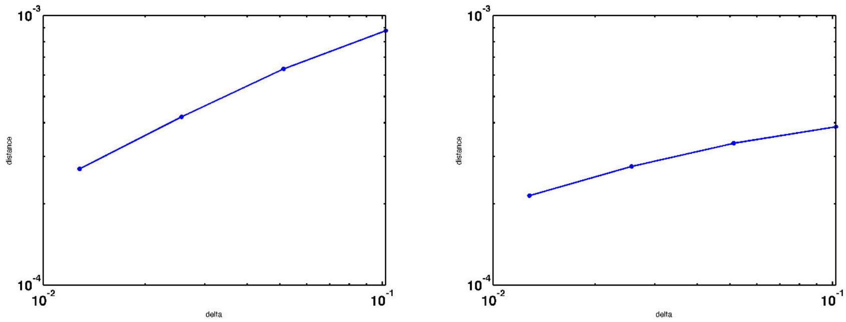

(a) Mean

(b) Second moment

Figure 4.11: Flat vortex sheet: Cauchy rates with respect to δ left (mean) right (second moment $\xi_2\xi_2$).

$\delta \to 0$. The results are shown in Figure 4.14. (A) displays the pointwise values $\mathcal{W}_1(\nu^{\delta,\rho}_{x,t}, \nu^{\delta/2,\rho})$, while (B) is a plot of the mean rates

$$\int \mathcal{W}_1(\nu^{\delta,\rho}_{x,t}, \nu^{\delta/2,\rho}_{x,t})\, dx,$$

at different times $t = 0, 1, 2, 4$.

Unexpectedly, We observe convergence even in the much stronger Wasserstein metric. This type of strong convergence was also observed in the context of compressible Euler equations of gas dynamics in [22].

4.3 Further properties of the vortex sheet

The numerical experiments for the flat vortex sheet initial data (4.4) show that single realizations (samples) do not show any convergence with respect to the numerical resolution or stability with respect to the perturbation parameter. On the other hand, the computed Young measures do converge (even strongly in the Wasserstein metric) with respect to both the number of Fourier modes as well as the perturbation parameter.

In this section, we will investigate the computed (admissible) measure valued solution of the Euler equations, corresponding to the flat vortex sheet data (4.4) in considerable detail. To begin with, we can fix the smoothing parameter $\rho > 0$ and the perturbation parameter δ and let the number of Fourier modes $N \to \infty$. Numerical results, presented in figures 4.10, show that the approximation converge to a Young measure $\nu^{\rho,\delta}$. In fact, one can also realize $\nu^{\rho,\delta}$ as the law of the random field $X_{\rho,\delta}$ which corresponds to the solution of the Euler equations with initial data $X^0_{\rho,\delta}$. Note that we can construct a unique $X_{\rho,\delta}(\omega)$ for every fixed $\omega \in \Omega$ as the two-dimensional

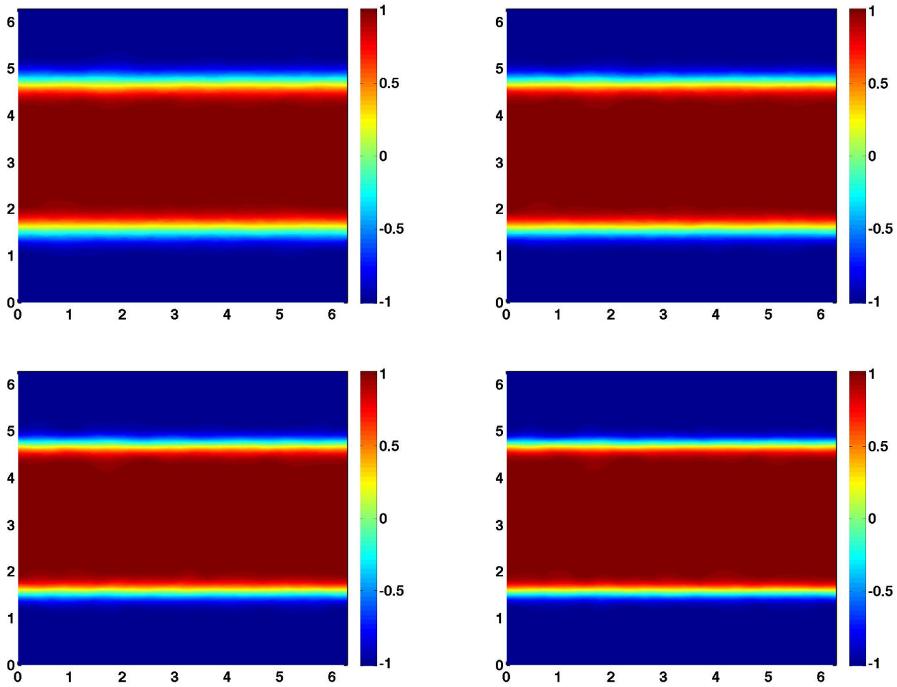

Figure 4.12: Flat vortex sheet: Convergence of mean of the first component of the velocity field at time $t = 2$ wrt δ (perturbation parameter). Top left $\delta = 0.1024$, Top right $\delta = 0.0512$, Bottom left $\delta = 0.0256$ and Bottom right $\delta = 0.0128$.

Euler equations are well-posed as the initial data $X^0_{\rho,\delta}(\omega)$ is smooth [37]. We summarize this fact and some other interesting analytical properties of the limit measure $\nu^{\rho,\delta}$ below.

Theorem 4.1 *For all values of ρ, δ, the measure-valued solution $\nu^{\rho,\delta}$ has the following properties.*

1. *$\nu^{\rho,\delta}$ is translationally invariant with respect to the x_1-direction, i.e. we have*

$$\nu^{\rho,\delta}_{x_1,x_2,t} = \nu^{\rho,\delta}_{x_1+h,x_2,t}$$

for any $h \in \mathbb{R}$ and $(x_1, x_2, t) \in \mathbb{T}^2 \times \mathbb{R}_+$.

2. *The mean $\overline{v}^{\rho,\delta} = \langle \nu^{\rho,\delta}, \xi \rangle$ has vanishing second component.*
3. *If $\nu^{\rho,\delta}$ is atomic, then it is stationary.*
4. *For each fixed $\omega \in \Omega$, the $X_{\rho,\delta}(\omega)$ are smooth solutions to the Euler equations with $X^0_{\rho,\delta}(\omega)$ smooth initial data, such that $X^0_{\rho,\delta}(\omega) \to v^0$ in L^2 as $\rho, \delta \to 0$. Moreover, we have a uniform bound on the vorticity in the H^{-1} norm.*

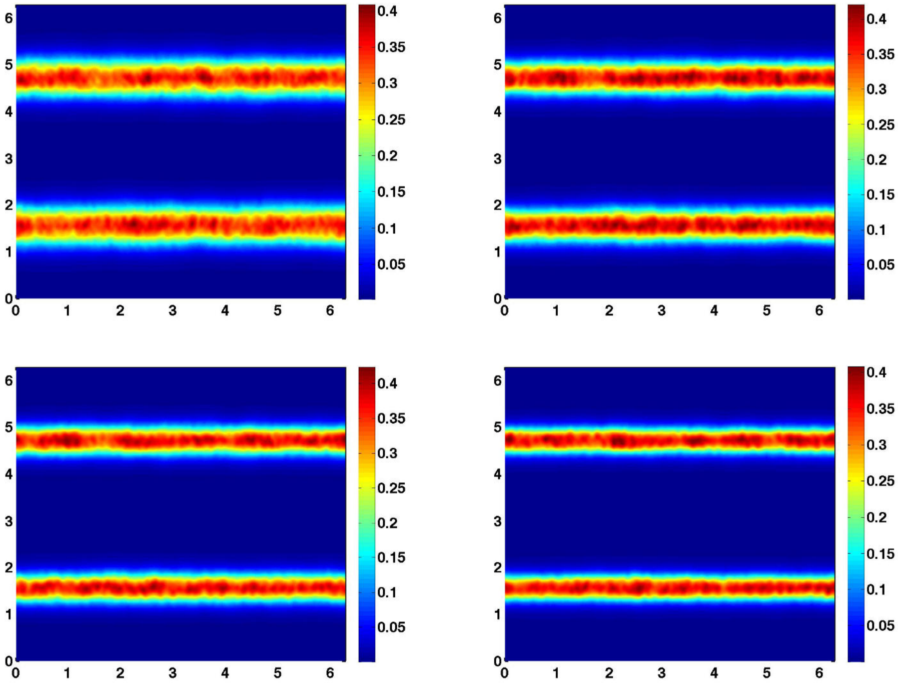

Figure 4.13: Flat vortex sheet: Convergence of second-moment of the second component of the velocity field at time $t = 2$ wrt δ (perturbation parameter). Top left $\delta = 0.1024$, Top right $\delta = 0.0512$, Bottom left $\delta = 0.0256$ and Bottom right $\delta = 0.0128$.

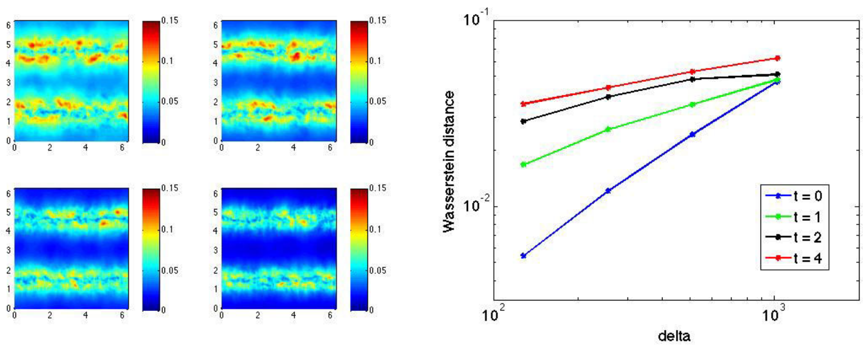

(a) distribution in space, $t = 4$, $\delta \to 0$

(b) Cauchy rates in the mean

Figure 4.14: Cauchy rates in the Wasserstein distance $\mathcal{W}_1$

All of these properties – except for the smoothness of the random fields $X_{\rho,\delta}$ – also hold for any limiting measure $\nu^{\rho,\delta}_{x,t} \overset{*}{\rightharpoonup} \nu_{x,t}$, obtained in the limit $\rho, \delta \to 0$, i.e. we are allowed to formally set $\delta = \rho = 0$.

Proof We start with the proof of property (1). The statistics of the perturbation ansatz for each interface

$$p_\delta(x) = \sum_{k=1}^{N} \alpha_k \sin(kx_1 - \beta_k)$$

is invariant with respect to translation in the x_1-direction. For any $h \in \mathbb{R}$, the values $\beta_1 - h/1, \ldots, \beta_N - h/N$ have the same probability of occuring as $\beta_1, \ldots, \beta_N$. Hence

$$\mathrm{Prob}[p_\delta(x + he_1) \in A] = \mathrm{Prob}[p_\delta(x) \in A]$$

for any measurable set A and any $h \in \mathbb{R}$. We obtain equality of the law

$$\mathcal{L}(v^0_\rho(x_1, x_2 - p_\delta(x_1))) = \mathcal{L}(v^0_\rho(x_1 + h, x_2 - p_\delta(x_1 + h)))$$

and hence of the initial data

$$\mathcal{L}(X^0_{\rho,\delta}(x_1, x_2)) = \mathcal{L}(X^0_{\rho,\delta}(x_1 + h, x_2)).$$

Finally, because the Euler equations are translation-invariant, it follows that

$$\nu^{\rho,\delta}_{x_1,x_2,t} = \mathcal{L}(X_{\rho,\delta}(x_1, x_2)) = \mathcal{L}(X_{\rho,\delta}(x_1 + h, x_2)) = \nu^{\rho,\delta}_{x_1+h,x_2,t}.$$

To prove (2), we proceed as follows. Let $\eta^{\rho,\delta}$ be the vorticity corresponding to the random field $X_{\rho,\delta}$. Taking the mean and interchanging integration and differentiation, we see that $\overline{\eta}^{\rho,\delta}$ is the vorticity corresponding to the mean $\overline{v}^{\rho,\delta}$. By property (1), the mean is independent of x_1. The same must be true of the mean vorticity $\overline{\eta}^{\rho,\delta}$, i.e. we have $\partial_{x_1}\overline{\eta}^{\rho,\delta} = 0$. It follows that also for the second component of $\overline{v}^{\rho,\delta}$, we have

$$\overline{v}^{\rho,\delta}_2 = \Delta^{-1}\partial_{x_1}\overline{\eta}^{\rho,\delta} = 0.$$

We come to property (3). Assume that $\nu^{\rho,\delta}_{x,t} = \delta_{v(x,t)}$. By property (2), the second component of the mean $\overline{v}^{\rho,\delta}_{x,t} = v(x,t)$ vanishes, i.e. $v_2 = 0$. Furthermore, v is independent of x_1 by property (1). It is straightforward to check that these two observations imply that v is a stationary solution.

We recall that the Leray projection is an orthogonal L^2 projection $(*)$ and that $X^0_{\rho,\delta}(\omega)$ is obtained in three steps $(**)$: In the first step, the intital datum v^0 is mollified to obtain a smooth field v^0_ρ. In a second step, we determine a random perturbation of the interfaces $p_\delta(x)$, which yields a field $v^0_{\rho,\delta}(x) = v^0_\rho(x - p_\delta(x))$. In the last step, we project this field to the space of divergence-free vector fields using the Leray projection to obtain $X^0_{\rho,\delta}(\omega)$. In particular, we find that

$$\|v^0 - X^0_{\rho,\delta}\|_{L^2} \overset{(*)}{\leq} \|v^0 - v^0_{\rho,\delta}\|_{L^2} \overset{(**)}{\leq} \|v^0 - v^0_\rho\|_{L^2} + \|v^0_\rho - v^0_{\rho,\delta}\|_{L^2}$$

Next, note that we have uniform L^∞ bounds $\|v^0\|_{L^\infty}, \|v^0_\rho\|_{L^\infty}, \|v^0_\delta\|_{L^\infty} \leq 1$ and that all of these fields are pointwise $= \pm e_1$, except in a region with width of order $O(\delta + \rho)$. We conclude that $\|v^0 - X^0_{\rho,\delta}\|_{L^2} \leq O(\rho + \delta)$. Finally, a uniform L^2 bound on a vector field implies a uniform H^{-1} bound on its vorticity. This concludes the proof. □

4.4 Non-atomicity of the limit measure valued solution

4.4.1 Non-zero variance

One of the most important questions concerning the measure valued solution realized as a limit of the approximations computed using Algorithm 4.2 applied to the flat vortex sheet initial data (4.4) is whether this measure is atomic or not, i.e. whether the limit measure valued solution is a weak solution of the Euler equations (1.1)? To answer this question, we focus on the variance of the computed approximations. By property (2) of theorem 4.1, we see that for a fixed ρ, δ, the computed Young measures will be invariant in the x_1-direction. We fix $N = 512$, and present a $x_1 =$ const slice of the mean and the variance of the velocity field v_1 in the x_2 direction for different values of δ. The results shown in figure 4.15 show that there is convergence as $\delta \to 0$. Furthermore, the mean as δ is reduced does not coincide with the initial velocity discontinuity. The variance is also very different from zero, at least at two patches (symmetric with respect to $x_2 = \pi$). We can denote these two patches as the turbulence zones. This is the first indication that the computed measure valued solution is *not atomic*.

4.4.2 Spread of the turbulence zone in time

To further test the issue of atomicity of the limit measure, we use property (3) of theorem 4.1. This property provides a clear criterion for atomicity i.e, if the limit measure is atomic, then it must be stationary (coincide with the initial flat vortex sheet (4.4)). We investigate the stationarity of the limit measure by considering the time dependent map for (the spatial mean of) the variance,

$$t \mapsto \int_{\mathbb{T}^2} \mathrm{Var}\left(\nu^{\rho,\delta}_{x,t}\right)\, dx,$$

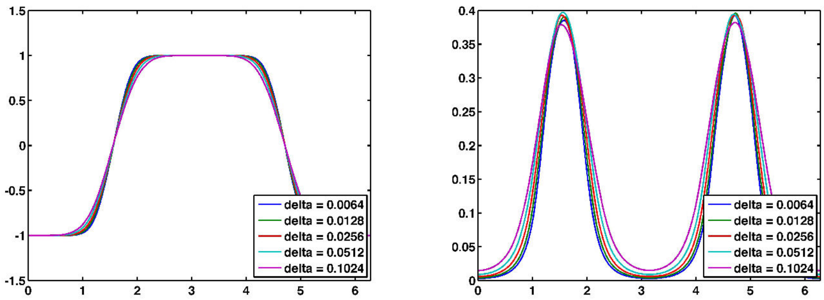

(a) mean

(b) variance

Figure 4.15: 1-D slices of the mean and the variance computed with different values of δ

as $\delta \to 0$. Given the fact that the variance is non-zero, only in the turbulence zone, we can interpret the above quantity as the mean spreading rate (in time) of the turbulence zone. In figure 4.16, we show how the zone spreads in time with respect to different values of δ. We observe that

- The spread rate of the turbulence zone converges as $\delta \to 0$.

- The limiting spread rate is *non-zero*, implying that the turbulence zone spreads out at a linear rate in time.

Thus, the limit Young measure is not stationary and hence, non-atomic.

Although, we do not have a rigorous proof of the linear spread rate of the turbulence zone and of the consequent non-atomicity of the limit measure, we can give a rigorous upper bound on the rate at which variance increases. To see this, we let $(\nu, \nu^\infty, \lambda)$ be an (admissible) measure valued solution (MVS) with atomic initial data, concentrated on v_0. Then $(\nu, \nu^\infty, \lambda)$ satisfies

$$\begin{aligned} \int_0^T \int_{\mathbb{T}^2} \langle \nu_{x,t}, \xi \rangle \chi'(t) \varphi(x) + \langle \nu_{x,t}, \xi \otimes \xi \rangle : \nabla \varphi(x) \chi(t)\, dx\, dt \qquad (4.3) \\ + \int_0^T \left(\int_{\mathbb{T}^2} \langle \nu^\infty_{x,t}, \theta \otimes \theta \rangle : \nabla \varphi(x) \chi(t)\, \lambda_t(dx) \right) dt = - \int_{\mathbb{T}^2} v_0(x) \cdot \varphi(x)\, dx, \end{aligned}$$

for all $\varphi \in C^\infty(\mathbb{T}^2; \mathbb{R}^2)$, and $\chi \in C_c^\infty([0,T))$ with $\chi(0) = 1$.

If we take $\varphi * \rho_\varepsilon$ as a test function, where $\rho_\varepsilon = \varepsilon^{-2}\rho(x/\varepsilon)$, $\rho \in C_c^\infty(\mathbb{T}^2)$ is a standard mollifier on $\mathbb{T}^2$ and $*$ denotes convolution, then we obtain

$$\begin{aligned} \int_0^T \int_{\mathbb{T}^2} \langle (\rho_\varepsilon * \nu)_{x,t}, \xi\rangle \chi'(t)\varphi(x) + \langle (\rho_\varepsilon * \nu)_{x,t}, \xi \otimes \xi\rangle : \nabla\varphi(x)\chi(t)\, dx\, dt \\ + \int_0^T \int_{\mathbb{T}^2} \Big(\int_{\mathbb{T}^2} \rho_\varepsilon(x-y) \langle \nu^\infty_{x,t}, \theta\otimes\theta\rangle\, \lambda_t(dx)\Big) : \nabla\varphi(y)\chi(t)\, dy\, dt \\ = -\int_{\mathbb{T}^2} (v_0 * \rho_\varepsilon)(x)\cdot\varphi(x)\, dx \end{aligned} \tag{4.4}$$

after an application of Fubini's theorem in (4.3). In the following, we will denote

$$\langle \nu^\varepsilon_{x,t}, f(\xi)\rangle := \langle (\rho_\varepsilon * \nu)_{x,t}, f(\xi)\rangle, \quad \langle \lambda^\varepsilon_{y,t}, f(\theta)\rangle := \int_{\mathbb{T}^2} \rho_\varepsilon(x-y)\langle \nu^\infty_{x,t}, f(\theta)\rangle\, \lambda_t(dx).$$

Similarly, we will write $v_0^\varepsilon(x) := (\rho_\varepsilon * v_0)(x)$ for the mollified initial data. With this notation, equation (4.4) takes the form

$$\begin{aligned} \int_0^T \int_{\mathbb{T}^2} \langle \nu^\varepsilon_{x,t}, \xi\rangle \chi'(t)\varphi(x) + \langle \nu^\varepsilon_{x,t}, \xi\otimes\xi\rangle : \nabla\varphi(x)\chi(t)\, dx\, dt \\ + \int_0^T \int_{\mathbb{T}^2} \langle \lambda^\varepsilon_{x,t}, \theta\otimes\theta\rangle : \nabla\varphi(x)\chi(t)\, dx\, dt = -\int_{\mathbb{T}^2} v_0^\varepsilon(x)\cdot\varphi(x)\, dx \end{aligned} \tag{4.5}$$

for all $\varphi \in C^\infty(\mathbb{T}^2;\mathbb{R}^2)$, and $\chi \in C_c^\infty([0,T))$ with $\chi(0) = 1$. Thus, $(\nu^\varepsilon, \lambda^\varepsilon\, \mathrm{d}x)$ is seen to be a MVS with mollified initial data given by v_0^ε. [1]

At this point, let us observe that for any suitable function f, we have

$$\begin{aligned} \int_{\mathbb{T}^2} \langle \nu^\varepsilon_{x,t}, f(\xi)\rangle\, dx &= \int_{\mathbb{T}^2} \langle \nu_{x,t}, f(\xi)\rangle\, dx, \\ \int_{\mathbb{T}^2} \langle \lambda^\varepsilon_{y,t}, f^\infty(\theta)\rangle\, dx &= \int_{\mathbb{T}^2} \langle \nu^\infty_{x,t}, f^\infty(\theta)\rangle\, \lambda_t(dx), \end{aligned} \tag{4.6}$$

as follows from an application of Fubini's theorem.

Fix $\varepsilon > 0$ for the moment. In the spirit of [5], we define

$$F(t) = \int_{\mathbb{T}^2} \langle \nu_{x,t}, \frac{1}{2}\,|\xi - v_0^\varepsilon|^2\rangle + \lambda_t(\mathbb{T}^2) \tag{4.7}$$

$$F^\varepsilon(t) = \int_{\mathbb{T}^2} \langle \nu^\varepsilon_{x,t}, \frac{1}{2}\,|\xi - v_0^\varepsilon|^2\rangle + \left(|\lambda^\varepsilon_{x,t}|\, dx\right)(\mathbb{T}^2), \tag{4.8}$$

$$E(t) = \int_{\mathbb{T}^2} \langle \nu_{x,t}, \frac{1}{2}\,|\xi|^2\rangle + \frac{1}{2}\lambda_t(\mathbb{T}^2) \tag{4.9}$$

$$E^\varepsilon(t) = \int_{\mathbb{T}^2} \langle \nu^\varepsilon_{x,t}, \frac{1}{2}\,|\xi|^2\rangle + \frac{1}{2}\left(|\lambda^\varepsilon_{x,t}|\, dx\right)(\mathbb{T}^2). \tag{4.10}$$

[1] We will have no need to bring the concentration measure $\langle \lambda^\varepsilon_{x,t}, \cdot\rangle\, dx$ into the sliced form $\langle \tilde{\nu}^\infty, \cdot\rangle \tilde{\lambda}_t(dx)$. Though, this could certainly be done.

By our observation (4.6), we have $F(t) = F^\varepsilon(t)$ and $E(t) = E^\varepsilon(t)$ for all $t \geq 0$.

It is shown in Lemma A.1, following the proof of [5, Theorem 2], that for any MVS (admissible or not) with sufficiently smooth initial data $v_0^\varepsilon(x)$, and with corresponding (strong) solution $v^\varepsilon(x,t)$, the following inequality holds:

$$F^\varepsilon(t) \leq E^\varepsilon(t) - \frac{1}{2}\int_{\mathbb{T}^2} |v_0^\varepsilon|^2\,dx + \frac{1}{2}\int_0^t \|\nabla v_0^\varepsilon + (\nabla v_0^\varepsilon)^T\|_\infty F^\varepsilon(\tau)\,d\tau. \qquad (4.11)$$

Assume now that $(\nu, \nu^\infty, \lambda)$ is in fact an *admissible* solution, so that $E(t) \leq \frac{1}{2}\int_{\mathbb{T}^2} |v_0|^2\,dx$ for all t. Then

$$\begin{aligned} F(t) &= F^\varepsilon(t) \\ &\leq E^\varepsilon(t) - \frac{1}{2}\int_{\mathbb{T}^2} |v_0^\varepsilon|^2\,dx + \frac{1}{2}\int_0^t \|\nabla v_0^\varepsilon + (\nabla v_0^\varepsilon)^T\|_\infty F^\varepsilon(\tau)\,d\tau \\ &\leq \frac{1}{2}\int_{\mathbb{T}^2} |v_0|^2\,dx - \frac{1}{2}\int_{\mathbb{T}^2} |v_0^\varepsilon|^2\,dx + \frac{1}{2}\int_0^t \|\nabla v_0^\varepsilon + (\nabla v_0^\varepsilon)^T\|_\infty F(\tau)\,d\tau. \end{aligned}$$

Note that the first difference is of order ε, while (for a suitable mollifier) $\|\nabla v_0^\varepsilon + (\nabla v_0^\varepsilon)^T\|_\infty$ can be bounded by ε^{-1}. Gronwall's inequality thus implies that

$$F(t) \leq \frac{1}{2}\left(\int_{\mathbb{T}^2} |v_0|^2 - |v_0^\varepsilon|^2\,dx\right) \mathrm{e}^{\frac{1}{2}\int_0^t \|\nabla v_0^\varepsilon + (\nabla v_0^\varepsilon)^T\|_\infty\,d\tau} \leq C\varepsilon\,\mathrm{e}^{\frac{t}{2\varepsilon}},$$

where $C \geq 0$ satisfies $\frac{1}{2}\int_{\mathbb{T}^2} |v_0|^2 - |v_0^\varepsilon|^2\,dx \leq C\varepsilon$.

The particular choice $\varepsilon = t/2$ now gives the bound

$$\int_{\mathbb{T}^2} \langle \nu_{x,t}, \frac{1}{2}|\xi - v_0^{(t/2)}|^2\rangle\,dx + \lambda_t(\mathbb{T}^2) \leq \frac{C\mathrm{e}}{2}t, \qquad (4.12)$$

for $t > 0$.

Corollary 4.2 *The mea* $\bar{\nu}_{x,t} \overset{t\to 0}{\longrightarrow} v_0(x)$ *converges* strongly *in* $L^2(\mathbb{T}^2;\mathbb{R}^2)$ *for any admissible MVS with initial data the vortexsheet* v_0*. Furthermore, we see that the spatially averaged variance cannot grow more than linearly for such solutions.*

Proof This is an immediate corollary of estimate (4.12). We have

$$\begin{aligned} \int_{\mathbb{T}^2} |\overline{\nu} - v_0|^2\,dx &\leq 2\int_{\mathbb{T}^2} |\overline{\nu} - v_0^{(t/2)}|^2\,dx + 2\int_{\mathbb{T}^2} |v_0 - v_0^{(t/2)}|^2\,dx \\ &\leq 2\int_{\mathbb{T}^2} \langle \nu_{x,t}, |\xi - v_0^{(t/2)}|^2\rangle\,dx + 2\int_{\mathbb{T}^2} |v_0 - v_0^{(t/2)}|^2\,dx \\ &\to 0, \end{aligned}$$

as $t \to 0$, and

$$\int_{\mathbb{T}^2} \mathrm{Var}(\nu_{x,t})\,dx = \int_{\mathbb{T}^2} \langle \nu_{x,t}, \frac{1}{2}|\xi - \overline{\nu}|^2\rangle\,dx \leq \int_{\mathbb{T}^2} \langle \nu_{x,t}, \frac{1}{2}|\xi - v_0^{(t/2)}|^2\rangle\,dx \leq \frac{C\mathrm{e}}{2}t. \qquad \square$$

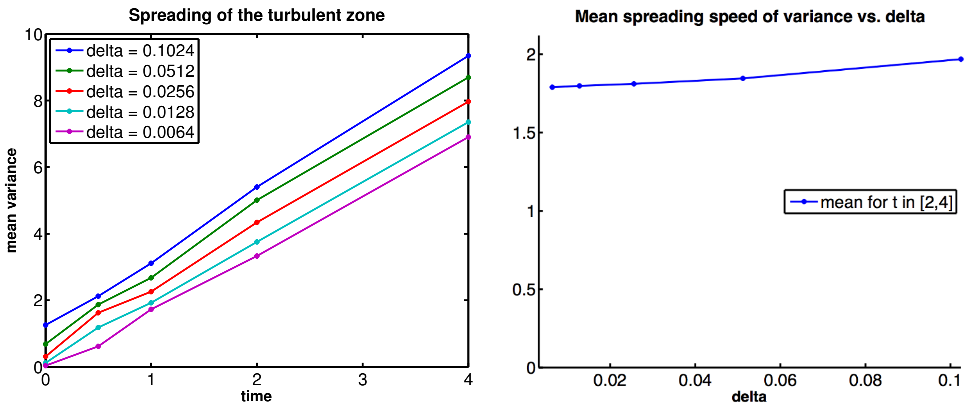

(a) Spreading at different values of time for varying values of δ.

(b) Mean spreading rate against δ over the time interval $[2,4]$.

Figure 4.16: Spreading of the turbulence zone in time.

For the particular choice of a piecewise linear function v_0^ε

$$v_0^\varepsilon(x) = \begin{cases} +e_1, & x_2 < \pi/2 - \varepsilon \text{ or } x_2 > 3\pi/2 + \varepsilon, \\ \dfrac{\pi/2 - x}{\varepsilon} e_1, & |\pi/2 - x_2| \le \varepsilon, \\ -e_1, & \pi/2 + \varepsilon \le x_2 < 3\pi/2 - \varepsilon, \\ \dfrac{x - 3\pi/2}{\varepsilon} e_1, & |3\pi/2 - x_2| \le \varepsilon, \end{cases}$$

we obtain a value of $C = 4\pi/3$, and the argument implies a bound on the spreading with constant $\frac{Ce}{2} = \frac{2\pi e}{3} \approx 5.7$.

The results of our computation as presented in figure 4.16 are consistent with the above corollary in establishing that mean variance (concentrated in the turbulence zone for the flat vortex sheet initial data) does spread out at a rate that is linear in time but at a rate of approximately 1.8 (or about a third of the rigorous upper bound).

4.4.3 Probability distribution functions

As a further test of the non-atomicity of the computed limit measure, we plot the empirical histogram at a point in space and different values of the perturbation parameter δ over time, in figure 4.17. The histograms serve as approximation of the probability density function (pdf), corresponding to the measure valued solution [22]. The figure shows that the pdfs converge as $\delta \to 0$. Furthermore, we observe that even if the initial measure is atomic (for small values of the perturbation parameter δ), the resulting pdf is non-atomic at points in the turbulent zone. Thus, we provide considerable evidence that the limiting measure valued solution is non-atomic.

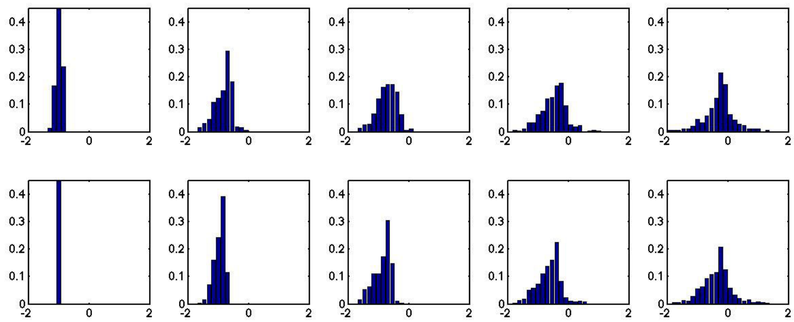

Figure 4.17: PDFs at a point $x = 2\pi \cdot (0.25, 0.77)$ and different times $t = 0, 0.5, 1, 2, 4$, for different values of $\delta = 0.0512$ (top), $\delta = 0.0064$ (bottom).

Remark 4.3 *The samples from which the computed measure-valued solution is obtained appear to be bounded in L^∞. Hence, by theorem 2.3, the corresponding Young measure does not exhibit any concentration effects.*

4.4.4 Contrast between incompressible Euler and incompressible Navier-Stokes

We have also investigated the effect that the introduction of a small amount of viscosity $\nu > 0$ has on the spreading rate as $\delta \to 0$. To this end we consider the solutions to the incompressible Navier-Stokes equations in the fully resolved case. The results on the spreading rate which were obtained from these computations are shown in 4.18.

In contrast to the situation encountered for the incompressible Euler equations, there is a clear slowing down in the growth of variance as $\delta \to 0$ in the fully resolved Navier-Stokes case. The limiting spreading rate is expected to be 0 because of the smoothing effect of the viscosity term.

In particular, we do not expect the zero viscosity and zero uncertainty limits to be interchangeable.

4.5 Possible non-uniqueness of Delort solutions

As mentioned in the introduction, Delort in [17] showed the *first rigorous existence results* for vortex sheets in two space dimensions provided that the vorticity belonged to a certain class defined below,

Definition 4.4 *A vector field $v \in L^\infty([0,T]; L^2(\mathbb{T}^2; \mathbb{R}^2))$ will be said to belong to the Delort class, if the vorticity $\eta = \operatorname{curl} v$ is a bounded measure of distinguished sign i.e, $\eta \in H^{-1}(\mathbb{T}^2) \cap \mathcal{BM}_+$.*

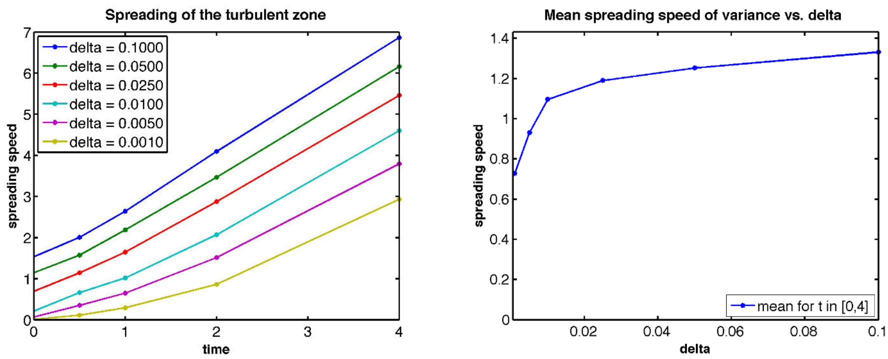

(a) Spreading of the variance for different values of δ.

(b) Limiting behaviour of spreading rate as $\delta \to 0$.

Figure 4.18: Spreading of the turbulent zone for the case of the Navier-Stokes equations with constant viscosity. In contrast to the observed behaviour for the Euler equations, a slowing down of the spreading is clearly visible in the limit $\delta \to 0$.

Delort proved the following celebrated result,

Theorem 4.5 [17]*: Under the assumption that the initial vorticity* $\eta_0 = \mathrm{curl}(v_0)$ *is in the Delort class, as defined above there exists a weak solution* v *of the 2-D incompressible Euler equations* (1.1)*, corresponding to the initial data* v_0*, that also belongs to the Delort class 4.4.*

The proof is based on mollifying the initial data, resulting in the generation of a sequence of approximate (smooth) solutions to the Euler equations. The resulting vorticity will be of a definite sign as it satisfies a maximum principle. The strong compactness of the approximating sequence is based on a localized L^1 control of the vorticity and uses the fact that the vorticity is of definite sign in a crucial manner, see also [47].

The uniqueness of the solution constructed by Delort is still open. It turns out that we can use property (4) of theorem 4.1 to numerically investigate this interesting question of uniqueness of solutions of (1.1) in the Delort class. However, as we analyze the Euler equations with periodic boundary conditions in this article, we *cannot restrict ourselves to the Delort class of vorticity being a bounded measure with a distinguished sign*. We need to extend to the following class of solutions,

Definition 4.6 *A vector field* $v \in L^\infty([0,T]; L^2(\mathbb{T}^2;\mathbb{R}^2))$ *will be said to belong to the* extended Delort *class, if the vorticity* $\eta = \mathrm{curl}\, v$ *is a bounded measure i.e,* $\eta \in H^{-1}(\mathbb{T}^2) \cap \mathcal{BM}$.

The existence proof of Delort in [17] can be readily extended to the case of extended Delort class initial data in the sense of definition 4.6 provided that vortices of opposite sign do not interact with each other (at least for a finite time period). We formalize this argument in the following theorem,

Theorem 4.7 *Let the initial velocity field v_0 belong to the extended Delort class as defined above. Further, assume that there exists a constant $c > 0$ and a terminal time $T > 0$, such that the time-dependent regions*

$$\mathcal{D}_{\pm}(t) = \{x \in \mathbb{T}^n;\ \exists N \in \mathbb{N},\ \eta_N(x,t) \gtrless 0\},$$

satisfy

$$\operatorname{dist}(\mathcal{D}_+(t), \mathcal{D}_-(t)) \geq c, \quad \forall t \in [0,T], \tag{4.13}$$

then there exists a weak solution v of the incompressible Euler equations (1.1) *that belongs to the extended Delort class 4.6.*

The proof follows from a straightforward repetition of the arguments of the proof of theorem B.1 in [17] and [47], while replacing the distinguished sign of the resulting vorticity field with assumption (B.1). A proof is given in appendix B.

Here, we will investigate the uniqueness of weak solutions of (1.1) that belong to the extended Delort class. To this end, we return to the flat vortex sheet initial data (4.4) and consider the perturbed random field initial data $X^0_{\rho,\delta}$ and the resulting solutions $X_{\rho,\delta}$. We collect some properties of this set of solutions below,

Lemma 4.8 *The solutions $X_{\rho,\delta}$ of the 2-D Euler equations* (1.1) *with randomly perturbed flat vortex sheet data $X^0_{\rho,\delta}$ satisfy for every realization $\omega \in \Omega$: There exist $\rho_k, \delta_k \to 0$ such that*

- *$X_{\rho_k,\delta_k}(\omega) \to X(\omega)$ in $C([0,T]; L^2_w(\mathbb{T}^2;\mathbb{R}^2))$,*
- *$\int |\eta_{\rho_k,\delta_k}(\omega)|\, dx \leq C$ uniformly for some constant C with $\eta_{\rho,\delta} = \operatorname{curl} X_{\rho,\delta}$*
- *Under the further assumption that vortices of distinguished sign are separated i.e, $\eta_{\rho,\delta}(\omega)$ satisfies* (B.1) *(uniformly) for all ω, we have a uniform lack of concentration of vorticity, in the sense that*

$$\lim_{r\to 0} \sup_{0\leq t\leq T} \sup_{N} \int_{B_r(x)} |\eta(\omega)_{\rho_k,\delta_k}|\, dx = 0, \qquad \forall\, x \in \mathbb{T}^2,$$

Then for each $\omega \in \Omega$, $X(\omega)$ is a weak solution of the Euler equations that belongs to the extended Delort class *4.6. Furthermore,*

$$\lim_{t\to 0} X(t,\omega) = v_0, \quad in \quad L^2(\mathbb{T}^2;\mathbb{R}^2),$$

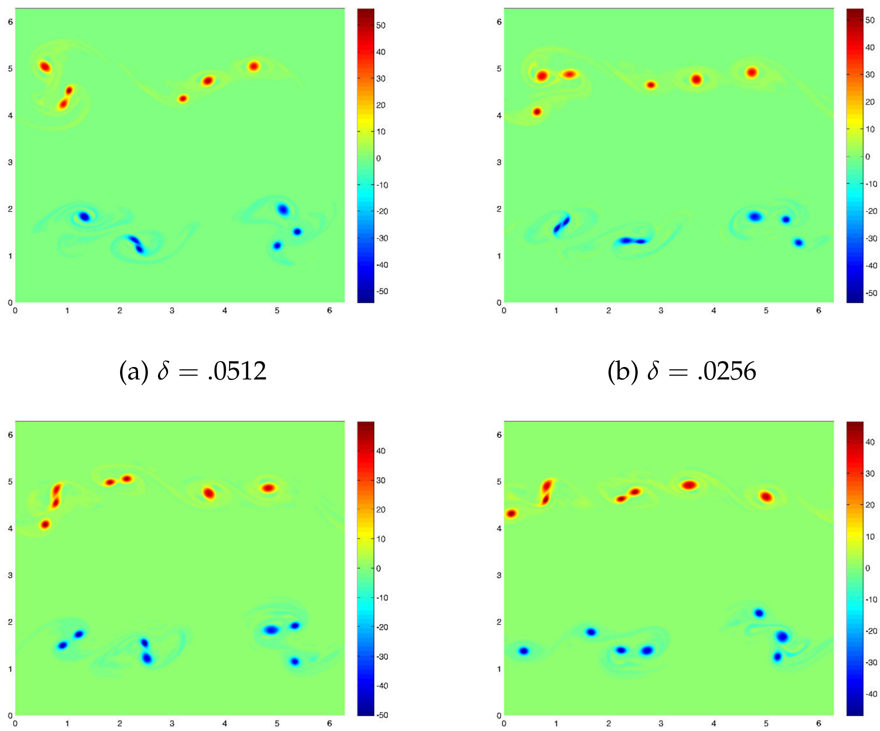

(a) $\delta = .0512$ (b) $\delta = .0256$

(c) $\delta = .0128$ (d) $\delta = .0064$

Figure 4.19: Illustration of the strict spatial separation of the vorticities of different signs for different values of δ at $t = 4$.

The first and second assertions of the above lemma are straight forward consequences of energy conservation and the maximum principle on vorticity for the smooth solutions $X_{\rho,\delta}$. Once, we assume (B.1), the compactness of the approximating sequence is established by repeating the arguments of the proof of Theorem B.1 as presented in [17] and [47].

We are unable to provide a rigorous proof for the assumption (B.1) for the case of perturbed flat vortex sheet initial data. However, this assumption can be readily verified *a posteriori* in our numerical computations. As an example, we fix a single sample (realization) and present the vorticity, obtained with spectral method with $N = 512$ nodes and $\rho = 0.008$ for different values of δ at time $T = 4$ in figure 4.19. The figure clearly shows that the vortices of positive and negative sign for any value of the perturbation parameter δ are well separated even at this relatively late time $T = 4$. In fact, we observe that the time of separation as required by the assumption (B.1) is $T \geq 4$ for all tested $\omega \in \Omega$. Hence, we can assert that each of our realizations (samples) converges (upto a subsequence) to a weak solution of (1.1) that belongs to the extended Delort class. This in turn, results in the following statement about the mean of the (admissible) measure valued solution $\nu_{\rho,\delta}$ constructed by the ensemble based algorithm 4.2 applied to the vortex sheet initial data (4.4),

Lemma 4.9 *Let v_0 be the flat vortex sheet initial data* (4.4) *and $\nu_{\rho,\delta}$ be an (admissible) measure valued solution of the Euler equations* (1.1)*, corresponding to this atomic initial data δ_{v_0}. Further, if we assume that the solutions of the Euler equations that belong to the* extended Delort class *4.6 are unique, then*

$$\langle \nu_{x,t}, \xi \rangle = v_0(x), \quad \textit{in} \quad L^2(\mathbb{T}^2; \mathbb{R}^2).$$

Proof Clearly, the flat vortex sheet v_0 is a stationary weak solution of the Euler equations that belongs to the extended Delort class 4.6 for all time $T \in [0, \infty)$. Under our assumption of uniqueness, v_0 is the unique weak solution in this class. Therefore, for every $\omega \in \Omega$, we can extract a further subsequence of $X_{\rho_k,\delta_k}(\omega)$converging weakly to the unique solution v^0. The uniqueness of the weak limit in turn implies that we in fact must have $\lim_{\rho,\delta\to 0} X_{\rho,\delta}(\omega) = v^0$ in the weak L^2 sense. From this, and the fact that the $X_{\rho,\delta}$ are uniformly bounded in the L^2 norm, we obtain that for any test function φ, we have

$$\begin{aligned}
\int_{\mathbb{T}^2\times[0,\infty)} \langle \nu_{x,t}, \xi \rangle \varphi(x,t)\, dx\, dt &= \lim_{\rho,\delta\to 0} \int_{\mathbb{T}^2\times[0,\infty)} \langle \nu_{x,t}^{\rho,\delta}, \xi \rangle \cdot \varphi \, dx\, dt \\
&= \lim_{\rho,\delta\to 0} \int_{\Omega} \left(\int_{\mathbb{T}^2\times[0,\infty)} X_{\rho,\delta}(\omega) \cdot \varphi \, dx\, dt \right) dP(\omega) \\
&= \int_{\Omega} \lim_{\rho,\delta\to 0} \left(\int_{\mathbb{T}^2\times[0,\infty)} X_{\rho,\delta}(\omega) \cdot \varphi \, dx\, dt \right) dP(\omega) \\
&= \int_{\Omega} \int_{\mathbb{T}^2\times[0,\infty)} v^0 \cdot \varphi \, dx\, dt\, dP(\omega) \\
&= \int_{\mathbb{T}^2\times[0,\infty)} v^0 \cdot \varphi \, dx\, dt.
\end{aligned}$$

We have used the uniform bound on

$$\int_{\mathbb{T}^2\times[0,\infty)} |X_{\rho,\delta}(\omega) \cdot \varphi| \, dx\, dt \le \|X_{\rho,\delta}\| \|\varphi\| \le C\|\varphi\|,$$

to justify passing to the limit inside of the dP-integral. Hence $\langle \nu_{x,t}, \xi \rangle = v^0(x)$ for any possible limiting measure-valued solution. □

We use the admissibility of measure valued solutions to show the following,

Lemma 4.10 *Let ν be an admissible measure-valued solution to the Euler equations* (2.3) *with atomic initial data. If the barycenter $\overline{v}(x,t) = \langle \nu_{x,t}, \xi \rangle$ is an energy conserving weak solution to* (1.1)*, then $\nu_{x,t} = \delta_{\overline{v}(x,t)}$ is atomic.*

Proof We have the following decomposition of the energy $E(t)$ at time t:

$$\begin{aligned} E(t) &= \frac{1}{2}\int_{\mathbb{T}^n} |\overline{v}(x,t)|^2\, dx + \frac{1}{2}\int_{\mathbb{T}^n} \langle \nu_{x,t}, |\xi - \overline{v}(x,t)|^2 \rangle\, dx + \lambda_t(\mathbb{T}^n) \\ &= \frac{1}{2}\int_{\mathbb{T}^n} |\overline{v}(x,t)|^2\, dx + \frac{1}{2}\mathrm{Var}_t(\nu) + \lambda_t(\mathbb{T}^n). \end{aligned}$$

The admissibility assumption $E(t) \le E(0)$ combined with the assumption of energy conservation for $\overline{v}(x,t)$ now yields

$$E(0) = \frac{1}{2}\int_{\mathbb{T}^n} |\overline{v}(x,0)|^2\, dx = \frac{1}{2}\int_{\mathbb{T}^n} |\overline{v}(x,t)|^2\, dx \le E(t) \le E(0).$$

Thus, all inequalities in these estimates are equalities. In particular, this implies that $\mathrm{Var}(\nu) = 0$ and $\lambda = 0$, hence $\nu_{x,t} = \delta_{\overline{v}(x,t)}$ a.e.. $\square$

We combine the above two lemmas to obtain the following theorem about the measure valued solutions corresponding to the flat vortex sheet initial data,

Theorem 4.11 *If the stationary solution v_0 is unique in the extended Delort class of flows with vorticity $\omega \in H^{-1}(\mathbb{T}^2) \cap \mathcal{BM}$, then the (admissible) measure valued solutions $\nu_{\rho,\delta}$, constructed by applying algorithm 4.2, then we have $\nu^{\rho,\delta} \rightharpoonup \delta_{v^0}$ (narrowly) as $\rho, \delta \to 0$.*

The main conclusion of all the above arguments is that if the week solutions of the Euler equations were unique in the extended Delort class, then the measure valued solution, computed using algorithm 4.2 would be *an atomic measure concentrated on the initial flat vortex sheet*. However, we provided considerable numerical evidence in sub-section 4.4 that the computed solutions are *non-atomic*. In fact, the turbulence zone (region where the variance is non-zero) increases linearly in time. Thus, we conclude that the **weak solutions in the extended Delort class are not unique**.

Comparison with the admissible weak solutions of Szekelyhidi.

In [49], Szekelyhidi was able to construct infinitely many admissible (finite kinetic energy) weak solutions to the 2-D Euler equations for the flat vortex sheet (4.4). Although admissible, these weak solutions are highly oscillatory. Hence, they may not belong to the (extended) Delort class as the resulting vorticity is no longer a bounded measure.

The single samples that we consider lie in the (extended) Delort class but converge to non-unique weak solutions. Furthermore, the computed measure

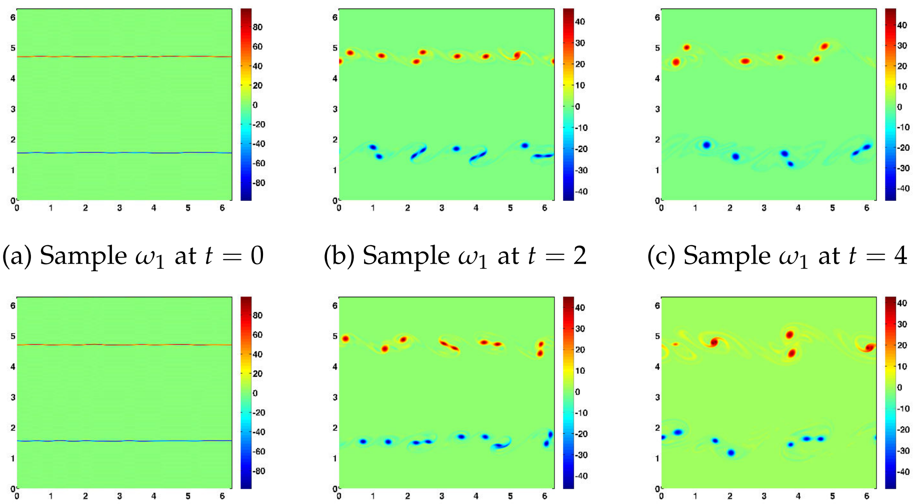

(a) Sample ω_1 at $t = 0$ (b) Sample ω_1 at $t = 2$ (c) Sample ω_1 at $t = 4$

(d) Sample ω_2 at $t = 0$ (e) Sample ω_2 at $t = 2$ (f) Sample ω_2 at $t = 4$

Figure 4.20: Comparison of the vorticity distribution $\eta(\omega_i)$ of two different samples ω_1 and ω_2 for $(\rho, \delta) = (0.008, 0.0064)$, illustrating the possible non-uniqueness in the evolution of extended Delort solutions.

valued solution has a turbulence zone (patches of non-zero variance) that spreads linearly in time. This is remarkably analogous to the construction of Szekelyhidi in [49] where a well defined turbulence zone is also defined and spreads linearly in time. Moreover, the empirical spread rate obtained by us is within the bounds provided by [49].

4.5.1 Stability (uniqueness) of the computed measure valued solution.

Admissible (weak) solutions of the Euler equations are not unique [12, 49]. Furthermore, the numerical evidence in the last subsection shows that even weak solutions, restricted to the considerably narrower Delort class, may not be unique. Since, every weak solution is also a measure valued solution, we cannot expect any uniqueness (stability) in the class of (admissible) measure valued solutions. However, the measure valued solution that we compute by application of algorithm 4.2 is not a generic measure valued solution but is one that is obtained with a very specific construction. Is this solution unique in a suitable sense? Is it stable? We explore these questions in this section.

4.5.2 Stability with respect to different perturbations

After having demonstrate the robustness of algorithm 4.2 with respect to choice of the numerical method in Step 2, we investigate if the algorithm is sensitive with respect to the type of perturbations in step 1. To do this, we consider the most general perturbation to the initial data (4.4) by adding a random field that is constant on local patches, and which exhibits uncorrelated fluctuations of equal strength in all of space. More precisely, we considered random fields of the form $X^0 = \sum_{i,j} X^0_{i,j} 1_{\mathcal{C}_{i,j}}$, where the patches

$$\mathcal{C}_{i,j} = \{(x,y) \in \mathbb{T}^2 : ik\Delta x \leq x < (i+1)k\Delta x,\ jk\Delta y \leq y < (j+1)k\Delta y\}$$

with $k = 16$ comprise 16×16 mesh cells, and the $X^0_{i,j}$ are independent, identically distributed $[-1,1]^2$-valued random variables. We obtain our initial perturbations Z^0_δ as the projection of $v^0 + \delta X^0$ to the space of divergence free vector fields. We refer to the results obtained from this perturbation procedure as 'uncorrelated', below.

Note that we can rewrite the evolution equation for the mean $\overline{v}$ of the MVS as,

$$\partial_t \overline{v} + \overline{v} \cdot \nabla \overline{v} + \nabla p = -\operatorname{div}\langle \nu, (\xi - \overline{v}) \otimes (\xi - \overline{v}) \rangle.$$

If the fluctuations of the mean $\overline{v}$ in the neighborhood of any given point are an indication of the fluctuations of ν, then we should expect the relevant contributions to the evolution of $\overline{v}$ to originate at the two interfaces, where $\overline{v}$ has a large jump. Hence, we localize the above uncorrelated perturbation to the initial data by multiplying it with cutoff functions that are supported around the two interfaces. We refer to the results from these localizations as 'uniform' or 'Gaussian' according to the corresponding distribution the values of the $X^0_{i,j}$ were chosen from. The results of applying algorithm 4.2 with these perturbations, with amplitude $\delta = .5$ and at time $T = 4$ are shown in figures 4.21 (mean) and 4.22 (variance). Clearly the computed solutions are very similar to those computed with the sinusoidal perturbations. The results are also shown in figure 4.21 and 4.22. Again, the nature of underlying distribution does not seem to affect the computed measure valued solution (at least with respect to mean and the second moment).

Summarizing the results of this subsection, we remark that the measure valued solution of the two-dimensional Euler equations, computed with the algorithm 4.2, are stable with respect to perturbations as well as robust vis a vis the choice of numerical method used to approximate them. This indicates that the computed measures may have MV stability, a weaker stability concept introduced in [22]. Although stability (uniqueness) does not hold for generic (admissible) measure valued solutions, the solutions computed by algorithm 4.2 do belong to a subset of admissible MVS, within which a suitable notion of stability (uniqueness) may hold. Further elaboration of these ideas is envisaged to be the subject of forthcoming articles.

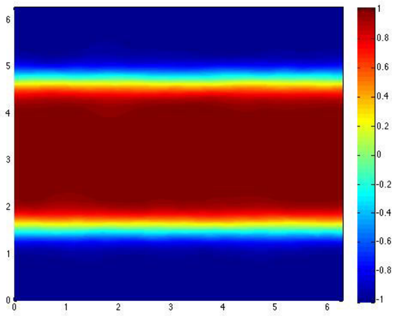

(a) interfaces

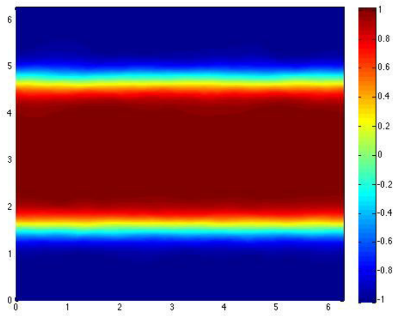

(b) uniform

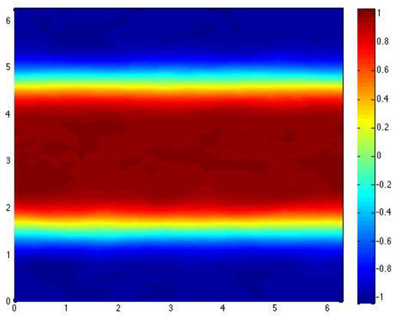

(c) uncorrelated

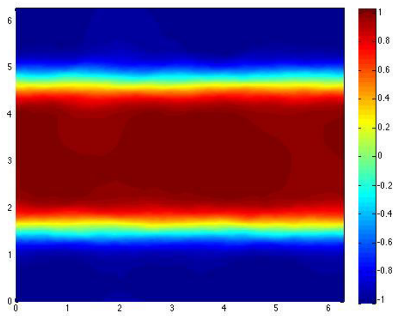

(d) Gaussian

Figure 4.21: Mean for different types of perturbations

4.5.3 The effects of smoothing

The computations presented in figure 4.16 have been carried out at a small, but fixed value of $\rho > 0$ with the goal of approximating the limit $\delta \to 0$. However, for fixed ρ, the unperturbed initial data is smooth. According to theorem 2.9 it then follows that $\lim_{\delta\to 0} \nu^{\rho,\delta}$ must be atomic, if we were to take this one-sided limit in full, while keeping $\rho > 0$ fixed.

Numerical experiments show that indeed, a corresponding sudden drop in the spreading rate is observed for values $\delta \ll \rho$. In particular, we expect that the particular order of taking the limits $\rho \to 0$, $\delta \to 0$ will be important. Our computed measure-valued solution corresponds to the limit

$$\nu = \lim_{\delta\to 0} \lim_{\rho\to 0} \nu^{\rho,\delta}.$$

To provide further evidence for a limiting measure-valued solution with constant spreading rate, we now consider the behaviour $\lim_{\rho\to 0} \nu^{\rho,\delta}$ for fixed $\delta > 0$. A representative plot of the resulting spreading of the variance for the case of uncorrelated perturbations with grid size N^2 and $\rho = 12/N$ is

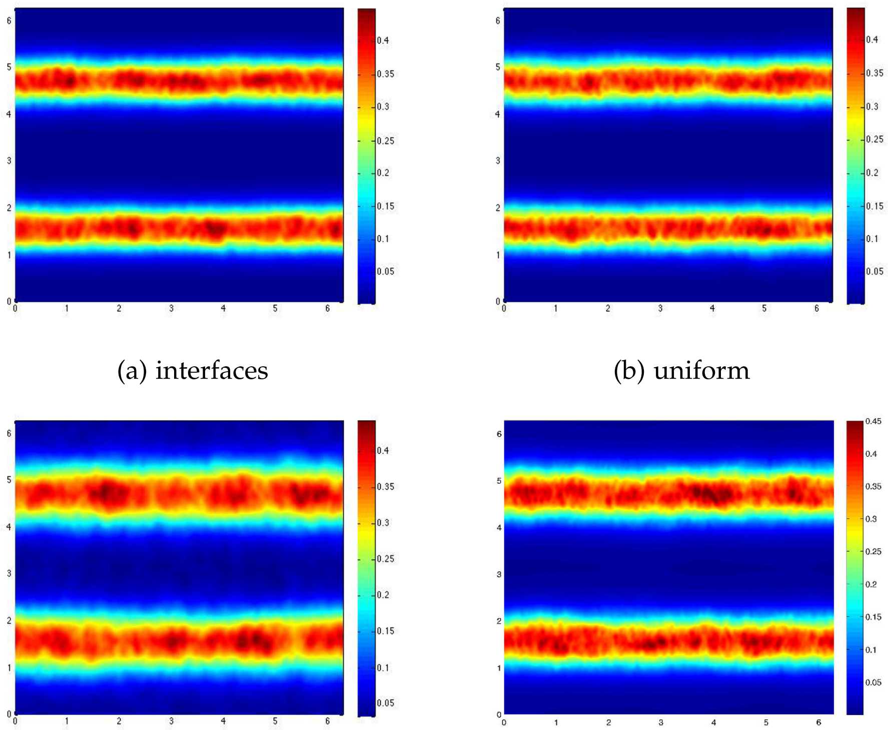

(a) interfaces (b) uniform

(c) uncorrelated (d) Gaussian

Figure 4.22: Second moments for different types of perturbations

shown in figure 4.23. The asymptotic behaviour indicated by 4.23 as $\rho \to 0$ and for fixed perturbation magnitude δ is clearly linear.

4.6 Discussion

Well-posedness results for the incompressible Euler equation (1.1) in two space dimensions are restricted to smooth initial data and exclude such physically interesting flows like vortex sheets. Although Delort [17] was able to show the existence of weak solutions for vortex initial data in 2D, uniqueness of such solutions is still open. Similarly, many different types of numerical schemes are available but rigorous convergence results exist only for special cases.

The starting point of the current chapter was the observation that even a well established numerical method, like the spectral (viscosity) method may not converge, even in 2D. Finer and finer scale oscillations are uncovered as the resolution is increased. Furthermore, the same numerical experiments

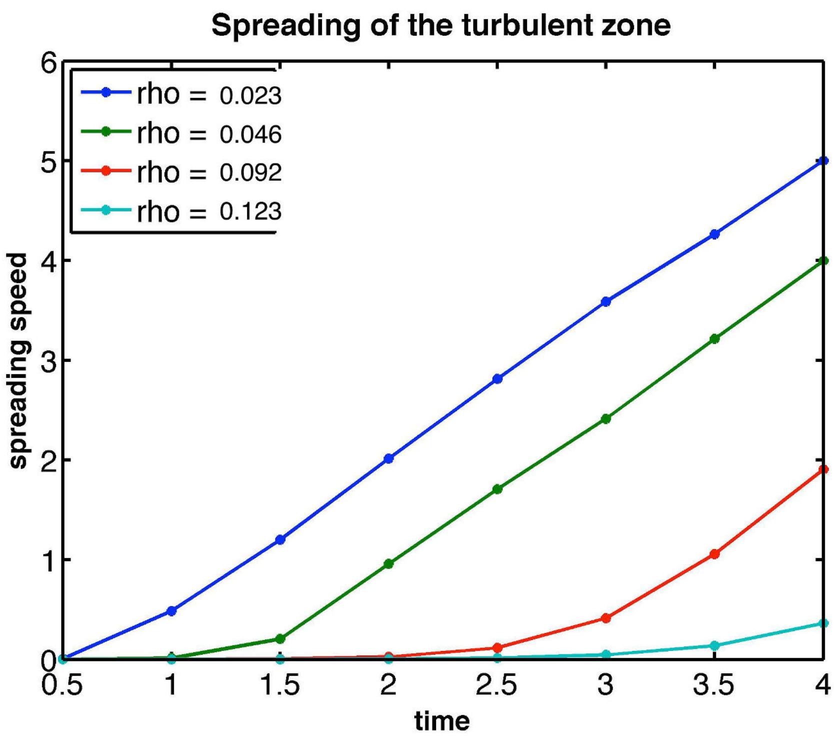

Figure 4.23: Spreading of the turbulent zone in the limit $\rho \to 0$ for fixed $\delta > 0$.

indicated the instability of some set of initial data with respect to perturbations.

Given the appearance of structures at smaller and smaller scales on increase of numerical resolution, we follow a recent paper [22] and investigate whether (admissible) measure valued solutions, introduced by DiPerna and Majda [19] might be an appropriate solution framework for the incompressible Euler equations, particularly with regard to the stability of initial data and the convergence of approximation schemes.

Our main aim was to design an algorithm to compute measure valued solutions of the Euler equations in a robust and efficient manner. To this end, we modified the ensemble based algorithm proposed in the paper [22] by combining it with the spectral (viscosity) method. The resulting approximate Young measures converge to an admissible measure valued solution of the Euler equations as the number of Fourier modes increases and the perturbation parameters converge to zero.

We present a wide variety of numerical experiments to illustrate the theoretical results on the proposed algorithm. In particular, we focus on an extensive case study for the two-dimensional flat vortex sheet. The numerical

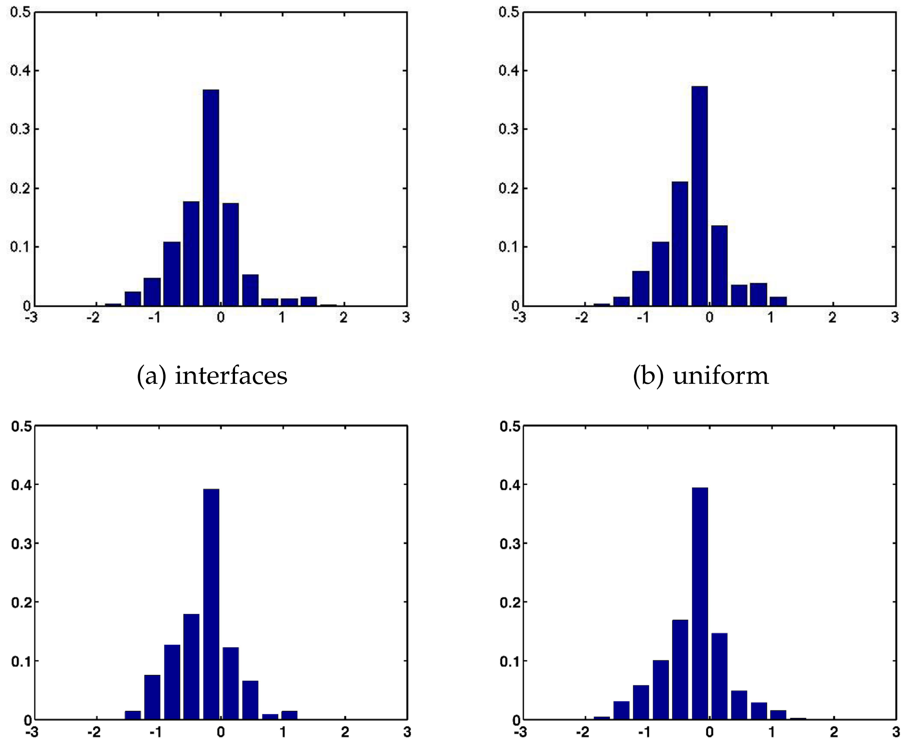

(a) interfaces

(b) uniform

(c) uncorrelated

(d) Gaussian

Figure 4.24: Different perturbations – distribution of x_1-velocity at a point near the interface, $t = 4$

experiments reveal that

- Single realizations (samples) may not converge as the number of Fourier modes is increased. Furthermore, there is no convergence as the perturbation amplitude is reduced indicating instability of the flat vortex sheet, at least at realistic numerical resolutions.
- Statistical quantities of interest such as the mean and variance do converge as the predicted by the theory.
- Furthermore, the approximate Young measure convergence with respect to the Wasserstein metric, indicating a considerably stronger form of convergence of the approximate Young measures than the predicted narrow convergence.
- The computed measure valued solution is robust with respect to the nature of the initial perturbations, suggesting stability of the computed measure valued solution in a suitable sense, for instance in the sense of MV stability of [22].

- The computed measure valued solution is non-atomic. The variance is concentrated (spatially) into two patches, symmetric with respect to line line $x_2 = \pi$. This *turbulence zone* spreads in time at a linear rate and is consistent with our theoretical upper bound.

We show analytically that if the weak solutions of the Euler equations are in the (extended) Delort class, i.e, the vorticity is a bounded measure, then the resulting measure valued solution, corresponding to the flat vortex sheet, will be atomic and concentrated on the initial data. However, given the observed non-atomicity of the measure, we conclude that the *weak solutions belong to the Delort class may not be unique*. This numerical evidence provides a new perspective on an interesting open question and calls for further theoretical investigation.

Chapter 5

Conclusion

In this chapter, we will give a quick summary of the main points discussed in this thesis, discuss its strengths and weaknesses and point out some open problems and possible future directions.

5.1 Summary

In chapter 1, a brief introduction to the incompressible Euler equations is given, as well as references for further reading. We show how the equations can be derived based on physical principles of mass and momentum conservation, incompressibility and the assumption that the fluid is ideal, i.e. frictionless. We also touch upon the corresponding situation for non-ideal fluids, which leads to the incompressible Navier-Stokes equations. Furthermore, the special role of the pressure as a Lagrange multiplier, enforcing the incompressible constraint, is pointed out. Well-known existence results from the mathematical theory of the Euler equations are then cited. A formal derivation of the Euler equations in terms of the vorticity is given. The resulting simplified form of the Euler equations in terms of the vorticity are essential for our numerical simulations described in chapter 4; all of them were carried out using the vorticity formulation.

Chapter 2 discusses the problems encountered when trying to pass to a weak limit in a non-linear equation. This is first illustrated using an explicit example. Then, it is shown how the notion of generalized Young measures can be employed to overcome this obstacle. The price one has to pay for this luxury in return is that weaker notions of solutions must be considered – namely measure-valued solutions (MVS). It is shown that the zero-viscosity limit of Leray solutions to the Navier-Stokes equations gives rise to a MVS. In particular, this can be combined with known existence results for the Navier-Stokes equations to show existence of MVS for L^2 initial data. The remainder of chapter 2 focusses on uniqueness questions for measure-valued solutions. Points of particular interest are

- the energy admissibility criterion,
- the resulting weak-strong uniqueness result, proving that admissible MVS coincide with classical solutions if they exist,
- the non-uniqueness results due to DeLellis, Szekelyhidi and co-workers, showing that non-uniqueness of weak solutions is generic [16],
- and finally the result due to Szekelyhidi and Wiedemann [48], which shows that the non-uniqueness encountered for MVS vs. the usual notion of weak solutions is equally bad. In particular, there seems to be no a priori mathematical reason to prefer (single-valued) weak solutions over MVS. On the other hand, MVS have the benefit that they allow us to pass limits more naturally.

In Chapter 3, we derive our numerical scheme based on spectral methods. This chapter contains a new convergence result for these schemes. We show that, in the limit of infinite grid size, an energy admissible MVS is obtained. As a first consequence, we obtain convergence of the scheme in L^2 in the presence of a strong classical solution. As a second consequence, we obtain a general existence result for MVS with given L^2 initial data. The algorithm for the concrete computation of MVS from [22] is cited with the necessary minimal adaptions to the case of incompressible flows. Another novel result of chapter 3 is the proof of equivalence of the 2D incompressible Euler equations and their vorticity formulation *on the discrete level*. This justifies our use of the vorticity formulation for all of our numerical experiments in chapter 4. The vorticity formulation has the important benefit that the incompressibility constraint does not have to be taken into account explicitely. This leads to faster algorithms which, in addition, we have found to be much more stable than solving the original system formulated in terms of the fluid velocity vector, directly.

Chapter 4 finally contains a description of numerical experiments that were carried out in 2D. We start out by illustrating the convergence of our algorithm for vortex patch initial data. This is in agreement with the weak-strong uniqueness result discussed in chapter 2, and was to be expected. The resulting MVS is atomic. In the remainder, we consider the particular case of vortex sheet initial data. This data is interesting in the present context, because it has been proved that infinitely many wild solutions in the sense of DeLellis, Szekelyhidi exist for flat vortex sheet initial data. In this case, the numerical scheme does not converge on the level of single samples. It is therefore necessary to consider approximate MVS, instead. On the level of these computed MVS, the situation is drastically different. Computed statistical quantities such as the mean and variance are shown to converge.

This is consistent with our results from chapter 3. More surprisingly, the convergence actually is seen to be much stronger. Our scheme appears to converge not only on the level of individual statistical quantities, but even with respect to the 1-Wasserstein metric. Another astonishing result of our experiments of chapter 4 is that the limiting MVS seems to be non-atomic. Our main argument for non-atomicity in the limit comes from the behaviour of the variance. It is argued that the variance grows linearly in time – even after taking the zero-uncertainty limit – at a finite, non-zero limiting spreading rate. Experiments based on varying different numerical parameters (such as grid-size, smoothing, perturbation magnitude, numerical viscosity, ...) are all consistent with such a finite, limiting spreading rate. Based on this observation, a link to the weak solutions constructed by Delort is made. For this, a class of extended Delort solutions is introduced. Delort's existence result is carried over to this class under an additional assumption of separation of regions of positive and negative vorticity. This additional assumption is found to be satisfied in all of our computations. It is then shown that non-atomicity of the limiting MVS implies non-uniqueness of weak solutions in the extended Delort class. This non-uniqueness is illustrated at the hand of two samples at the smallest computed perturbation magnitude. Finally, we also ask whether the computed MVS is stable with respect to different perturbation mechanisms. A visual comparison indicates that this is indeed the case.

5.2 Open problems

In our view, the most important points that have either not been established beyond any reasonable doubt, or have not been touched upon at all, are the following.

Convergence with respect to the Wasserstein metric: Our experiments indicate that the computed MVS converges in the 1-Wasserstein metric. The theory described in chapters 1-3 give no indication whatsoever that this should be the case. Judging from the theory described in chapter 2 alone, there seems to be no good reason for the convergence of the entire measure in such a strong sense. No attempt has been made to explain this observation in this thesis. This point is under current investigation.

Instability vs. non-wellposedness for the flat vortex sheet: Our result for the non-uniqueness of extended Delort solutions ultimately hinges on the fact that even the smallest perturbation of a flat vortex sheet will lead to an instantaneous, steadily expanding turbulent zone (effecting the linear increase of the variance of the computed MVS even in the zero-uncertainty limit). It has been known for a long time that the linear stability analysis indicates that the flat vortex sheet is unstable in the sense that perturbations should be expected to grow at least exponentially in time. Such an exponential instability would not be enough to prove a non-uniqueness result – rather, we need a stronger non-wellposedness result. Our evidence for such a non-wellposedness result is rather circumstantial. It would therefore be desirable to either give an analytical proof of the non-atomicity of our computed MVS, settling the matter once and for all, or at least to have a quantitative measure that can be efficiently computed and which can be used to distinguish between exponential instability and non-wellposedness, numerically.

Delort class vs. extended Delort class: Due to obvious technical reasons (Fourier expansion), we have restricted our attention to flows in a doubly periodic geometry. Because of this, we had to consider a flat vortex sheet which had both positive and negative signs in the vorticity (separated in space). In consequence, this required the introduction of the extended Delort class. It would be interesting to carry out similar experiments for vortex sheets of distinguished sign. This has been done in the forthcoming paper [33]. The results appear to be similar.

Strict separation of the regions $\mathcal{D}_\pm(t)$: In our proof of the possible non-uniqueness of extended Delort solutions we had to introduce an additional assumption that $d(D_+(t), D_-(t)) \geq c > 0$, uniformly for all approximations.[1] We have not been able to establish such a separation rigorously, although it seems to be very clearly satisfied in our computations. It would be interesting to find an analytical proof. This would not only make our non-uniqueness argument more rigorous, but it would also allow one to establish the existence result of Delort in greater generality.

Stability of the computed MVS: We have presented some visual evidence that the computed MVS is stable with respect to different perturbation mechanisms. This opens up two possible directions for future work. On the one hand, it would be interesting to compare not only the results of different perturbation mechanisms, but also the results of different numerical schemes, which have been shown to converge to an admissible MVS. If MVS are a suitable solution concept, then clearly we would want stability also with respect to other schemes. An approach based on finite difference schemes [33] does indeed show similar results. On the other hand, our comparisons between different perturbation mechanisms and numerical schemes have only been done by visual comparison of plots of the mean, variance and distribution functions, as of yet. A more quantitative study of these stability proper-

[1] We recall that $\mathcal{D}_\pm(t)$ denotes the set of points of vorticity with sign $\pm$ at time t.

ties would be advisable. Can we establish converge to the same limit in a quantitative way by numerical experiments?

5.3 Contributions

Many of the results on which this thesis is based, have been known for at least twenty years [1, 17, 19, 20, 38, 47, 50, 52]. Some are more recent [4, 5, 12, 13, 14, 15, 16, 22, 48]. To the best of our knowledge, novel contributions of *this* work include:

- the proof of convergence of spectral schemes to MVS,
- the proof of equivalence between the 2D incompressible Euler equations and the vorticity formulation *on the discretized level*,
- extensive experiments for the computation of a MVS in the case of the flat vortex sheet in 2D, using our spectral scheme,
- the observed non-atomicity of the computed MVS for the incompressible Euler euqations *even for atomic initial data*,
- a link between non-atomicity of our computed MVS for the flat vortex sheet and non-uniqueness in the extended Delort class.

We would finally like to mention that parts of this work have been submitted for publication. A pre-print is already available [32].

Appendix A

Weak-Strong Uniqueness

We provide the general proof for the weak-strong uniqueness theorem 2.9. It will be a straight forward consequence of the following lemma.

Lemma A.1 *Let ν be any (admissible or not) MVS with atomic initial data given by the divergence-free vector field $v_0 \in C^\infty(\mathbb{T}^n;\mathbb{R}^n)$. Assume that there exists a smooth solution $v \in C^\infty([0,T]\times\mathbb{T}^n;\mathbb{R}^n)$ of the Euler equations with initial data given by v_0. Denote*

$$F(t) = \frac{1}{2}\int_{\mathbb{T}^n} \langle \nu_{x,t}, |\xi - v(x,t)|^2\rangle \, dx + \frac{1}{2}\lambda_t(\mathbb{T}^n),$$

and let

$$E(t) = \frac{1}{2}\int_{\mathbb{T}^n} \langle \nu_{x,t}, |\xi|^2\rangle \, dx + \frac{1}{2}\lambda_t(\mathbb{T}^n).$$

Then the following estimate holds

$$F(t) \leq E(t) - \frac{1}{2}\int_{\mathbb{T}^n} |v_0|^2 \, dx + \frac{1}{2}\int_0^t \|\nabla v + (\nabla v)^T\|_{L^\infty} F(\tau)\, d\tau.$$

Proof Let $\chi \in C^\infty([0,T])$, $\chi \geq 0$. Then

$$\begin{aligned}\int_0^T \chi' F \, dt = & \frac{1}{2}\int_0^T \int_{\mathbb{T}^n} \chi' \langle \nu, |\xi|^2\rangle \, dx\, dt + \frac{1}{2}\int_0^T \chi' \lambda_t(\mathbb{T}^n)\, dt \\ & - \int_0^T \int_{\mathbb{T}^n} \chi' \bar{v}\cdot v \, dx\, dt + \frac{1}{2}\int_0^T \int_{\mathbb{T}^n} \chi' |v|^2 \, dx\, dt.\end{aligned}$$

Since v is a strong solution, the second term on the second line vanishes. The expression on the first line can be rewritten using $E(t)$. Hence

$$\int_0^T \chi' F \, dt = \int_0^T \chi' E \, dt - \int_0^T \int_{\mathbb{T}^n} \chi' \bar{v}\cdot v \, dx\, dt \tag{A.1}$$

The second term can be rewritten

$$\int_0^T \int_{\mathbb{T}^n} \chi' \bar{v} \cdot v \, dx \, dt = \int_0^T \int_{\mathbb{T}^n} \bar{v} \cdot \partial_t(\chi v) \, dx \, dt - \int_0^T \int_{\mathbb{T}^n} \chi \bar{v} \cdot \partial_t v \, dx \, dt.$$

Using the fact that ν is a MVS, we have

$$\begin{aligned}
\int_0^T \int_{\mathbb{T}^n} \bar{v} \cdot \partial_t(\chi v) \, dx \, dt &= \int_0^T \int_{\mathbb{T}^n} \langle \nu, \xi \otimes \xi \rangle : \nabla(\chi v) \, dx \, dt \\
&\quad + \int_0^T \int_{\mathbb{T}^n} \langle \nu^\infty, \theta \otimes \theta \rangle : \nabla(\chi v) \, \lambda_t(dx) \, dt \\
&= \int_0^T \chi \int_{\mathbb{T}^n} \langle \nu, \xi \otimes \xi \rangle : \nabla v \, dx \, dt \\
&\quad + \int_0^T \chi \int_{\mathbb{T}^n} \langle \nu^\infty, \theta \otimes \theta \rangle : \nabla v \, \lambda_t(dx) \, dt.
\end{aligned}$$

Using the fact that v is a classical solution and the incompressibility constraint on $\bar{v}$, we obtain

$$\begin{aligned}
-\int_0^T \int_{\mathbb{T}^n} \chi \bar{v} \cdot \partial_t v \, dx \, dt &= \int_0^T \int_{\mathbb{T}^n} \chi \bar{v} \cdot [v \cdot \nabla v + \nabla p] \, dx \, dt \\
&= \int_0^T \chi \int_{\mathbb{T}^n} v \cdot \nabla v \cdot \bar{v} \, dx \, dt
\end{aligned}$$

On the other hand, we also have

$$\begin{aligned}
\int_{\mathbb{T}^n} \bar{v} \cdot \nabla v \cdot v \, dx &= \int_{\mathbb{T}^n} \bar{v} \cdot \nabla \left(\frac{1}{2} |v|^2 \right) \, dx \\
&= 0,
\end{aligned}$$

again by the incompressibility constraint on $\bar{v}$. Similarly, we see that

$$\int_{\mathbb{T}^n} v \cdot \nabla v \cdot v \, dx = 0.$$

Adding all of these terms together and substituting in (A.1), we obtain

$$\begin{aligned}
\int_0^T \chi' F\,dt &= \int_0^T \chi' E\,dt - \int_0^T \int_{\mathbb{T}^n} \chi' \bar{v}\cdot v\,dx\,dt \\
&= \int_0^T \chi' E\,dt + \int_0^T \chi \int_{\mathbb{T}^n} \langle \nu, \xi\otimes\xi\rangle : \nabla v\,dx\,dt \\
&\quad + \int_0^T \chi \int_{\mathbb{T}^n} \langle \nu^\infty, \theta\otimes\theta\rangle : \nabla v\,\lambda_t(dx)\,dt \\
&\quad + \int_0^T \chi \int_{\mathbb{T}^n} v\cdot\nabla v\cdot\bar{v}\,dx\,dt + \int_0^T \chi \int_{\mathbb{T}^n} \bar{v}\cdot\nabla v\cdot v\,dx\,dt \\
&\quad + \int_0^T \chi \int_{\mathbb{T}^n} v\cdot\nabla v\cdot v\,dx\,dt \\
&= \int_0^T \chi' E\,dt + \int_0^T \chi \int_{\mathbb{T}^n} \langle \nu, (\xi - v)\cdot\nabla v\cdot(\xi - v)\rangle\,dx\,dt \\
&\quad + \int_0^T \chi \int_{\mathbb{T}^n} \langle \nu^\infty, \theta\otimes\theta\rangle : \nabla v\,\lambda_t(dx)\,dt
\end{aligned}$$

Now, choose χ to be a sequence of smooth approximations of $\chi_{[s,t]}$ for $0 < s < t < T$. Then, for almost all such s, t we have that $\int_0^T \chi' F\,dt \to -[F(t) - F(s)]$, $\int_0^T \chi' E\,dt \to -[E(t) - E(s)]$. Thus, for any such s, t, we obtain

$$\begin{aligned}
F(t) = E(t) + [F(s) - E(s)] &+ \int_s^t \int_{\mathbb{T}^n} \langle \nu, (\xi - v)\cdot\frac{1}{2}[\nabla v + (\nabla v)^T]\cdot(\xi - v)\rangle\,dx\,dt \\
&+ \int_s^t \int_{\mathbb{T}^n} \langle \nu^\infty, \theta\otimes\theta\rangle : \frac{1}{2}[\nabla v + (\nabla v)^T]\,\lambda_t(dx)\,dt.
\end{aligned}$$

Next, observe that

$$F(s) - E(s) = -\int_{\mathbb{T}^n} \bar{v}(x,s)\cdot v(x,s)\,dx + \frac{1}{2}\int_{\mathbb{T}^n} |v(x,s)|^2\,dx.$$

The expression on the right hand side converges to

$$-\int_{\mathbb{T}^n} v_0\cdot v_0\,dx + \frac{1}{2}\int_{\mathbb{T}^n} |v_0|^2\,dx = -\frac{1}{2}\int_{\mathbb{T}^n} |v_0|^2\,dx,$$

as $s \to 0$. Letting $s \to 0$, we obtain

$$\begin{aligned}
F(t) &= E(t) - \frac{1}{2}\int_{\mathbb{T}^2} |v_0|^2\,dx + \int_0^t \int_{\mathbb{T}^n} \langle \nu, (\xi - v)\cdot \frac{1}{2}[\nabla v + (\nabla v)^T]\cdot(\xi - v)\rangle\,dx\,dt \\
&\quad + \int_0^t \int_{\mathbb{T}^n} \langle \nu^\infty, \theta\otimes\theta\rangle : \frac{1}{2}[\nabla v + (\nabla v)^T]\,\lambda_t(dx)\,dt \\
&\le E(t) - \frac{1}{2}\int_{\mathbb{T}^2} |v_0|^2\,dx + \int_0^t \left(\int_{\mathbb{T}^n} \langle \nu, |\xi - v|^2\rangle\,dx\right) \frac{1}{2}\|\nabla v + (\nabla v)^T\|_{L^\infty}\,dt \\
&\quad + \int_0^t \lambda_t(\mathbb{T}^n)\frac{1}{2}\|\nabla v + (\nabla v)^T\|_{L^\infty}\,dt \\
&= E(t) - \frac{1}{2}\int_{\mathbb{T}^2} |v_0|^2\,dx + \frac{1}{2}\int_0^t \|\nabla v + (\nabla v)^T\|_{L^\infty} F(t)\,dt.
\end{aligned}$$

This is the claimed estimate. □

We finally finish the general proof of weak-strong uniqueness.

Proof (Theorem 2.9) By energy admissibility,

$$E(t) \le \frac{1}{2}\int_{\mathbb{T}^2} |v_0|^2\,dx,$$

for all $t \ge 0$. Lemma A.1 thus implies that

$$F(t) \le \frac{1}{2}\int_0^t \|\nabla v + (\nabla v)^T\|_{L^\infty} F(\tau)\,d\tau.$$

By Gronwall's inequality, this implies that

$$F(t) \le e^{\frac{1}{2}\int_0^T \|\nabla v + \nabla v^T\|_{L^\infty}\,dt}\, F(0).$$

Since $F(0) = 0$, the right hand side vanishes and we must have $\nu_{x,t} = \delta_{v(x,t)}$, $\lambda = 0$. This proves weak-strong uniqueness. □

Appendix B

Vortex sheets

In [17], Delort gave the first existence proof of solutions for the incompressible Euler equations in 2D with vortex sheet initial data. The main theorem of [17] is the following.

Theorem B.1 [17]*: Under the assumption that the initial vorticity $\eta_0 = \mathrm{curl}(v_0)$ is in the Delort class, as defined above there exists a weak solution v of the 2-D incompressible Euler equations* (1.1)*, corresponding to the initial data v_0, that also belongs to the Delort class 4.4.*

The uniqueness of the solutions constructed by Delort was not addressed in [17] and remains an open problem. The purpose of this section is to review the proof of theorem B.1. In fact, we shall need a slight (but straight forward) extension of this theorem. We have to extend the class in definition 4.4. We recall Definition 4.6.

Definition B.2 *A vector field $v \in L^\infty([0,T]; L^2(\mathbb{T}^2;\mathbb{R}^2))$ will be said to belong to the* extended Delort *class, if the vorticity $\eta = \mathrm{curl}\, v$ is a bounded measure i.ef, $\eta \in H^{-1}(\mathbb{T}^2) \cap \mathcal{BM}$.*

The existence proof of Delort in [17] can be readily extended to the case of extended Delort class initial data in the sense of definition 4.6 provided that vortices of opposite sign do not interact with each other (at least for a finite time period). We formalize this argument in the following theorem,

Theorem B.3 *Let the initial velocity field v_0 belong to the extended Delort class as defined above. Further, assume that there exists a constant $c > 0$ and a terminal time $T > 0$, such that the time-dependent regions*

$$\mathcal{D}_\pm(t) = \{x \in \mathbb{T}^n;\ \exists N \in \mathbb{N},\ \eta_N(x,t) \gtrless 0\},$$

satisfy

$$\mathrm{dist}(\mathcal{D}_+(t), \mathcal{D}_-(t)) \geq c, \quad \forall t \in [0,T], \tag{B.1}$$

then there exists a weak solution v of the incompressible Euler equations (1.1) *that belongs to the extended Delort class 4.6.*

Our proof will be based on the following fundamental lemma concerning the limiting behaviour of approximate solutions of the Euler equations.

Lemma B.4 *Let v_N be an approximate solution sequence. Let $\eta_N = \operatorname{curl} v_N$. If*

- *$v_N \to v$ in $C([0,T]; L^2_w)$,*
- *$\int |\eta_N|\, dx \leq C$ uniformly for some constant C,*
- *and we have a uniform lack of concentration of vorticity, in the sense that*

$$\lim_{r\to 0} \sup_{0\leq t\leq T} \sup_N \int_{B_r(x)} |\eta_N|\, dx = 0, \qquad \forall\, x \in \mathbb{T}^2,$$

then v is a weak solution of the Euler equations.

This result is implicitly proved in the original article [17]. The more explicit statement is taken from [47].

Proof Following Delort [17], given vortexsheet initial data v_0 with vorticity $\eta_0 \in H^{-1} \cap \mathcal{BM}$, we can produce an approximating solution sequence v_N satisfying the assumptions of lemma B.4 as follows.

We start by mollifying v_0 to obtain a smooth approximation. To this end, let ρ be a standard smooth mollifier with compact support and define $\rho_N(x) = N^2\rho(x/N)$. The mollified initial data $v_N(x,0) := (\rho_N * v_0)(x)$ will have vorticity $\eta_N(x,0)$ with controlled L^1 norm,

$$\|\eta_N(\cdot,0)\|_{L^1(\mathbb{T}^2)} \leq \|\eta_0\|_{\mathcal{BM}}.$$

By Theorem 1.5, we can solve the Euler equations for these smooth approximating initial data to obtain a smooth solution v_N. The L^1-bound is conserved in time, so that

$$\int_{\mathbb{T}^2} |\eta_N(x,t)|\, dx = \|\eta_N(\cdot,t)\|_{L^1(\mathbb{T}^2)} = \|\eta_N(\cdot,0)\|_{L^1(\mathbb{T}^2)} \leq \|\eta_0\|_{\mathcal{BM}}$$

uniformly in N.

The uniform L^2-bound on v_N provides a weakly convergent subsequence $v_{N_k} \rightharpoonup v$ in $L^2(\mathbb{T}^2)$. The uniform L^1-control on η_N together with the negative Sobolev regularity in time implies that we can find a subsequence such that also $\eta_N \overset{*}{\rightharpoonup} \eta$ in $\mathcal{BM}$, where $\eta = \operatorname{curl} v$ in the distributional sense. The crucial missing part of the argument then consists in proving that

$$\lim_{r\to 0} \sup_{0\leq t\leq T} \sup_N \int_{B_r(x)} |\eta_N|\, dx = 0, \qquad \forall\, x \in \mathbb{T}^2.$$

This is where the uniform separation in space of the negative and positive parts of the vorticity η_N is used. In this case, the following bound can be established, [37]. We have

$$\int_{B_r(x)} |\eta_N|\, dx = \int_{B_r(x)} \eta_N\, dx \leq C|\log(2r)|^{-1/2},$$

for $0 < r < c$ and all $x \in \mathbb{T}^2$. The constant C depends only on the initial data and can be chosen independent of N for the sequence obtained from our construction.

The argument is based on the conservation of the pseudo-energy

$$H_N(t) = \int_{\mathbb{T}^2\times\mathbb{T}^2} K(x-y)\eta_N(x,t)\eta_N(y,t)\, dx\, dy$$

for smooth flows. The function $z \mapsto K(z)$ is the fundamental solution of the Laplace equation (with singularity $K(z) \sim -(2\pi)^{-1}\log(z)$ as $z \to 0$). We can estimate (for small $r > 0$)

$$\begin{aligned}\left(\int_{B_r(x_0)} \eta_N\, dx\right)^2 &= \int_{B_r(x_0)\times B_r(x_0)} \eta_N(x,t)\eta_N(y,t)\, dx\, dy \\ &\leq C|\log(2r)|^{-1}\int_{|x-y|<2r} K^-(x-y)\eta_N(x,t)\eta_N(y,t)\, dx\, dy,\end{aligned}$$

where $K^-(z) = \max(0, -K(z))$. The integral term on the right hand side can be estimated by

$$|\log(2r)|^{-1}\int_{|x-y|<2r} K(x-y)\eta_N(x,t)\eta_N(y,t)\, dx\, dy = |\log(2r)|^{-1}H_N(t).$$

On the other hand, we have $H_N(t) = H_N(0)$. Combining these facts, we obtain the required bound to conclude

$$\lim_{r\to 0}\sup_{0\leq t\leq T}\sup_N \int_{B_r} |\eta_N|\, dx \leq \lim_{r\to 0} C|\log(2r)|^{-1/2} = 0.$$

This shows that Lemma B.4 applies to the present situation. Therefore, the weak limit $v_{N_k} \rightharpoonup v$ is a weak solution of the Euler equations. Furthermore, we have the bound $\|\eta\|_{\mathcal{BM}} \leq \|\eta_0\|_{\mathcal{BM}}$. This proves the existence of a weak solution *in the Delort class* for vortexsheet initial data with distinguished sign; the proof also works under the assumption of a strict separation of regions $\mathcal{D}_+$ and $\mathcal{D}_-$. □

Bibliography

[1] J. J. Alibert and G. Bouchitté. Non-uniform integrability and generalized Young measures, *J. Convex. Anal.,* 4 (1), 1997, 129-147.

[2] C. Bardos and E. Tadmor. Stability and spectral convergence of Fourier method for nonlinear problems. On the shortcomings of the 2/3 dealiasing method *Num. Math.,* 2014, to appear.

[3] J. B. Bell, P. Colella and H. M. Glaz. A second-order projection method for the incompressible Navier-Stokes equations. *J. Comput. Phys*. 85 (1989), no. 2, 257–Äì283.

[4] T. Buckmaster, C. DeLellis, P. Isett and L. Székelyhidi Jr. Anomalous dissipation for 1/5- Hölder Euler flows. *Ann. Math.,* 2014, to appear.

[5] Y. Brenier and C. De Lellis and L. Székelyhidi Jr. Weak-Strong Uniqueness for Measure-Valued Solutions. *Comm. Math. Phys.,* 305 (2), 2011, 351–361.

[6] A. Chorin and J. E. Marsden. A mathematical introduction to fluid mechanics. *Texts in Applied Mathematics.,* (4), Springer, 1993.

[7] A. Chorin. Numerical solution of the Navier-Stokes equations. *Math. Comp.* 22, 1968, 745–Äì762.

[8] A. Chorin. On the convergence of discrete approximations to the Navier-Stokes equations. *Math. Comp.*, 23, 1969, 341–Äì353.

[9] A. Chorin. A vortex method for the study of rapid flow. *Proceedings of the Third International Conference on Numerical Methods in Fluid Mechanics (Univ. Paris VI and XI, Paris, 1972),* Vol. II, pp. 100–104. Lecture Notes in Phys., Vol. 19, Springer, Berlin, 1973.

[10] G. M. Coclite, S. Mishra and N. H. Risebro. Computing measure valued solutions of multi-phase flows in porous media. *In preparation*

[11] C.M. Dafermos. Maximal dissipation in equations of evolution. *J. Diff. Eq.*, 256, 2012.

[12] C. De Lellis, L. Székelyhidi Jr. The Euler equations as a differential inclusion. *Ann. of Math.* (2) 170 (2009), no. 3, 1417–1436.

[13] E. Chiodaroli, C. De Lellis, O. Kreml. Global ill-posedness of the isentropic system of gas dynamics. Preprint, 2013.

[14] C. De Lellis, L. Székelyhidi Jr. The h-principle and the equations of fluid dynamics. *Bull. Amer. Math. Soc.,* 49 (3), 2012, 349-375.

[15] C. De Lellis, L. Székelyhidi Jr. Dissipative continuous Euler flows. *Invent. Math.,* 193 (2), 2013, 377-407.

[16] C. De Lellis, L. Székelyhidi Jr. On admissibility criteria for weak solutions of the Euler equations. *Arch. Ration. Mech. Anal.*, 195(1):225–260, 2010.

[17] J. M. Delort. Existence de nappes de tourbillon en dimension deux. *Jl. Amer. Math. Soc.,* 4 (3), 1991, 553–586.

[18] R. J. DiPerna. Measure-valued solutions to conservation laws. *Arch. Rational Mech. Anal.*, 88(3):223–270, 1985.

[19] R. J. DiPerna and A. Majda. Oscillations and concentrations in weak solutions of the incompressible fluid equations. *Comm. Math. Phys.* 108 (4), 1987, 667–689.

[20] R. J. DiPerna and A. Majda, Concentrations in regularizations for 2-D incompressible flow *Comm. Pure Appl. Math.,* 40 (3), 1987, 301–345.

[21] G. L. Eyink and K. Srinivasan. Onsager and theory of hydrodynamic turbulence. *Rev. Modern. Phys.,* 78 (1), 2006, 87–135.

[22] U. S. Fjordholm, R. Käppeli, S. Mishra and E. Tadmor. Construction of approximate entropy measure valued solutions for hyperbolic systems of conservation laws. *Preprint*, 2014, available from ArXiv 1402.0909.

[23] U. S. Fjordholm and S. Mishra. Computing measure valued solutions of conservation laws with strictly convex entropy. *In preparation*, 2014.

[24] S. Gottlieb, C.-W. Shu and E. Tadmor. High order time discretizations with strong stability properties. *SIAM. Review* 43, 2001, 89–112.

[25] D. Gottlieb, Y. M. Houssaini and S. Orszag. Theory and application of spectral methods. *Spectral methods for PDEs*, 1-54, SIAM, 1984.

[26] S. Gottlieb and L.-A. J. Gottlieb. Strong stability preserving properties of Runge-Kutta time discretization method for linear constant coefficient operators. *J. Sci. Comput.*, 18(1):83–109, 2003.

[27] S. Gottlieb. On high order strong stability preserving Runge-Kutta and mutli step time discretizations. *J. of Sci. Comput.*, 25(1): 105–128, 2005.

[28] R. Krasny. A study of singularity formation in a vortex sheet by the point-vortex approximation. *J. Fluid Mech.* 167 (1986), 65,Äì93.

[29] R. Krasny. Vortex sheet computations: roll-up, wakes, separation. *Vortex dynamics and vortex methods (Seattle, WA, 1990),* 385–402, Lectures in Appl. Math., 28, Amer. Math. Soc., Providence, RI, 1991.

[30] S. Nazarenko, S. S. Ray, U. Frisch and T. Matsumuto. Resonance phenomenon for the Galerkin-truncated Burgers and Euler equations. *Phys. Rev. E*, 84, 2011.

[31] Landau, L. D. and Lifshitz, E. M. Course of theoretical physics. Vol. 6, Second Edition *Fluid mechanics*, Translated from the third Russian edition by J. B. Sykes and W. H. Reid, *Pergamon Press, Oxford*, 1987

[32] S. Lanthaler and S. Mishra. Computation of measure-valued solutions for the incompressible Euler equations. *Submitted*, http://arxiv.org/abs/1411.5064.

[33] F. Leonardi and S. Mishra. A projection-finite difference method for computing measure valued solutions of the incompressible Euler equations. *In preparation*.

[34] Leray, Jean Selected papers. Œuvres scientifiques. Vol. II Fluid dynamics and real partial differential equations *Springer-Verlag, Berlin; Société Mathématique de France, Paris*, 1998

[35] J. S. Lowengrub and M. J. Shelley. Exact desingularization and local regridding for vortex methods. *Vortex dynamics and vortex methods (Seattle, WA, 1990),* 341,Äì362, Lectures in Appl. Math., 28, Amer. Math. Soc., Providence, RI, 1991.

[36] A. Majda. Vorticity, turbulence, and acoustics in fluid flow. *SIAM Rev.* 33 (1991), no. 3, 349–388.

[37] A. Majda and A. Bertozzi. Vorticity and incompressible flow. *Cambridge university press,* 2002.

[38] A. Majda. Remarks on weak solutions for vortex sheets with a distinguished sign. *Indiana Univ. Math. J.*, 42 (3), 1993, 921–939.

[39] S. Mishra and C. Schwab. Sparse tensor multi-level Monte Carlo finite volume methods for hyperbolic conservation laws with random initial data. *Math. Comput.*, 81(180), 2012, 1979–2018.

[40] S. Mishra, Ch. Schwab and J. Sukys. Multi-level Monte Carlo finite volume methods for nonlinear systems of conservation laws in multi-dimensions. *J. Comput. Phys* 231 (8), 2012, 3365–3388.

[41] S. Mishra, Ch. Schwab and J. Sukys. Monte Carlo and multi-level Monte Carlo finite volume methods for uncertainty quantification in nonlinear systems of balance laws. *Uncertainty Quantification in Computational Fluid Dynamics.* Lecture Notes in Computational Science and Engineering Volume 92, 2013, 225–294

[42] L. Onsager. Statistical hydrodynamics. *Nuovo Cimento (9) 6*, Supplemento, 2 (Convegno Internatzionale di Meccanica Statistica) (1949), 279–287.

[43] R. Robert. Statistical hydrodynamics (Onsager revisited). *In Handbook of mathematical fluid dynamics*, Vol II, North Holland, 2003, 1–54.

[44] P. Sagaut. Large eddy simulation for incompressible flows. *Springer-Verlag, Berlin,* Scientific Computation, 2006.

[45] V. Scheffer. An inviscid flow with compact support in space-time. *J. Geom. Anal.,* 3 (4), 1993, 343–401.

[46] A. Shrirelman. Weak solutions with decreasing energy of the incompressible Euler equations. *Comm. Math. Phys.,* 210 (3), 2000, 541–603.

[47] S. Schochet. The weak vorticity formulation of the 2-D Euler equations and concentration-cancellation. *Comm. Partial Differential Equations*, 20 (5-6), 1995, 1077–1104.

[48] L. Székelyhidi and E. Wiedemann. Young measures generated by ideal incompressible fluid flows *Arch. Rat. Mech. Anal.,* 206 (1), 2012, 333–366

[49] L. Székelyhidi. Weak solutions to the incompressible Euler equations with vortex sheet initial data. *C. R. Math. Acad. Sci. Paris*, 349 (19-20), 2011, 1063–1066.

[50] E. Tadmor. Convergence of spectral methods for nonlinear conservation laws. *SIAM Jl. Num. Anal.,* 26 (1), 1989, 30–44.

[51] E. Tadmor. Total variation and error estimates for spectral viscosity approximations *Math. Comput.,* 60, 1993, 245–256.

[52] L. Tartar. Compensated compactness and applications to partial differential equations. *Nonlinear analysis and mechanics: Heriot-Watt Symposium*, Vol. IV, Pitman, 1979, 136–212.